OZONE- AND ULTRAVIOLET RADIATION-INDUCED SIGNALLING IN PLANTS

By

Godfrey Preston Miles

B.Sc., Western Washington University, USA, 1995

A THESIS SUBMITTED IN PARTIAL FULFILLMENT OF

THE REQUIREMENTS FOR THE DEGREE OF

DOCTOR OF PHILOSOPHY

In

THE FACULTY OF GRADUATE STUDIES

(Faculty of Agricultural Sciences)

PLANT SCIENCE

THE UNIVERSITY OF BRITISH COLUMBIA

December 2004

ABSTRACT

Plant cells respond to a myriad of environmental stresses, including oxidant-generating agents such as ozone and ultra-violet radiation, by mobilizing a complex of cellular defenses. This response is made possible by an integration of signalling networks that mediate the perception of, and response to, these environmental stresses. However, the signalling networks linking perception of these various stress-related perturbations with the ultimate defense responses remain largely undefined.

Exposure of tobacco suspension-cultured cells to ozone, UVC [254nm, monochromatic] or hydrogen peroxide was found to induce the rapid activation of a specific 46 kDa mitogen-activated protein kinase ($MAPK^{46}$) (salicylic acid-induced protein kinase). Oxidant activation of $MAPK^{46}$ is transient, calcium-dependent, and can be suppressed by pre-treatment with free radical traps. The observed response is not restricted to tobacco, since oxidant treatment of plants such as *Arabidopsis*, poplar, spruce and *Physcomitrella* also resulted in rapid activation of a similar protein kinase. Treatment of the tobacco cells with PD98059, a specific inhibitor of human MEK-1 & 2, blocked ozone- and hydrogen peroxide-induced activation of $MAPK^{46}$, but not UVC-induced activation. These results indicate that the ozone- and hydrogen peroxide-induced activation of $MAPK^{46}$ is signalling through a cognate MAPKK(s) that is sensitive to PD98059, whereas UVC may utilize a MAPKK which is insensitive to PD98059.

To explore where these oxidants might initiate this signal response, suramin, a non-membrane permeable reagent that interferes with membrane

receptor-mediated signalling in mammalian cells, was employed. Pretreatment of tobacco suspension-cultured cells with suramin strongly attenuated the oxidant-induced activation of MAPK[46] in a concentration-dependent manner, indicating that reactive oxygen species (ROS) signalling to the MAPK cascade may be initiated in large part at the cell membrane, perhaps through oxidative activation of membrane receptors.

An *Arabidopsis* AtMPK6-RNAi, loss-of-function genotype was constructed in order to better understand the role of this MAPK in cellular responses to oxidant signalling. When exposed to ozone, the RNAi-AtMPK6 genotype displayed more intense and prolonged AtMPK3 activation, as detected by Western blotting, when compared to WT, indicating that AtMPK6 is somehow involved in the regulation of this second MAPK in an oxidant background. The RNAi-AtMPK6 genotype was also found to be more sensitive than the WT to ozone fumigation, over a 24-hour period of continuous exposure, as evidenced by visible leaf damage and leaf-localized hydrogen peroxide accumulation.

To identify a possible oxidant-induced MAPKK involved in the activation of AtMPK6, a transgenic *Arabidopsis* loss-of-function genotype was developed using RNAi technology directed at AtMKK5, a candidate cognate MAPKK for AtMPK6. When exposed to ozone, the RNAi-MKK5 genotype showed a reduction in the activation of AtMPK3 and AtMPK6. I show that even partial silencing of MKK5 is sufficient to render the transgenic genotype highly susceptible to ozone damage, as determined by visible leaf damage and abnormally high levels of hydrogen peroxide accumulation in leaf tissue. This sensitivity to ozone was not lost over

successive generations of the AtMKK5 genotype. The MKK5-RNAi genotype is more sensitive to the injurious effects of ozone than is the AtMPK6-RNAi genotype.

Mastoparan (MP), a cationic, amphiphilic tetradecapeptide isolated from wasp venom, is capable of directly stimulating the guanine nucleotide exchange reaction of the α-subunit of animal heterotrimeric G proteins via a mechanism analogous to that of G protein coupled receptors (GPCR). This leads to a range of downstream events including the activation of MAPKs. I show that the induction of plant MAPK signaling by MP does not require the participation of either the Gα- or Gβ-subunits of the *Arabidopsis* heterotrimeric G-proteins, but is reliant on ROS, a cognate MAPKK, and an influx of extra-cellular Ca^{2+} ions. While these findings do not preclude a role for a heterotrimeric G protein in MAPK signaling, they highlight the need for caution in drawing conclusions from published experiments using MP.

To gain some additional insight into the cellular changes associated with oxidant stress, and the possible role of MPK6 in regulating those changes, I used isotope-coded affinity tagging (ICAT) technology to examine ozone-induced changes in protein expression in *Arabidopsis*, where the proteomes of both WT and MPK6-RNAi genotypes were compared in the context of an ozone challenge.

Functional classification of the proteins from ozone treated tissue that were differentially expressed in the MPK6-suppressed and WT backgrounds was conducted based on the GO ontology system (**Table 5.4, p148**). The majority of the 0 hr-air and 8 hr-O_3 proteins are annotated as being located in the chloroplast, while the rest are associated with the mitochondria, nucleus, and cytosol. The categories of 'other metabolic processes', electron transport, energy pathways or

antioxidant-related make up the bulk of the 0 hr-air and 8 hr-O_3 protein entries with an assortment of other categories covering the rest of the protein entries.

The data presented in this thesis provide evidence for the ability of oxidants (ozone & UVC) to activate MAPK signalling in plants, and demonstrate that the initial events leading to this activation originate at the cell membrane, possibly through a receptor-based mechanism. Further, I present one of the first large-scale proteomic studies directed at plant signal transduction. The data from this study will help us to better understand the involvement of MPK6 in the overall response to oxidative stress.

TABLE OF CONTENTS

List of Abbreviations

APX	ascorbate peroxidase
bp	base pair
BSA	bovine serum albumin
CaMV	cauliflower mosaic virus
dATP	deoxyadenosine triphosphate
dCTP	deoxycytidine triphosphate
ddH_2O	double distilled water
DAB	diaminobenzidine
DEPC	diethyl pyrocarbonate
dGTP	deoxyguanosine triphosphate
DNA	deoxyribonucleic acid
dNTPs	deoxynucleotide triphosphate
DTT	dithiothreitol
dTTP	deoxythymidine triphosphate
EDTA	ethylenediaminetetra acetic acid
EV	empty vector
g	gravitational force
GST	glutathione S-transferase
HEPES	N-(2-hydroxyethyl)piperazine-N'-(2-ethanesulfonic acid)
HR	hypersensitive response
IP	immunoprecipitation
JA	jasmonic acid
kDa	kilodalton
LB	Luria Broth
MAPK	mitogen-activated protein kinase
MAPKK	mitogen-activated protein kinase kinase
MBP	myelin basic protein
MS	Murashige & Skoog culture medium
MOPS	3-(N-morpholino) propane-sulfonic acid
mRNA	messenger ribonucleic acid
μE	micro Einsteins
Nos	nopaline synthase

ORF	open reading frame
PAGE	polyacrylamide gel electrophoresis
PCR	polymerase chain reaction
ppb	parts per billion
PVPP	polyvinylpolypyrrolidone
RH	relative humidity
RNAi	ribonucleic acid interference
RNA	ribonucleic acid
ROS	reactive oxygen species
rpm	revolutions per minute
RT	room temperature
SA	salicylic acid
SAR	systemic acquired resistance
SDS	sodium dodecyl sulfate
SIPK	salicylate-induced protein kinase
Taq	*Thermus aquaticus*
UTR	untranslated sequences
UV	ultra-violet
WIPK	wound-induced protein kinase

List of Schemes, Tables, and Pie Charts

List of Figures and Legends

Acknowledgements

I am deeply indebted and grateful to my research supervisor Dr. Brian E. Ellis, for offering me this opportunity to work in this wonderful lab. I am thankful to him for all his help and positive guidance throughout this study, and for his tremendous, supportive interest in my research. I am also grateful to the members of my committee, Dr. Steven Pelech, Dr. Murray B. Isman, and Dr. Ross T. A. MacGillivary who provided me with excellent feed-back on my work. I would also like to thank all the marvelous people I had the privilege to work with in Dr. Ellis' multi-cultural lab - Amrita Kumar, Stefanie Butland, Rishi Gill, Jason Galpin, Somrudee 'Lukpla' Sritubtim, Alana Clegg, Hardy Hall and Greg Lampard, the support staff in Plant Science - Robyne, Ashley, and Peter Garnett, who maintained those finicky ozone systems, and Dr. Naza Azizbekova for all her technical help with my tissue culture. Special thanks are owed to my good friend and colleague for almost six years, Dr. Marcus Samuel. Finally, I also give special thanks to my very supportive and wonderful parents, George and Marie Miles, my sister, Eddree and brother, Arthur, who have always been a positive influence in my life, and my most special and sweet daughter, Zoë E. Miles, who is the center of my Universe.

Chapter 1

General Introduction

1.1 Tropospheric ozone formation and distribution

Approximately two billion years ago, early aquatic organisms started to utilize the sun's energy to split molecules of H_2O and CO_2, recombining them into various organic compounds and molecular oxygen (O_2) in a process known as photosynthesis. This O_2 made its way into the atmosphere where it gradually accumulated ultimately producing a massive ecological change that greatly disadvantaged the already existing anaerobic organisms. In the upper layers of the stratosphere, O_2 molecules absorbed UV radiation from the sun in a photochemical reaction that eventually forms ozone (O_3). The resulting stratospheric O_3 layer that surrounds the Earth acted as a "filter" against incoming UV radiation.

Ozone is formed (Retzlaff et al., 1991) in the stratosphere by the photochemical mechanism first identified by Chapman (1930) and thus often referred to as the "Chapman mechanism." The reaction sequence starts with the ultraviolet photolysis of diatomic oxygen, which creates two oxygen radicals:

(R1) $O_2 + h\nu\ (\leq 242\text{nm}) \rightarrow O + O$

each of these then reacts with another molecule of oxygen, forming ozone:

(R2) $O + O_2\ (+M) \rightarrow O_3\ (+M)$

In these reaction descriptions, $h\nu$ denotes a quantum of radiation of appropriate energy, and the symbol M refers to another molecule, such as N_2 or O_2, which

stabilizes the reaction by absorbing a portion of the energy released in ozone formation. In the overall Chapman mechanism ozone loss is allowed via the following reactions:

(**R3**) $O_3 + h\nu \rightarrow O + O_2$ (i.e. the reverse of R2)

(**R4**) $O + O_3 \rightarrow 2O_2$

Ozone produced in the stratosphere can enter the troposphere via what is known as the stratosphere – troposphere exchange phenomenon (Shapiro et al., 1980). This process appears to involve large-scale eddies in the jet stream region, and results in net movements of ozone from the stratosphere to the troposphere. This process, though it exists, accounts for only a small part of the tropospheric, or ground-level ozone, whereas; the majority of ground-level O_3 is formed *in situ* by photochemical reactions involving volatile organic compounds (VOCs) and nitrogen oxides (NOx), which are produced in large quantities in and around heavily industrialized areas.

In the Los Angeles Basin, the Federal Ambient Air Quality Standard of 0.12 ppm (averaged over a one-hour period) is exceeded 90 – 100 days a year (Mudd et al., 1997) and peak ozone levels can exceed 0.4 ppm (1 hr daily maxima) (McCurdy 1994). Because the complex series of reactions are driven by temperature and sunlight, ozone formation varies hourly, daily and seasonally.

1.2 Ultraviolet Radiation: origin and types

The solar radiation arriving in the Earth's atmosphere is made up in large part of radiation consisting of wavelengths (λ) that are shorter than visible light (400-700

nM). These shorter, and more energetic, wavelengths (100 to 400 nM) constitute what is known as the UV spectral region. This region is further divided into three sub-regions, designated UVA (315-400nM), the least energetic, UVB (280-315nM), and finally UVC (100-280nM), the shortest and most energetic of the three divisions. The UVC portion of the spectrum is essentially completely absorbed by atmospheric oxygen and ozone. UVB is absorbed efficiently, but not completely, by ozone and various trace atmospheric gases. UVA is only weakly absorbed by ozone and easily makes its way to the surface of the Earth.

A number of atmospheric trace gases such as ozone, hydrogen peroxide, formaldehyde (HCHO), nitric acid (HNO_3), and nitrogen dioxide (NO_2) undergo photolysis when they absorb UVB radiation. These photolysis products (O, NO, OH, H, HCO and eventually HO_2 and organic peroxy radicals) exist as highly reactive species in the atmosphere. The increased production of these reactive species adds to the oxidizing capacity of the troposphere, and thus to the oxidant challenge faced by living organisms (Tang et al., 1998).

1.3 Effects of ozone exposure on mammals and plants

In mammals, the effects of ozone exposure include airway hyper-reactivity, increased epithelial macromolecular permeability, neutrophil infiltration, DNA damage, increased frequency of K-ras mutations (resulting in lung neoplasms in mice) and increased levels of glutathione (GSH) and catalase (CAT) (Pryor et al., 1995; Sills et al., 1995; Vender et al., 1994).

The detrimental effects of this pollutant on plants include diminished photosynthesis (Runeckles and Krupa, 1994; Darral 1989); flecks, chlorosis and necrotic lesions (Manning and Krupa, 1992); retarded growth, increased lipid peroxidation (Hewitt et al., 1990); membrane damage (Heath 1988); and accelerated foliar senescence (Pauls and Thompson, 1980). All of these symptoms can be related to the initial production of reactive oxygen species (ROS) in the affected tissues (Grimes et al., 1983; Amundsen et al., 1986, 1987; Patton and Garraway, 1986; Darrall et al., 1989; for a review see Runeckles and Chevone, 1992).

Recent studies have shown that ozone and other atmospheric oxidants are responsible for as much as 90% of agricultural crop loss due to air pollution (Heck et al., 1984a; 1984b). Similarly, in forest systems, ozone is believed to cause more damage to trees than any other gaseous pollutant (Koch et al., 1998; Langebartels et al., 1998). Over the past twenty years in North America, ambient concentrations of ozone have increased 1% to 2% per year with no indication of leveling off (Stockwell et al., 1997).

1.4 Biological effects of ultraviolet radiation

The thickness of the UV-screening ozone layer varies with season, meteorological conditions and latitude (Madronich et al., 1995). Decreased stratospheric ozone levels are now evident over large parts of the globe, allowing increased penetration of solar UVB radiation to the Earth's surface. This increase in UVB radiation is predicted to have adverse effects on terrestrial and aquatic life. These include UVB-induced life-cycle timing problems, alteration of plant form, increased accumulation of specialized plant chemicals and damage to genetic

mechanisms. For example, UVB has been shown to increase the frequency of somatic homologous DNA rearrangements in *Arabidopsis* and tobacco plants (Ries et al., 2000). In addition to direct impacts on individual plants, UVB can have broader ecological effects by affecting the balance of competition between plant species or genotypes. This could result, for example, from UV-susceptible plants falling victim more readily to pathogens and insects compared with non-susceptible plants.

In aquatic ecosystems, as well, increased levels of UVB and UVA have been linked to adverse effects on the growth, protein and pigment content, and on reproduction of phytoplankton, thus directly affecting the homeostasis of aquatic food webs.

1.5 Ozone-and ultraviolet-induced oxidative stress in plant tissues: *in vivo* production of ROS

1.5.1 Ozone

In plants, ozone enters the mesophyll via the stomata, and diffuses through the inner air spaces to reach the cell wall and plasmalemma (Salater et al., 1992, Sharma et al., 1997). In this environment, ozone is immediately converted to ROS including $^{\bullet}O_2^-$, $HO^{\bullet}$ and H_2O_2, by contact with water, the plasmalemma, or other cellular components (Kanofsky and Sima, 1995 Morgan and Wenzel, 1985). It can also form ozonides and lipid peroxides that can initiate a series of reactions producing further damaging reactive oxygen intermediates (Sharma et al., 1997).

ROS consist of oxygen-centered redox derivatives of molecular oxygen. The parental molecule for these derivatives is the free radical superoxide anion ($^{\bullet}O_2^-$). The

family of ROS species derived from $^{\bullet}O_2^-$ consists of a number of other free radicals, most notably the hydroxyl radical ($^{\bullet}OH$) and the hydroperoxyl radical ($HO_2^{\bullet}$), which is the conjugate acid to the superoxide anion. In addition to these $^{\bullet}O_2^-$ derived free radicals, various oxygen derivatives that are not free radicals, e.g., hydrogen peroxide (H_2O_2), are also formed. Reactive nitrogen species (RNS) such as the parental radical, nitric oxide (NO), and an array of redox-active derivatives such as nitrogen dioxide ($NO_2^{\bullet}$) and peroxinitrite ($ONOO^{\bullet}$), are also formed, but the impact of RNS is outside of the scope of this study.

Ozone can also act directly on unsaturated hydrocarbons in living cells, to produce H_2O_2 via the oxidation of singlet Criegee diradicals (**Scheme 1**). The 1, 2, 3-trioxolane (primary ozonide) derivative formed when ozone reacts with an alkene (Squadrito et al., 1992) is extremely unstable and usually forms a secondary ozonide, which is more stable. The *cis*- or *trans*-Criegee ozonide (secondary ozonide (**Scheme, path B**) is in dynamic equilibrium with the carbonyl oxide (existing as a singlet diradical) and the aldehyde. Hydrogen peroxide can form directly from the oxidation of the carbonyl oxide with water (Scheme, path A), forming the hydroxyhydroperoxide (HHP), or via the secondary ozonide. Pellinen et al. (1999) recently demonstrated that hydrogen peroxide build-up in ozone-challenged plant tissue occurs at the cell wall and plasma membrane. It is worth noting that if this ozone-induced hydrogen peroxide encounters Fe^{2+} ions, the production of very reactive hydroxyl radicals could result from what is

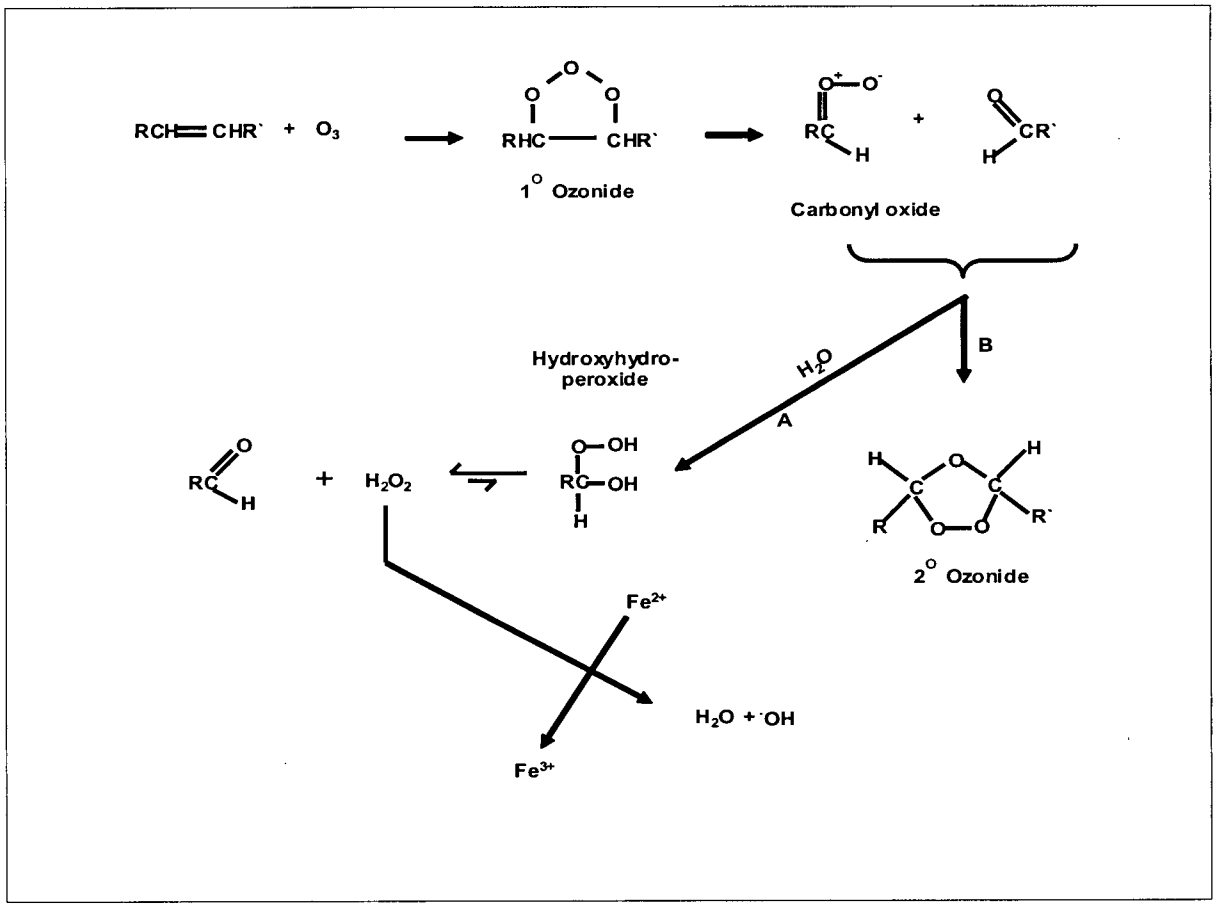

Scheme 1.1, Mechanistic representation of the fate of ozone after addition across unsaturated cellular lipids (adapted from Squadrito et al., 1992).

known as the Haber-Wilstätter / Weiss cycle, via Fe-catalyzed Fenton chemistry (Grimes et al., 1983; Runeckles and Vaartnou, 1997; reviewed in Storz and Imlay, 1999). However, no matter what form the oxidizing species take, it is reasonable to predict that ozone could be eliciting its downstream effects, at least in part, through the initial rapid oxidation of cell signalling components situated at or near the cell surface.

1.5.2 Ultraviolet radiation (UVR)

ROS have been established to be important in UVB-induced plant signal transduction (A.-H.-Mackerness and Jordan, 1999) and epidermal growth factor-mediated (EGF) signalling in human keratinocytes (Peus et al., 1999). However, unlike ozone, which can act as a primary oxidant, UVR has to 'stimulate' the production of ROS by indirect chemistry.

A recent paper by Desikan et al. (1996), demonstrated that the first ROS formed after UVB exposure is $^{\bullet}O_2^-$. The authors also showed that application of the superoxide dismutase (SOD) inhibitor *N*, *N*-diethyldithiocarbamate (DDC), drastically attenuated the level of UVB-induced pathogenesis-related gene (*PR-1*) expression. Since DDC induces the accumulation of $^{\bullet}O_2^-$, this observation connects $^{\bullet}O_2^-$ signalling to the regulation of this defense gene. When Tiron, a known scavenger of $^{\bullet}O_2^-$ was used, the effect of UVB on the *PR-1* gene was drastically reduced, which supported the idea that the first ROS generated as a consequence of UVB exposure is $^{\bullet}O_2^-$. Using a pharmacological approach, Mackerness et al. (2001) showed that in UVB-exposed *Arabidopsis* seedlings, $^{\bullet}O_2^-$ is both NADPH oxidase- and peroxidase-derived.

Ozone and UVR also induce additional stress-related genes such as lipoxygenase (LOX), polyphenol oxidase (PPO), phenylalanine-ammonia-lyase (Pal), and proteinase inhibitors I and II (Pin) (Bell and Mullet, 1993; Lois and Hahlbrock, 1992; Maccarrone et al., 1992; Sharma and Davis, 1994; Sano et al., 1994). This

indicates that these stressors may share all or part of the subsequent signal transduction cascades.

1.6 Origins of metabolic reactive oxygen species

While ROS are produced in cells as a result of environmental stresses such as ozone and UVR, they are also produced in unstressed cells as a result of normal metabolic events (Foyer et al., 1994; Abe et al., 1998; Blumwald et al., 1998). The metabolic event with perhaps the greatest propensity for ROS production in plants is photo-oxidation in chloroplasts, where the major ROS produced is $^{\bullet}O_2^-$ (Asada 1992; Foyer et al., 1994). In this oxygen-rich microenvironment, $^{\bullet}O_2^-$ is formed via direct donation of an electron to oxygen from reduced ferredoxin residing in the photosynthetic electron transport chain (Asada, 1992; Foyer et al., 1994; Kangasjarvi et al., 1994).

The initial step in the reduction of O_2 by electrons leaking from these high energy systems produces the short-lived hydroperoxyl ($HO_2^{\bullet}$) and $^{\bullet}O_2^-$ radicals. $HO_2^{\bullet}$ and $^{\bullet}O_2^-$ radicals form hydroperoxides with unsaturated carbon skeletons such as membrane fatty acids, and also oxidize specific amino acids, such as histidine, methionine and tryptophan. $HO_2^{\bullet}$, the conjugate acid of $^{\bullet}O_2^-$ easily moves across lipid barriers due to its low electronegative character.

Further reduction of $^{\bullet}O_2^-$ yields H_2O_2, a relatively long-lived molecule with the ability to diffuse longer distances and to readily cross cellular membranes. H_2O_2 can oxidize –SH groups, a process that is greatly enhanced by the presence of metal ion catalysts such as Cu^{2+} and Fe^{2+}. Still further reduction of H_2O_2 yields the $^{\bullet}OH$ radical,

an extremely reactive species with a propensity to oxidize biological targets very near to its site of production before it has a chance to diffuse to more distant points.

1.6.1 Plant mitochondria

Mitochondria are also important producers of cellular ROS (Poyton and McEwen, 1996; Braidot et al., 1999; reviewed in Kowaltowski and Vercesi, 1999). In fact, it is estimated that up to 2% of the oxygen reduced by the plant mitochondria, is transformed into ROS (Boveris and Chance, 1973; Lie 1997; reviewed in Kowaltowski and Vercesi, 1999). This 2% conversion rate of molecular oxygen to ROS is increased under biotic and abiotic stresses (Tenhaken et al., 1995). The main sites for ROS production in plant mitochondria (Rich and Bonner, 1978; Braidot et al., 1999) are similar in mammalian mitochondria (Boveris et al., 1976; Turrens and Boveris, 1980; Chakrabort et al., 1999). The sites of mitochondrial ROS production are complexes I (NADPH-Q-reductase) and the ubiquinone reductase site (complex III) of the respiratory chain. In a recent paper (Braidot et al., 1999) demonstrated that in pea stem mitochondria, H_2O_2 is produced at complex II (succinate dehydrogenase).

1.6.2 Plant peroxisomes

Plant peroxisomes play important roles in a myriad of metabolic processes including photorespiration, fatty-acid β-oxidation, the glyoxylate cycle and the generation/degradation of hydrogen peroxide (reviewed in Corpas et al., 2001), subsequently producing the following oxygen and nitrogen species: H_2O_2, $^{\bullet}O_2^{-}$, and NO. Plant peroxisomes, in addition to chloroplasts and mitochondia, should be considered as cellular compartments able to produce and deliver important oxygen- and nitrogen-based signalling molecules into the cytosol.

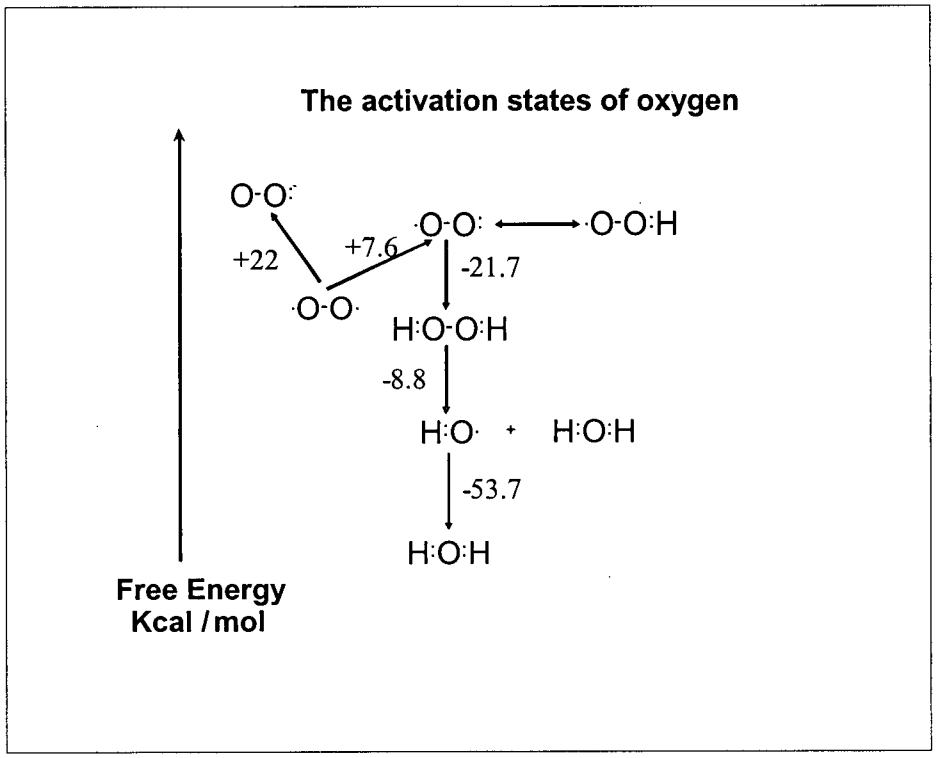

Figure 1.1 Representation of the various activation states of oxygen that can be expected to be found in a physiologically normal cell.

1.7 Antioxidant metabolites and enzymes

Plants constitutively produce a basal level of anti-oxidant metabolites and enzymes which help to protect them from the potential damaging effects of exogenous and endogenous ROS. Ozone- and UVR-exposure are also known to increase, in a number of plants, the expression of numerous antioxidant enzymes including: superoxide dismutase (SOD), peroxidases, catalase (CAT), and ascorbate peroxide (APX) (Tanaka et al., 1988; Conklin and Last, 1995; Roa et al., 1995; Boldt and Scandalio, 1997).

Superoxide dismutase (SOD) catalyzes the dismutation of the superoxide anion (and its conjugate acid $HO_2^{\bullet}$) to H_2O_2 and O_2 (Foyer et al., 1994; Kangasjarvi et al., 1994). There are different types of SOD located in the chloroplasts, mitochondria and

the cytosol (Bowler et al., 1992). Some peroxidases catalyze reduction of alkyl-peroxides to H_2O and an alcohol in a reaction coupled to oxidation of a reductant (AH_2). Catalase, a hydroperoxidase, catalyzes the decomposition of H_2O_2 into O_2 and H_2O, without the production of free radicals (Foyer et al., 1994).

APX is an important part of the ascorbate-glutathione cycle (Kargasjarvi et al., 1994). There are different types of APX located in the cytosol (soluble), cytosol (membrane bound), chloroplast (thylakoid membrane bound), and chloroplast (stromal) (Kubo et al., 1992; Newman et al., 1994; Jespersen et al., 1997; Santos et al., 1998). APX catalyses the first step in the ascorbate-glutathione cycle by reducing H_2O_2 to H_2O, where ascorbate is the electron donor (Mittler and Zilinskas, 1991). The ascorbate-glutathione (Halliwell-Asada) pathway starts, as stated above, by the reduction of H_2O_2 to form monodehydroascorbate (MDHA). The regeneration of ascorbate from MDHA can come about by two different mechanisms. The first is catalytic reduction of MDHA by NADH, mediated by monodehydroascorbate reductase, while the second is spontaneous diproportionation of MDHA into ascorbate and dehydroascorbate (DHA). In a connected set of reactions, ascorbic acid can be reclaimed from DHA via the dehydroascorbate reductase reaction, in which reduced glutathione (GSH) is oxidized to form GSSG. Subsequently, GSH is reformed from GSSG by reduction with NADPH, a reaction catalyzed by glutathione reductase.

In addition to these direct antioxidant defenses, plants have evolved, as a first line of defense against UVR, both constitutive and inducible UV-screening metabolites, including flavonoids, carotenoids and phenolic conjugates.

1.8 ROS Signalling

In recent years there has been increasing recognition that the cellular impacts of ROS are not all mediated through chemical damage of cellular constituents. There is considerable evidence that ROS also have the ability to alter cell function by acting as, mimicking, or affecting intermediates (second messengers) in signal transduction pathways. Oxidant increases can signal the induction of antioxidant enzymes, mimic the effects of receptor-mediated ligand responses (e.g., insulin in mammals), and activate signal transduction pathways. The effects of oxidants on signalling mechanisms may be a major factor in the oxidative stress responses associated with inflammation, aging, and cancer in mammals, and in oxidant-induced growth retardation and induction of systemic acquired resistance (SAR) in plants.

The molecular mechanisms whereby oxidative stress impacts signal transduction pathways are not well understood, but several studies have pointed to the involvement of iron-catalyzed free radicals (Musicki and Behrman, 1993; Breuer et al., 1995; Abe et al., 1998; Guyton et al., 1996; Keyer and Imlay, 1996). These findings indicate that, in mammalian systems, hydrogen peroxide can undergo a metal-catalyzed oxidation, producing hydroxyl and hydroxyl-like radicals which oxidize cysteine-rich regions of various membrane receptors or protein phosphatases. This oxidation ultimately results in a ligand-independent activation of the affected signalling networks.

1.9 The sensing of oxidative stress by prokaryotes and eukaryotes

Sies (1991) defined oxidative stress as a perturbation in the prooxidant-antioxidant balance in favor of prooxidant, leading to potential damage. In other words,

oxidative stress occurs when production of damaging free radicals and other oxidative molecules exceeds the capacity of the organism's antioxidant defenses to detoxify them.

There are a number of proteins in bacteria whose synthesis is specifically induced by perturbations in the organism's redox-balance. Of these, the most thoroughly examined are the OxyR and SoxR proteins. The OxyR protein is sensitive to H_2O_2, while the SoxR protein is sensitive to $^{\bullet}O_2^-$ and $NO^{\bullet}$. Activation of the SoxR protein is dependent on the formation of a redox-sensitive [2Fe-2S] center. H_2O_2 does not stimulate the synthesis of OxyR but rather converts the reduced form of OxyR into its oxidized and regulatory competent form (Stroz et al., 1990; Zheng et al., 1998). Activation of the OxyR protein relies on the H_2O_2-induced, oxidation of Cys-199 to a sulfenic acid derivative that forms an intramolecular disulfide bond with Cys-208. Once activated, the OxyR protein induces the transcription of at least nine antioxidant genes. By contrast, the SoxR protein operates in a unique two-stage system of transcriptional control upon activation. It binds to and induces the transcription of only a single gene, SoxS. The SoxS protein subsequently triggers the transcription of many genes.

In addition to providing immediate protection against redox stress, OxyR-regulated activities include functions that confer resistance to HOCl, organic solvents, and reactive nitrogen species while, the products of the SoxRS regulon can confer resistance to drugs, organic solvents, and reactive nitrogen species.

In higher organisms, such as the budding yeast *Saccharomyces cerevisiae*, H_2O_2 is sensed by the yAP-1 transcription factor. The yAP-1 transcription factor

belongs to the AP-1 group of transcription factors consisting of homo- and heterodimers of the ATF, Foc and Jun families of proteins (reviewed in Toone and Jones, 1999). The oxidative-induced modification of yAP-1 occurs at two cysteine-rich regions located at the C-terminus and N-terminus of the protein, respectively (Kuge et al., 2001). Once modified, the oxidized yAP-1 translocates from the cytoplasm to the nucleus, but oxidation of the C-terminal cysteine region modifies the protein's nuclear export signal, inhibiting its relocalization back to the cytoplasm (Kuge et al., 2001; reviewed in Costa and Moradas-Ferreira, 2001). yAP-1 is thus able to perform both the role of oxidant sensing and redox signal transduction to the nucleus (Klug et al., 1997).

In mammalian cells, the mechanisms involved in the perception of ROS are less well understood. A large number of oxidant-induced genes have been identified (Monteiro and Stern, 1996; Adler et al., 1997; Flohe et al., 1997; Piette et al., 1997; Adler et al., 1999; reviewed in Allen and Tresini, 2000), but many of these same oxidant-induced genes are also induced by other physiological signals. The oxidoreductase Trx, which is expressed in a number of cells, including lymphocytes, is one such gene that is induced by oxidants. Located within the 5'-upstream sequence of the human Trx gene, there are a number of putative binding sites for the redox-sensitive transcription factors AP-1 and NF-κβ (Nakamura et al., 1993; 1997). However, both the AP-1 and NF-κβ transcription factors are also activated by non-oxidant signals. To date, transcription factors solely controlled by ROS have not been identified.

1.10 The role of calcium ions in cellular processes

Calcium ions play important roles as a second messenger in metazoans Price et al., 1996; Clayton et al., 1999; and reviewed in White and Broadley, 2003). Intracellular ($[Ca^{2+}]_i$) levels regulate a large number of important cellular processes including gene expression, cell viability, cell proliferation, cell motility and cell shape and volume regulation (Hrabak et al., 1996; Sreeganga and Low, 1997). Plants, like all other organisms, maintain concentrations of this ion in the cytosol and nucleus three to four orders of magnitude lower than that of other cellular compartments (Felle 1988; Bush et al., 1989)

$[Ca^{2+}]_i$ also rapidly responds to many external activating agents, and the fluxes in this cation play a key role in regulating cell responses to environmental signals. The changes in Ca^{2+} levels within the cell induced by environmental challenges are controlled by ligand-gated and G protein-coupled ion channels in the plasma membrane, and by mobilization of Ca^{2+} from intracellular stores (Sreeganga and Low, 1997). The generation of cytosolic Ca^{2+} spikes and oscillations typically involves the coordinated release and uptake of Ca^{2+} from these stores, mediated by intracellular Ca^{2+} channels. These channels are sensitive to several second messengers including cytosolic ADP ribose, inositol triphosphate and Ca^{2+} itself.

Yano et al. (1998) demonstrated in plants that an influx of Ca^{2+} ions could be crucial for the early steps of the signal transduction pathway by which a proteinaceous elicitor, harpin, (a protein from the phytopathogenic bacterium *Erwinia amylovora*) induces hypersensitive cell death in suspension-cultured tobacco (*Nicotiana tabacum* cv. Xanthi) cells. An influx of Ca^{2+} ions has also been suggested to be involved in

other examples of local bacteria-induced cell death in plants (Atkinson et al., 1990; Levine et al., 1996).

Calcium plays a role in one of the earliest responses produced in plants after contact with pathogens, namely the transient production of reactive oxygen species such as H_2O_2, $^{\bullet}O_2^-$, and $^{\bullet}OH$ (Schwake and Hagar, 1992; Baker and Orlandi, 1995; Lamb et al., 1997), in a process called the 'oxidative burst'. There are often two distinct phases of the oxidative burst induced by plant-bacterial interactions: an early transient burst (Phase I), and a delayed, long-lived burst (Phase II) (Baker and Orlandi, 1995). Sreeganga and Low (1997), using aequorin-transformed tobacco cells, examined the relationship between changes in intracellular Ca^{2+} and induction of an oxidative burst by either oligogalacturonic acid, Mas-7 (a peptide known to activate G proteins and Ca^{2+} fluxes), hypo-osmotic stress, or harpin. All of these treatments, except harpin, rapidly induced a transient Ca^{2+} spike that lasted approximately 20 seconds before returning to basal levels. This was followed by a hydrogen peroxide buildup at around two minutes post-elicitation. The fact that harpin did not induce a Ca^{2+} influx during its stimulation of the oxidative burst is a surprising observation, and indicates that harpin must act via a different pathway, or induce a known pathway in a novel manner. Lee et al. (2001) showed in tobacco that harpin, from the bean halo-blight pathogen *Pseudomonas syringae* ($harpin_{Psph}$) was able to induce the accumulation of pathogenesis-related gene transcripts and also observed that this process was independent of Ca^{2+}.

1.11 Oxidative stress and calcium ions

It has previously been demonstrated that oxidants like ozone, UVR and H_2O_2 can induce a transient increase in intracellular Ca^{2+} in many types of plant cells. Clayton et al. (1999) demonstrated in aequorin-expressing *Arabidopsis* plants that ozone exposure elicited a rapid but transient biphasic increase in cytosolic free Ca^{2+}. Cytosolic calcium homeostasis may be sensitive to the oxidation status of the glutathione pool, which it responds to via the plasma membrane Ca^{2+}-ATPase (reviewed in Price et al., 1996). In this model, an increase in the ratio of oxidized (GSSG) to reduced (GSH) glutathione causes a pronounced reduction in the activity of calcium transport proteins responsible for removing Ca^{2+} from the cytosol, leading to an increase in $[Ca^{2+}]_i$.

This oxidant-induced elevation in intracellular Ca^{2+} ions may further induce the production of $^{\bullet}O_2^-$ (and eventually H_2O_2) via a Ca^{2+}-dependent NADPH oxidase-mediated mechanism, thus creating a positive feedback loop (Price et al., 1995; Izumi et al., 2004). Consistent with this mechanism, Larkindale and Knight (2002) showed that heat-induced oxidative damage in *Arabidopsis* cells was abrogated by pre-treatment with various Ca^{2+}-channel blockers, including La^{3+}. However, it has been demonstrated in *Arabidopsis* that the influx of Ca^{2+} also activates a Ca^{2+}/ calmodulin protein which binds to, and enhances the activity of, a specific isoform of catalase (AtCat-3) (Yang and Poovaiah, 2002). Since the activated *Arabidopsis* Ca^{2+}/ CaM had no effect on bacterial, fungal, bovine or human catalases, it seems that the increase in $[Ca^{2+}]_i$ could be negatively regulating H_2O_2 homeostasis in a plant-specific process.

While the role of NADPH oxidase in generating a short-lived "oxidative burst" has been well characterized in some mammalian cells, a role for the same enzyme in plant ROS has been more difficult to demonstrate unequivocally. Several reports have described the impact of the classical NADPH oxidase inhibitor, diphenyleneionium (DPI), on various ROS-linked processes in plants (Levine et al., 1994; Samuel et al., 2000), which is generally taken as *prima facie* evidence for the involvement of NADPH oxidase. However, it has been pointed out the DPI is also capable of inhibiting other flavoproteins, as well as peroxidases, all of which are both efficient producers of ROS and abundant in plant cells (reviewed in Bolwell 1999). Nevertheless, there is other evidence indicating that NADPH oxidase-like activities may be present in plants. Bioinformatics analysis has shown that both *Arabidopsis* and tomato possess multigene families of putative mammalian NADPH oxidase subunit homologs (Sagi and Fluhr, 2001), while antibodies, raised against human $p22^{phox}$, $p47^{phox}$, and $p67^{phox}$ have been demonstrated to cross-react with appropriate size protein bands in plant extracts (Tenhaken et al., 1995; Desikan et al., 1996; Xing et al., 1997).

In *Arabidopsis*, analysis of mutants of the NADPH oxidase, respiratory burst oxidase homologs (rboh), rbohD and rbohF, has demonstrated that these molecules are sources of $^{\bullet}O_2^-$ production in the pathogen-induced oxidative burst (Torres et al., 2001). Calcium ions also interacted functionally with recombinant rboh *in vitro*. Elevated levels of NADPH oxidase activity were induced by Ca^{2+} concentrations between 50 μM and 10 mM, indicating that the plant plasma membrane NADPH oxidase might be directly regulated by Ca^{2+} *in vivo*, unlike the neutrophil $gp91^{phox}$.

Another major difference between the plant NADPH oxidase activity and its mammalian counterpart is that the plant enzyme can reduce molecular oxygen to $^{\bullet}O_2^-$ in the absence of any cytosolic subunits. Torres et al. (2002) recently showed that knockouts of *AtrbohF* in *Arabidopsis* blocked H_2O_2 generation during bacterial and fungal challenge.

It is also worth noting that the importance of Ca^{2+} ions in the propagation of ROS during plant-pathogen interaction (Baker et al., 1993). They showed that pre-treatment of tobacco suspension-cultured cells with the calcium channel blocker, La^{3+} followed by elicitor treatment, inhibited the oxidative burst. An additional experiment demonstrated that spruce suspension-cultured cells pre-treated with EGTA (a Ca^{2+} chelator) greatly reduced the oxidative burst, demonstrating the importance of extracellular Ca^{2+} ions in the production of ROS (Schwacke and Hager, 1992).

1.12 Hypersensitive response (HR) and systemic acquired resistance (SAR)

Subsequent to the phase I oxidative burst (described in section (1.10)), the challenged plant cell initiates a series of metabolic changes whose overall goal is the survival of the plant. A response pattern that leads to disease resistance after pathogen attack is called the 'hypersensitive response'. It is characterized by rapid and localized cell death that eventually appears as visible lesions. This response pattern is accompanied by a second and substantial production of ROS (Phase II, described in Section 1.10, p18). In contrast, if the cell is unable to mount an effective defense, the response pattern allows the development of a pathogen-induced disease state, an outcome which is typically associated with induction of only the phase I ROS

burst (Lamb et al., 1997). The ROS produced in the HR have been postulated to contribute to three major defense features: hypersensitive cell death (Hahlbrock et al., 1995; Tenhaken et al., 1995; Bolwell 1996), cell wall strengthening (Baker and Orlandi, 1995; Bradley et al., 1992), and the activation of transcription-dependent responses against pathogens (Levine et al., 1994; Brisson et al., 1994; Lamb et al., 1997; Hahlbrock et al., 1995).

The significance of ROS production during HR has been emphasized by the recent finding that H_2O_2 functions as a second messenger in establishment of systemic acquired resistance (SAR) in plants (Chen et al., 1995; Alvarez et al., 1998; Chamnongpol et al., 1998). SAR is a process activated by local pathogen infection and characterized by an enhanced resistance throughout the plant against secondary infection from a range of pathogens (Sticher et al., 1997).

Salicylic acid (SA) levels rise in both challenged and non-challenged tissue upon pathogen infection, and considerable evidence suggests that SA accumulation is an integral component of the SAR signalling process, although it is not required for all cases of SAR (Camp et al., 1998). Much of the experimental evidence for this role of SA has been derived from studies with transgenic plants expressing a bacterial SA-dehydrogenase gene (*NahG*). The constitutive expression in the plant of this nahG gene product suppresses SA accumulation, and blocks the establishment of SAR (Vernooij et al., 1994).

A number of abiotic and biotic stressors, which also induce ROS accumulation, can induce the biosynthesis of SA (Yalpani et al., 1994; Sharma et al., 1996; Draper et al., 1997; Mur et al., 1997). Fumigation of tobacco seedlings with 200 ppb ozone for

one day induced a 66-fold accumulation of SA Yalpani et al., (1994). Kawano et al. (1998) showed that tobacco suspension cultured cells treated with SA accumulated $^{\bullet}O_2^-$.

The role of H_2O_2 in SAR was investigated in a system involving an incompatible interaction between *Pseudomonas syringae* and *Arabidopsis* (Lamb et al., 1998). This work histochemically demonstrated the production of ROS at both the initial infection site and in distal leaves. The systemic accumulation of ROS did not follow a uniform pattern, but was distributed in discrete tissue foci (micro-HRs) consisting of a single to a few cells, mostly adjacent to vascular bundles. The application of diphenyleneiodonium (DPI), an inhibitor of NADPH oxidase and the oxidative burst, stopped the formation of these local lesions, and also blocked the induction of SAR. This is strong evidence for the importance of the oxidative burst produced during HR as the first step in lesion formation and establishment of SAR in distal leaves.

1.13 Additional signalling species

Jasmonic acid (JA) is a 12-carbon fatty acid derivative, which is synthesized via the octadecanoid pathway from the 18-carbon substrate, linoleic acid. There is substantial evidence that JA plays an important role in determining plant stress response outcomes (Penninckx et al., 1996). Elevated levels of jasmonates have been detected in wounded tobacco leaves within thirty minutes (Baldwin et al., 1994). JA derivatives also accumulate as a result of plant-pathogen interactions (Gundlach et al., 1992; Blechert et al., 1995) and in ozone-treated *Arabidopsis* and hybrid poplar plants (Koch et al., 2000; Rao et al., 2000), but not in tobacco (Ellis, unpublished data).

Blechert et al., (1995) were the first to show that the use of a protein kinase inhibitor could eliminate the stress-induced accumulation of JA, thus linking JA to kinase signalling cascades. Elevated levels of JA have also been linked to the direct activation of specific stress-related genes, including Pal, proteinase inhibitors I and II (Pin), LOX, and polyphenol oxidase (PPO) (Farmer and Ryan, 1990; Gundlach et al., 1992; Bell and Mullet, 1993; Melan et al., 1993; Sembdner and Pathier, 1993; Constabel *et al.*, 1995). Genes encoding proteins important in photosynthesis and carbon assimilation, such as ribulose bisphosphate carboxylase / oxygenase small-subunit (RbcS), are down-regulated in the presence of elevated JA (Reinbothe et al., 1994).

In addition to ROS, JA, and SA, the gaseous plant hormone ethylene has been shown to act as a signalling component in wounding and defense responses (reviewed in Ecker, 1995; Morgan & Drew, 1997). The biosynthesis of ethylene is induced by many stresses including pathogen infection (Boller 1991; Enyedi et al., 1992; Hammond-Kosack & Jones, 1996), wounding (O'Donnel et al., 1996) and UVB irradiation (Predieri ey al., 1995). Transcription of a number of defense-related genes, including some basic PR genes, is induced upon exogenous application of ethylene (Brederode et al., 1991; Potter et al., 1993).

1.14 Signal transduction in metazoans

The mechanisms through which cells respond to environmental stresses such as pathogen challenge, tissue trauma, temperature extremes, or air pollutants are complex. Signals generated extracellularly, at the cell surface, or intracellularly are thought to be transmitted through highly regulated amplification pathways, and lead to

changes in both gene expression and the phenotypic character of the organism (Abe et al., 1998). If the stress is too severe, and the cellular damage is too great for repair, the cell dies. This trauma-induced cell death differs from the programmed cell death which cells may undergo as part of a developmental program, or a cooperative process for containment of a pathogen.

A common mechanism by which metazoan organisms achieve cellular signal amplification is reversible phosphorylation of regulatory proteins in a hierarchical cascade that links the receptor of the initial signal to an ultimate response. There are two main classes of transmembrane cell-surface receptors that enable the cell to respond to exogenous signals: G protein-linked receptors and the enzyme-linked receptors. The G protein-linked receptors act indirectly to regulate the activity of one or more separate plasma membrane-bound target proteins. In mammalian genomes, genes encoding this type of receptor; occur as a family of over 1000 distinct members, whose predicted gene products exhibit a major common structural motif consisting of seven membrane-spanning regions.

Enzyme-linked receptors either act directly as enzymes or are able to modify the activity of associated enzymes. Most enzyme-linked receptors are single-pass transmembrane proteins, with their ligand-binding domain outside the cell and an intracellular catalytic domain. Although these receptors form a heterogeneous group, the great majority appear to be protein kinases that phosphorylate specific sets of target proteins in the cell (Gutkind 1998; Blumwald et al., 1998).

1.15 Mitogen-activated protein kinases (MAPKs)

There are several different protein kinase-based signal amplification cascades known in eukaryotic organisms but the best characterized are those formed by the mitogen-activated protein kinases (MAPKs). The MAPK family (Boulton et al., 1991) represents a subgroup of one of the largest protein superfamilies, the eukaryotic protein kinase superfamily. Within this superfamily, MAPKs belong to the C-M-G-C group that is comprised of four sub-groups: (1) cyclin-dependent kinases; (2) MAPKs; (3) glycogen synthase kinase; and (4) cell division cycle-dependent (cdc)-like kinases (Hanks and Hunter, 1995).

The basic phosphorelay of eukaryotic MAPK pathways consists of a three-component module that appears to be conserved in plants, yeast, *Drosophila*, and humans. Several examples of the mammalian MAPK family include: 1) the extracellular-signal regulated kinases (ERKs), which are best known for their involvement in growth-factor dependent cell proliferation, 2) the c-jun NH_2-terminal kinases / stress-activated protein kinases (JNKs / SAPKs), which are involved in stress signalling pathways, and 3) p38, the mammalian homologue of the yeast stress MAPK, HOG1. In mammals, p38 is involved in controlling responses to an array of environmental stresses like osmotic shock and UV- irradiation, while in yeast the HOG1 is involved in responding to osmotic stress.

Within the mammalian MAPK family, the extracellular signal-regulated kinase (ERK) pathway (Raf $\rightarrow$MEK 1&2 $\rightarrow$ ERK 1&2) is the most completely characterized signal transduction cascade (Hirt et al., 1997). Activation of the ERK pathway in mammalian cells is usually initiated by the binding of a growth factor to a receptor-

tyrosine kinase, located at the plasma membrane. A series of phosphorylation events leads to the phosphorylation of c-Raf (as an example), a serine / threonine protein kinase (MAPKKK) located upstream of the ERKs. C-Raf is activated by this phosphorylation and, in turn, phosphorylates, and activates, the downstream protein kinase, MAPK/ERK kinase (MEK). MEK1&2 are dual-specificity protein kinases that directly activate ERK 1&2 by phosphorylating them at both threonine and tyrosine residues within a –T-E-Y- motif. Once ERKs are phosphorylated, they can be translocated to the nucleus where they phosphorylate a variety of transcription factors including ELK1, Ets1, Sap1a, c-Myc, Tal, and signal transducer and activator of transcription (STAT) proteins. Alternatively, or simultaneously, they may also phosphorylate target proteins directly within the cytoplasm, including EGF receptor, the Ras exchange factor Son-of-sevenless (SOS), Raf1, and MEK1. The phosphorylation of each of these proteins is thought to reduce their catalytic activity, which would create a negative feedback mechanism for controlling the activity of the upstream activators of the ERK1&2 cascade (Li and Spector, 1997; Abe et al., 1998).

MAPKs are proline-directed serine / threonine kinases which means that they phosphorylate polypeptide substrates that possess a proline residue immediately C-terminal (+ 1 site) within the substrate recognition consensus motif: ΨX [S T] P (Ψ - represents P or an aliphatic amino acid) (Clark-Lewis et al., 1991)

1.16 Plant signal transduction

Like other eukaryotic organisms, plants have developed cellular communication systems to ensure appropriate responses to the wide array of exogenous and endogenous stresses to which they are exposed (e.g. chilling, Prasad et al., 1994;

wounding, Olson and Varner, 1993; UV-irradiation, Green and Fluhr, 1995; and pathogen invasion, Legendre et al., 1993). Integral to these cellular communication systems are plant MAPK cascades. MAPK activation in plants has been connected to various treatments including touch, ROS, high salinity, drought, hyper- and hypo-osmolarity, pathogen infection, wounding and low temperature (Tena et al., 2001, and Morris, 2001; Ichimura et al., 2002).

In 1989, the first higher plant protein kinase cDNA sequences were published by Lawton et al., (1989). Since then, numerous genes encoding MAPKKK, MAPKK, and MAPK homologues have been identified from plants such as *Arabidopsis* (Mizoguchi et al., 1993; Nishihama et al., 1995), tobacco (Wilson et al., 1993; Shibatas et al., 1995; Banno et al., 1993; Seo et al., 1995; Zhang and Klessig, 1997), parsley (Ligterink et al., 1997), rice (Agrawal et al., 2003) and alfalfa (Jonak et al., 1996).

The biochemical characteristics of plant MAPKs, MAPKKs and MAPKKKs are very similar to those of yeast and mammals, but the number of plant MAPK cascade members is much higher than is found in either yeast (4 MAPKKKs, 4 MAPKKs and 6 MAPKs) or humans (14 MAPKKKs, 7 MAPKKs and 12 MAPKs). This indicates that MAPK signal modules could potentially have a broader array of roles in plants (Mizoguchi et al., 1997).

With the completion of the *Arabidopsis* genome sequencing project, the full array of protein kinases encoded in a plant genome could finally be identified. One thousand and seventy two genes encoding putative serine / threonine-specific and dual-specificity protein kinases have been revealed. These include genes for at least 20 MAPKs, 10 MAPKKs, 21 MEKK-like MAPKKKs, 48 RAF-related MAPKKKs, and 11

ZR1-interacting kinases (Z1K) (Ichimura et al., 2002; Jonak et al., 2002). A more detailed description of the *Arabidopsis* MAPK signalling components, including kinase class, named members, and signature motif, is presented in **table 1.1**. (Adapted from, Jonak et al., 2002). Based on this knowledge, a systematic nomenclature for the plant MAPKs, MAPKKs, and MAPKKKs has been proposed, to help bring some order to what has been up to now a complicated and somewhat random system of naming plant kinases (Ichimura et al., 2002). In this nomenclature, MAPKs and MAPKKs are renamed as MPKs and MKKs. In *Arabidopsis*, the 20 genes identified as possible MPKs could be further divided into four groups (A-D), based on sequence alignments. Plant MPKs occur as two types, those containing the TEY activation motif and those containing TDY. The TEY subtype makes up groups A, B and C while the TDY subtype compose group D.

The *Arabidopsis* genome also encodes at least 10 possible MKKs. The plant MKKs differ somewhat from their mammalian counterparts in their MKK phosphorylation motifs. Plants have an S/TxxxxxS/T in this motif while mammals have the sequence S/TxxxS/T in theirs. The plant MKKs can be sub-divided into four groups (A-D) based on their amino acid sequence similarities.

Compared with the relatively homogeneous MKKs and MPKs, plant MAPKKKs are both more numerous and more diverse in their primary structures and domain composition. The *Arabidopsis* MAPKKKs, based on the amino acid sequences of their catalytic domain, can be separated into two main classes, MEKKs and RAF-like, with each class subdivided further into groups and subgroups.

Common name	Number*	Group	Number*	Named members
MAPK	23	A B C D	3 5 4 8	MPK3/6/10 MPK4/5/11/12/13 MPK1/2/7/14 MPK8/9/15/16/17/18/19/20
MAPKK	10	A B C D	3 1 2 4	MKK1/2/3 MKK3 MKK4/5 MKK7/8/9/10
MAPKKK	80	MEKK-like ZIK Raf-like	21 11 48	MKK1, ANP1-3, MAP3Kel ZIK1 EDR1, CTR1
MAPKKKK	10	Ste20/PAK-like	10	

Table 1.1 The sequencing of the *Arabidopsis* genome has revealed the presence of 20 MAPKs, 10 MAPKKs, 80 MAPKKKs, and 10 MAPKKKKs. Key members of each class of kinase are identified via their names (adapted from Jonak et al. 2002).

Plant genomes encode large numbers of receptor-like kinases (RLK), which are structurally related to tyrosine-specific and serine / threonine-specific families of receptor kinases in mammals (Shiu & Bleecker, 2001; Cook et al., 2002). The *Arabidopsis* genome for example, encodes for 417 RLKs. The older term, RLK, is slowly being replaced by the term, plant receptor kinase (PRK). PRKs, like their mammalian homologs, consist of an extracellular domain, a single transmembrane domain and a cytosolic kinase domain (Shiu & Bleecker, 2001). The PRK structures are similar to those of the receptor tyrosine kinase (RTKs) and receptor serine / threonine kinases (RSKs) of the TGFβR (transforming growth factor β receptor) family

in metazoans (Shiu & Bleecker, 2001; Cook et al., 2002). In plants, there exist more than 20 structurally distinct extracellular domains making up the PRK superfamily, including epidermal growth factor (EGF) repeats, lectin domains, leucine-rich repeats (LRR), and S-domain, which are homologous to the self-incompatibility-locus glycoproteins found in *Brassica oleracea* (Nasrallah et al., 1988; Tori & Clark, 2000; Shiu & Bleecker, 2001).

1.17 Oxidative stress and plant MAPKs

There are numerous publications demonstrating the ability of ROS to induce the activation of MAPKs in plants. Desikan et al. (1999) was first to publish that treatment of *Arabidopsis* suspension-cultured cells with hydrogen peroxide, could induce the activation of a MAPK. Kovtun et al. (2000), through transient expression studies in protoplasts, provided evidence for activation of AtMPK6 (MPK6) and AtMPK3 (MPK3) by hydrogen peroxide, while Kumar and Klessig (2000) demonstrated that SIPK could be activated in tobacco suspension-cultured cells exposed to NO. H_2O_2 has been shown to induce the activation of the *Arabidopsis* MAPKKK, ANP1 (Kovtun et al., 1999). This H_2O_2-induced activation of ANP1, leads to the eventual activation of two downstream MAPKs (MPK6 and MPK3) the orthologues, of the tobacco MAPKS, SIPK and WIPK, respectively. The use of a constitutively active ANP was able to mimic this H_2O_2 effect, inducing expressing of a reporter gene under the control of the GST6 promoter. The GST6 gene is an oxidant stress-response gene.

In tobacco, the MAPKK, NtMEK2, is the upstream activator of SIPK and WIPK. While in alfalfa, the salt stress-induced MAPKK, SIMKK, (the alfalfa ortholoue of NtMEK2) interacts with and phosphorylates SIMK, the alfalfa ortholoue of SIPK.

1.18 Heterotrimeric G proteins in plants

The mammalian genome encodes over twenty Gα, five Gβ, and twelve Gγ isoforms, accompanied by at least 1000 different G protein-coupled receptors (GPCR). This versatile transducer module controls an enormous array of cellular functions, including cell division, pathogen defense, stress tolerance (including oxidant stress), and apoptosis (Karnik et al., 2003; Spiegel et al., 2004; Marinissen and Gutking, 2001). The binding of an extracellular ligand to a GPCR induces conformational changes which lead to dissociation of the trimeric complex by the C-terminal section of the GPCR. This process is accompanied by the exchange of GTP for GDP on the Gα-subunit, and separation of the Gα-subunit from the βγ-dimer. The GTP bound to the Gα-subunit is ultimately hydrolyzed by the intrinsic GTPase activity of the Gα-subunit followed by eventual reforming of the heterotrimeric complex.

In contrast to animals, plants seem to go through life with a very limited array of heterotrimeric G proteins. Nevertheless, Gα, Gβ, and Gγ homologues have been identified in *Arabidopsis* and other plant species (Ishikawa et al., 1995; Goto et al., 1996; Lee and Assmann, 1999; Saalbach et al., 1999; Ando et al., 2000; Perroud et al., 2000; Mason and Botella, 2001). In *Arabidopsis*, there appears to be a single prototypical Gα (*Arabidopsis* G PROTEIN, ALPHA SUBUNIT1 (GPA1)) and one proteotypical Gβ (*Arabidopsis* G PROTEIN, BETA SUBUNIT1 (AGB1)) subunits and

potentially, two Gγ subunits (*Arabidopsis* G PROTEIN, GAMMA SUBUNIT1 (AGG1 and AGG2)), are found. Interaction has been detected between the *Arabidopsis* Gγ and Gβ subunits (Mason and Botella, 2000), but there is no conclusive evidence for a functional heterotrimer of α-, β-, and γ-subunits in plants, or for a plant trimer dissociating into an α-subunit and a βγ-dimer as seen in mammals (reviewed in Fujisawa et al., 2001). Despite the abundance of putative receptor kinases in plants, as revealed by recent genome sequencing efforts, there is no convincing evidence for canonical GPCRs in this phylum.

However, through a combination of mutant analysis and pharmacology, plant heterotrimeric G protein subunits have been implicated in numerous physiological processes and phenotypic changes including auxin and gibberellin signalling, K^+ channel regulation, Ca^{2+} regulation, cell division, stomatal function, and secondary metabolite biosynthesis (Aharon et al., 1998; Jones et al., 1998; Mahady et al., 1998; Saalbach et al., 1999; Ullah et al., 2001; Wang et al., 2001).

1.19 Problem statements and thesis objectives

Over the millennia, plants have had to adapt to a vast array of potentially adverse environmental stresses including UV, ozone, pathogens, drought, and changes in temperature, and salinity. A common aspect of these environmental stresses is the enhanced production of ROS within the plant cell (Foyer and Mullineaux, 1994; Lamb and Dixon, 1997; Kovtun et al., 2000; Asai et al., 2002).

The mechanisms through which plant cells respond to these different environmental stresses are complex. Signals generated extracellularly, at the cell surface or intracellularly can be transmitted through highly regulated signalling

pathways leading to changes in both gene expression and phenotypic character of the plant. The study of signal transduction in plants in recent years has revealed that a number of different environmental stresses can elicit the same physiological response in plants. The fact that stresses other than ozone and UVR also initiate ROS accumulation, and that ozone and UVR share overlapping patterns of defense-related gene expression with other stresses, such as pathogens, points to the possibility that these stimuli share all or part of the subsequent signal transduction cascades. Eckey-Kaltenbach et al. (1994) have stated that ozone can function as a *cross-inducer*, a phenomenon in which the plant's response to ozone challenge mimics the plant responses to any stress that generates an oxidative burst (Sandermann et al., 1998; Rao and Davis, 2000). Under these criteria, UVR could also be considered a *cross-inducer*, since it induces an array of defence-related genes similar to that induced by ozone and by various pathogens.

Even though there are a number studies describing the responses, both biochemical and physiological, to oxidant stress in plants, there remain many aspects that need further study. First, we know very little about the immediate-early events involved in ozone- and UVR-induced signalling in plants. Second, the pathways(s) used by this oxidant-induced signal to induce a protective response in the challenged plant needs to be defined. Since this is likely to be a multi-layered response, it would be of interest to establish which components of the signalling pathway(s) are most important in attenuating oxidative damage in the challenged tissue.

In more specific terms, I set out to discover what role(s) in oxidant signalling might be played by MAPKs, and to identify the 'early response' proteins whose expression

levels are modified as a result of oxidant-induced signalling. Elucidation of these patterns should help us to better understand the signalling events both upstream and downstream of this MAPK activation that eventually lead to homeostatic recovery or cell death. I started my reseach with the following hypotheses: (1) that oxidants such as ozone, UVC, and hydrogen peroxide can activate plant MAPKs and (2) that these MAPKs are integral in the plant's ROS-related homeostasis.

Research Objectives

I. Establish whether oxidants such as ozone, UVC and hydrogen peroxide can activate MAPK signalling in plant cells.

II If so, carry out a pharmacological analysis of the signalling process linking oxidant stress to MAPK activation.

III. Investigate a role for heterotrimeric G proteins in oxidant signalling.

IV. Generate transgenic *Arabidopsis* plants in which expression of candidate, oxidant-induced MAPKK and MAPK genes have been suppressed via RNAi.

V. Evaluate biochemical and physiological responses of these transgenic genotypes to ozone exposure.

VI. Identify oxidant-induced changes in protein expression levels controlled by MAPK signalling by using isotope-coded affinity tag (ICAT) technology, and transgenic *Arabidopsis* genotypes.

Chapter 2

Ozone treatment rapidly activates MAP kinase in plants

2.1 Introduction

Ozone is a ubiquitous component of the terrestrial atmosphere. In the stratosphere, ozone provides a crucial barrier to incoming UV radiation, but within the troposphere it is a destructive gaseous pollutant that is estimated to cause more damage than all other atmospheric pollutants combined (Chameides et al., 1994; Heagle, 1989). Damage symptoms in plants depend on the ozone concentration, length of exposure, tissue age and genetic susceptibility of the plant, but they range from inhibition of photosynthesis and associated yield loss, to premature senescence and visible tissue necrosis (Darrall 1989; Hewitt et al., 1990; Krupa and Manning, 1989). Ozone enters the plant mesophyll via the stomata and diffuses through inner air spaces to reach the cell wall and plasmalemma (Sharma et al., 1997). There it is immediately converted to reactive oxygen species (ROS) such as $^{\bullet}O_2^-$, $HO^{\bullet}$, and H_2O_2 either by contact with water, plasmalemma or other cellular components (Pellinen et al., 1999). The reactivity of $\cdot O_2^-$ is limited but its pro-oxidant feature lies in its ability to be transformed into other reactive oxygen intermediates such as hydroperoxide radical ($HO_2^{\bullet}$) and H_2O_2 (Feher et al., 1987; Cadenas, 1995).

ROS are also an unavoidable product of the interaction of molecular oxygen with normal metabolic processes in plants, including the intense electron fluxes associated with both mitochondrial respiration and photosynthesis, and the activity of flavin-based oxidoreductases. Plant cells therefore have a continuing requirement to scavenge oxidizing species and their metabolic products, a basal demand that is met through constitutive accumulation of antioxidant metabolites (e.g. ascorbate, tocopherols, flavonoids, glutathione) and enzymic scavengers of ROS (e.g. ascorbate peroxidase, catalase, superoxide dismutase).

These constitutive scavenging mechanisms are also inducible. Various stresses, including wounding, chilling, ozone exposure, or pathogen attack, trigger a rapid release of ROS (oxidative burst) within the affected cells (Legendre et al., 1993; Prasad et al., 1994) and concomitantly elicit marked increases in the activities of scavenging enzymes as well as enhanced transcription of the corresponding genes (O'Kane et al., 1996; Conklin and Last, 1995; for review see Lamb and Dixon, 1997; Orvar et al., 1997).

Specific ROS such as superoxide anion radical have been proposed to act as early "second messengers" in the signal transduction pathway(s) that lie downstream of the initial event, but the mechanism by which oxidative stress is detected in plants, and the nature of the signal transduction pathway that enables appropriate transcriptional and metabolic responses, remains unknown.

Eukaryotic organisms possess a number of proteins whose function is sensitive to the cell's redox status, including known signal transduction components such as NFκB (Milligan et al., 1998), PKC (Taher et al., 1993), $p21^{ras}$ (Lander et al., 1995),

MAPK (Guyton et al., 1996), and phosphoprotein phosphatase (Caselli et al., 1998). In plants, rapid activation of MAPKs can be induced by wounding (Usami et al., 1995; Seo et al., 1995; 1999), cold (Jonak et al., 1996), virus infection (Zhang and Klessig, 1998), treatment with microbial elicitors (Suzuki and Sinshi, 1995; Adam et al., 1997), and by *R/Avr* recognition between host and pathogen (Romeis et al., 1999), all processes associated with induction of ROS accumulation. The apparent commonality of ROS generation as an immediate consequence of a wide range of cellular traumas, that also rapidly activate MAPKs, points to the possibility that ROS themselves may be responsible for triggering through MAPK cascades. Since challenge with ozone immediately creates ROS in plant tissues (Pellinen et al., 1999), this model predicts that exposure to ozone should also lead to rapid MAPK activation.

In the present study, exposure to ozone was found to induce activation of an ERK-type MAP kinase within minutes in tobacco, *Arabidopsis*, and poplar plants, and in tobacco and poplar suspension-cultured cells. This activation process is calcium-dependent, and can be blocked by free radical traps as well as by a specific inhibitor of MEK. The activated kinase in tobacco was determined to be the salicylate-induced protein kinase (SIPK) described from tobacco.

2.2 Materials and Methods

2.2.1 Whole plant and suspension-culture growth conditions

Tobacco (*Nicotiana tabacum*) genotype Xanthi nc (courtesy of Dr. John Ryals, Agricultural Biotechnology Research Unit, CIBA-GEIGY Corp.), plants were started from seeds, and grown in sterilized soil (50% Metro Mix 290, 50% soil with 3.5 kg m^{-3} Osmocote 14-14-14 controlled release fertilizer (Grace Sierra)), in controlled environmental growth chambers with 25/20°C (day/night) under 16 h photoperiod and RH 60% +/- 5%. Plants were watered weekly with tap water.

Hybrid poplar plants, *Populus tremula* X *P. alba*, 'INRA 717 1B4' (Leple et al., 1992), were maintained *in vitro* in Magenta boxes containing propagation medium [MS salts, MES buffer, myo-inositol, L-glutamine, vitamins, sucrose, and Phytagel; pH 5.8]. These plants were incubated at 25°C under a 16 hour photoperiod of cool-white fluorescent light (25 – 32 μmole/sec/m^2). Plants were sub-cultured every fourth week by aseptically transferring shoot apices to fresh medium.

Arabidopsis thaliana (ecotype Columbia) plants were grown in soil, in greenhouse conditions or in controlled environmental growth chambers with 25/20°C (day/night) under 16hr photoperiod and RH 60% +/- 5%. Plants were watered weekly with tap water.

Tobacco (Xanthi nc.) cell suspension cultures were established by placing approximately 0.5 g callus into 25 ml suspension culture medium containing 1X MS supplemented with 1 mg/l 2, 4-D and 0.1 mg/l of kinetin, and cultured in the dark (125 rpm on a gyratory shaker). Established cultures were sub-cultured at weekly intervals by placing 10 ml of one-week-old suspension culture into 40 ml of fresh medium.

Poplar suspension cultures (*Populus trichocarpa* X *deltoides* clone H11) obtained from Dr. M. Gordon (U. Washington), were maintained using the same

growth medium (with no 2, 4-D or kinetin) and growth conditions as tobacco. Transgenic *Arabidopsis* seedlings were started from seeds and maintained on 1/2 strength MS salts (pH 5.7) and 1% sucrose for two weeks.

2.2.2 Surface sterilization of plant tissue

Surface sterilization of *Arabidopsis* and tobacco seeds was carried out as follows. Seeds were placed into clean Eppendorf tubes containing 1 ml 70% ethanol for 1 minute with occasional swirling, followed by centrifugation of the tube for 5 seconds at 1000 rpm. In a flow hood, the ethanol was poured off and replaced with 1 ml 20% v/v mixture of bleach (from the bottle) (Clorox) and 0.05% Tween-20, and placed on a rotator for 15 minutes. After brief centrifugation, the seeds were washed five times with sterile water.

Leaves from mature tobacco plants were harvested, rinsed with water to remove any debris, placed in a large beaker containing 15% bleach (500 mls) with a few drops of Tween-20 and swirled gently for 20 minutes. Using aseptic technique, the leaf tissue was transferred to a sterile beaker and washed five times with sterile water.

2.2.3 Callus induction

In a flow hood under sterile conditions, small rectangular sections, 15mm (L) by 5mm (W), were cut from previously sterilized leaves, using a scalpel. These sections

were cut perpendicular to the main vein of each leaf, and placed onto callus induction medium, with the rib of the vein pushed gently into the agar. The callus induction plates (MS (1X) / 0.8% tissue culture Agar, B5 vitamins, 30 g/L sucrose, 0.1 mg/L kinetin (6-furfurylaminopurine), 1 mg/L 2,4-D (2,4-dichlorophenoxyacetic acid), at a pH of 5.7), with the leaf sections, were then placed in a dark location at room temperature. In approximately 4 weeks, the newly developing callus was sub-cultured by transferring 0.1 to 0.2 g (fresh weight) onto fresh callus induction medium.

2.2.4 Ozone fumigation of whole plants

Plants were grown for six weeks (tobacco), four weeks (poplar), or two weeks (*Arabidopsis*), followed by exposure to ozone (200 or 500 ppb) and harvesting at the pre-determined time points after ozone exposure started. Ozone was generated with a Delzone ZO-300 ozone generating sterilizer (DEL industries) and monitored with a Dasibi 1003-AH ozone analyzer (Dasibi Environmental Corp.). After exposure for different times, the third, fourth and fifth leaves, counting from the top, were harvested for both tobacco and poplar, and the rosette leaves were harvested from *Arabidopsis*. These were immediately frozen in liquid nitrogen and stored at -80° C to await analysis. Exposure levels within the ozone gassing chamber varied no more than +/- 10% over the course of the treatment.

2.2.5 Ozone fumigation of suspension-cultured cells

One-week-old tobacco (Xanthi nc) or poplar (*Populus trichocarpa* X *deltoides* clone H11) cell suspension cultures were uniformly distributed on a layer of Whatman 541 filter paper in Petri plates drilled with multiple holes to allow the medium to flow through. The resulting thin cell layer was then exposed to ozone (200- or 500 ppb) for a selected period of time in a flow-through chamber (3 L/min). Control plates were exposed to ambient air in a similar chamber. After exposure, the cells were immediately harvested by vacuum filtration, frozen in liquid nitrogen and stored at -80° C to await analysis. All experiments were repeated in triplicate, and representative data are shown in the figures.

2.2.6 Protein extraction and immunoblotting

The frozen tissue was ground in liquid nitrogen and the powder stirred with two volumes of extraction buffer (50 mM Hepes pH 7.5, 5 mM EDTA, 5 mM EGTA, 10 mM DTT, 1 mM sodium orthovanadate, 10 mM sodium fluoride, 1 mM PMSF, 2 μg/ml antipain, 2 μg/ml leupeptin, 10 μg/ml aprotinin, 5 μg/ml pepstatin, 10% glycerol, 7.5% polyvinylpolypyrrolidone) and kept on a reciprocating shaker (100 oscillations/minute) for 10 minutes, at 4°C , followed by centrifugation at 15,500 g for 30 minutes. The supernatant was assayed directly or flash-frozen and stored at -80° C. The protein content was quantified using the Bradford dye-binding assay.

Extracted proteins (80 μg total protein from leaves or 30 μg from suspension-cultured cells) or immuno-precipitated proteins were fractionated by 10% sodium dodecyl sulphate (SDS) - polyacrylamide gel electrophoresis (PAGE), and transferred onto polyvinylidenedifluoride (PVDF) membranes (Millipore). Polyclonal

phosphospecific MAPK (anti-pERK, p44/42) antibody (New England Biolabs) or polyclonal p44/42 MAPK-specific antibody (anti-ERK) (Santa Cruz Biotechnology) raised against a peptide which corresponds to amino acids 305-327 of ERK-1 (p44 MAP kinase of rat origin), were used as the primary antibodies. Peroxidase-conjugated goat anti-rabbit IgG (Dako) was used as the secondary antibody. MAPKs were visualized using an enhanced chemiluminescence (ECL) protocol according to the manufacturer's directions (Amersham).

2.2.7 In-gel kinase assay

Six-week-old tobacco or two-week-old *Arabidopsis* plants were exposed to ozone and extracted crude proteins (80 μg) from these samples were fractionated in a 10% SDS-PAGE gel co-polymerized with 100 μg/mL myelin basic protein (MBP). After electrophoresis, SDS was removed by washing the gel with washing buffer (25 mM Tris, pH 7.5, 0.5 mM DTT, 0.1 mM Na_3VO_4, 5 mM NaF, 0.5 mg/mL BSA, and 0.1% Triton X-100 [v/v]) three times for 30 min each at room temperature. The kinases were allowed to renature in 25 mM Tris, pH 7.5, 1 mM DTT, 0.1 mM Na_3VO_4, and 5 mM NaF at 4°C overnight with three changes of buffer. The gel was then incubated at room temperature in 30 ml reaction buffer (25 mM Tris, pH 7.5, 2 mM EGTA, 12 mM $MgCl_2$, 1 mM DTT, and 0.1 mM Na_3VO_4) with 200 nM ATP plus 50 μCi γ-^{32}P-ATP (3000 Ci/mmol) for 60 min. The reaction was stopped by placing the gel in 5% (w/v) trichloroacetic acid /1% NaPPi (w/v). The unincorporated γ-^{32}P-ATP was removed by washing in the same solution for at least 6 hr with five changes. The gel was dried

onto Whatman 3MM paper and exposed to Kodak XAR-5 film. Pre-stained size markers (Bio-Rad) were used to estimate the size of the kinases.

2.2.8 Immunoprecipitation and in-gel kinase assays

Extracted protein (40 μg) in 500 μl extraction buffer without PVPP was used for immuno-precipitation with 5 μg anti-SIPK antibodies (Dr. Yuko Ohashi, Tsukuba). After incubation overnight at 4°C, the immune complexes were recovered by incubation with 15μl Protein-A-Sepharose suspension for 2 hours, followed by centrifugation (15,500g) for 1 minute at 4°C. The pellet was washed thrice with extraction buffer without PVPP, and then 16 μl extraction buffer without PVPP and 4 μl 5X loading buffer (0.625 M Tris-HCl pH 6.8, 5% SDS, 40% glycerol, 0.125% bromophenol blue, 40% v/v β-mercaptoethanol) were added and the sample was boiled for 5 minutes. The released proteins were used for an in-gel kinase assay, carried out as described above for extracted total proteins from leaves.

2.2.9 Suspension-culture treatments

Tobacco and poplar suspension-cultured cells (1 week after subculture) were treated with 20 mM hydrogen peroxide for 15 minutes. The cells were then harvested by vacuum filtration, frozen in liquid nitrogen and stored at -80°C until analysis.

To test potential inhibitors, suspension culture cells were pretreated with specific reagents as follows: MEK 1 inhibitor PD98059 (100 μM) (New England Biolabs) for 1 hr, $LaCl_3$ (5 mM) for 15 minutes, N-acetyl cysteine (20 mM) for 45 minutes, or N-(2-mercaptopropionyl) glycine (20mM) for 45 minutes. Unless otherwise noted, all reagents were obtained from Sigma. The inhibitor-treated cells were either plated and exposed to 200- or 500ppb ozone as described above, or treated with 20

mM hydrogen peroxide, before extraction. Following treatment or exposure to either oxidant, cells were harvested by vacuum filtration, frozen in liquid nitrogen and stored at -80°C until needed.

2.3 Results

2.3.1 Ozone quickly induces MAPK in tobacco, *Arabidopsis* and poplar leaves

When proteins were extracted from ozone-treated leaves and tested for the presence of protein phosphorylating activity using an in-gel kinase assay, MBP-phosphorylating activity was detected (**Fig. 2.1**). This activity migrated as a single band in the tobacco sample, with an apparent molecular mass of ~46 kDa; whereas, there were two bands ~ (44- and 46-kDa) noticeable in the *Arabidopsis* sample. An in-gel kinase assay was not performed with poplar proteins. Since the estimated molecular mass and substrate utilization properties of these protein bands are consistent with those of known MAPkinases, anti-ERK 1&2 antibodies were used to probe Western blots of proteins from ozone-exposed leaves. In tobacco leaves, anti-

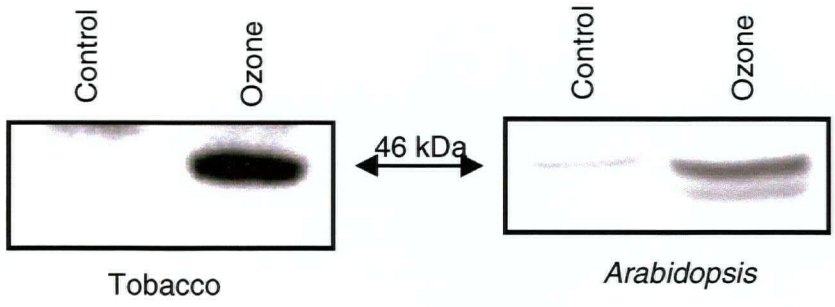

Figure 2.1 MBP phosphorylating activity is induced by ozone exposure. Tobacco and *Arabidopsis* plants were exposed to ozone (500 ppb) for 10 minutes and extracted leaf proteins (30 μg) were fractionated in an SDS-polyacrylamide gel polymerized with MBP as a substrate for MAPK. After denaturation and renaturation of the gel, protein kinase activity on MBP was detected by incubating the gel with γ^{32}P-labelled ATP.

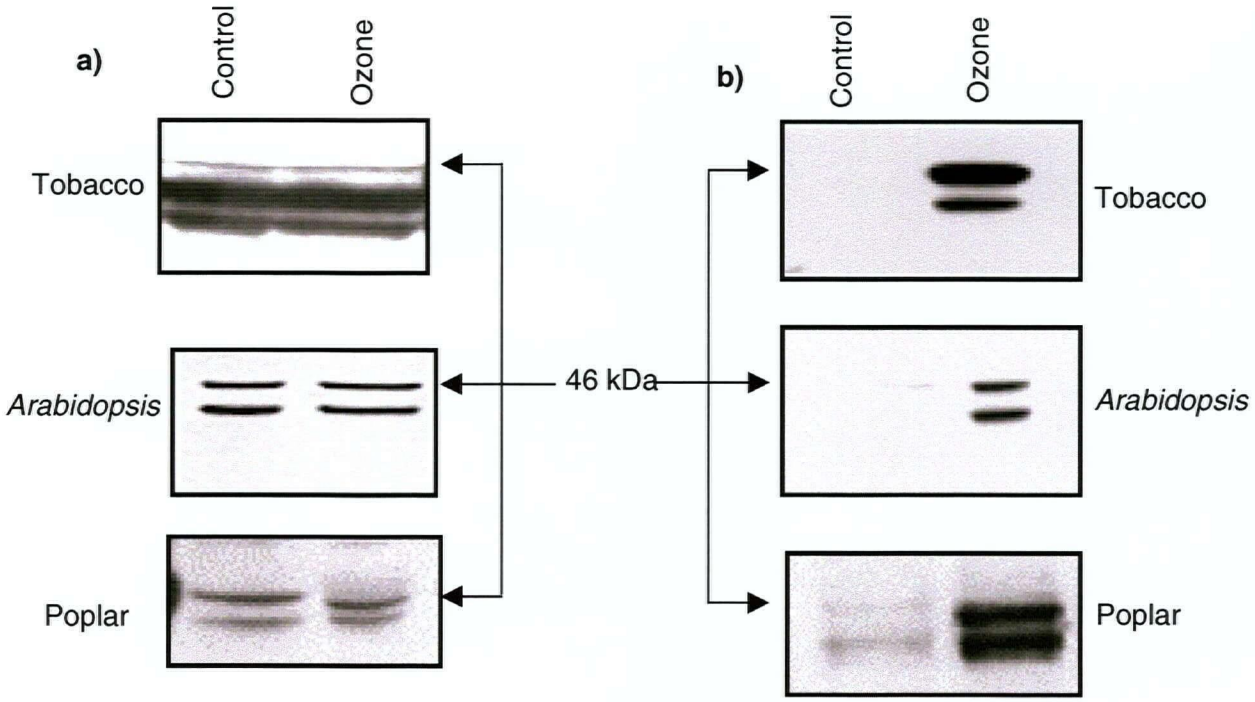

Figure 2.2 An ERK homologue is activated by ozone exposure. Tobacco, poplar and *Arabidopsis* leaves were exposed to ozone (500 ppb) for 10 minutes and proteins were then extracted. After fractionation of total proteins (80 μg) by SDS-PAGE, the blots was probed with either an anti-ERK (**a**) antibody, or with an anti-phosphoERK antibody (**b**) which recognizes only the active forms of ERK1&2.

ERK antibodies recognized a small number of proteins in the size range of 40 - 50 kDa, (Fig. **2.2a, top**) including a discrete 46 kDa band. In protein extracts from *Arabidopsis* and poplar, two distinct bands (44- and 46-kDa) were recognized, respectively (**Fig. 2.2a, middle and bottom**). The intensity of these bands appeared to be unaffected by the 10-minute ozone treatment, but when these samples were probed with anti-pERK antibodies, which recognize only the doubly phosphorylated (-**TXY**-) ERK epitope, two proteins ~ (44- and 46 kDa) were detected in the extracts from ozone-treated tissues, and none in the control treatment (**Fig. 2.2b**).

2.3.2 Ozone activates MAPkinases in suspension-cultured cells

Studying very short-term responses to ozone in whole plants is logistically challenging, and is further complicated by the stomatal diffusion barrier which restricts the amount of sub-epidermal tissue reached by the oxidant within the leaf. Plant tissues cultured *in vitro* have been shown to reflect whole plant metabolism in many cases, including responses to fungal elicitors (Romeis et al., 1999). When suspension-cultured tobacco (**Fig. 2.3a**) and poplar (**Fig. 2.3b**) cells were plated as thin layers, and exposed to ozone (500 ppb) for ten minutes, they too showed the phosphorylation of two protein bands with molecular masses of 44- and 46kDa when assayed by Western blotting analysis using anti-pERK antibodies, or a single band in the in-gel kinase (tobacco) assay (**Fig. 2.3c**). There were no detectable signals in the control cells.

A time-course analysis showed that, after a ten minute exposure to 500 ppb ozone and further culturing in liquid medium, the phosphoproteins remained

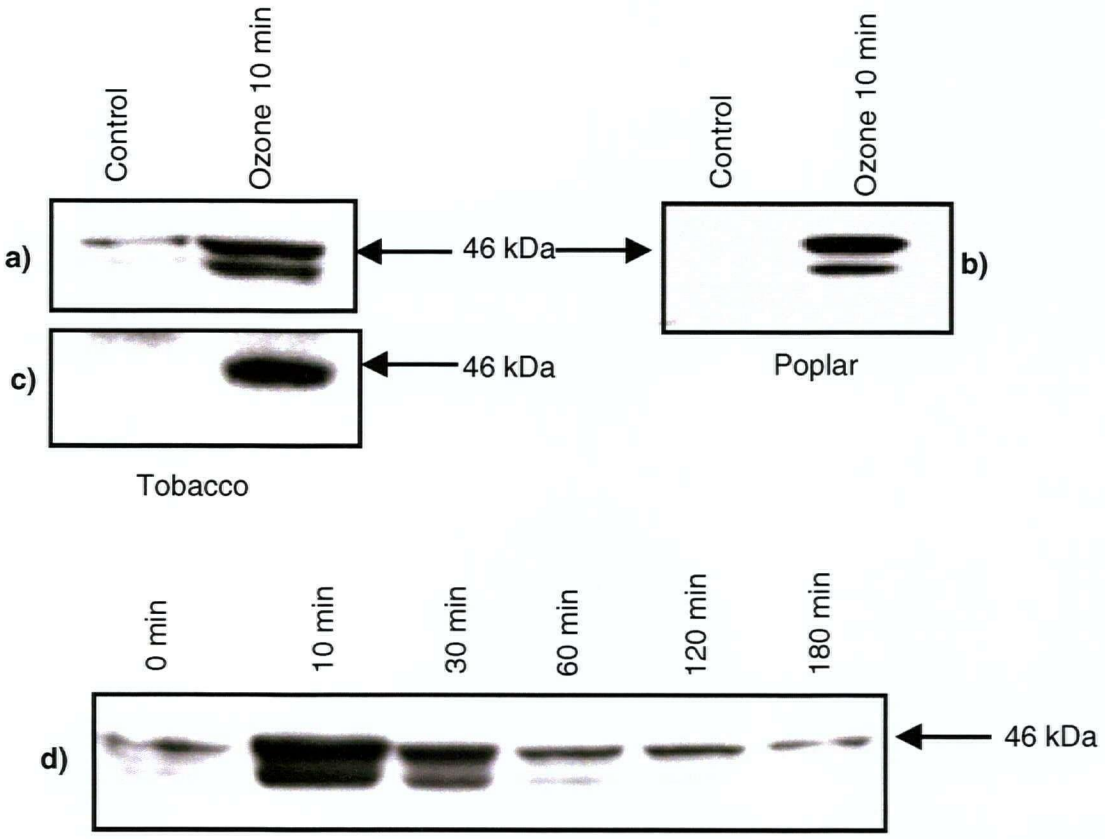

Figure 2.3 MAPK[46] is activated by ozone in both tobacco and poplar suspension-cultured cells. Total proteins (30 μg) from suspension-cultured cells of tobacco and poplar were plated, exposed to ozone (500 ppb) for 10 minutes followed by probing with anti-phospho ERK1&2 (**a, b**), or subjected to an in-gel kinase assay (tobacco) (**c**). Control cells were plated and exposed to ambient air for 10 minutes. (**d**) A time course analysis was performed to determine the activation profile of the ozone-activated tobacco MAPK. Immediately after ozone fumigation the treated cells were cultured in sterile liquid medium for 3 hr, and the proteins were extracted at different time points followed by Western blotting analysis using anti-phospho ERK 1&2 antibodies.

detectably activated in tobacco cells for at least one hour, but had returned to control levels by three hours post-treatment (**Fig. 2.3d**).

A number of MAP kinases have been described from tobacco, including SIPK. To establish whether the ozone-activated kinase(s) were related to SIPK, proteins from control and ozone-treated tissues were immunoprecipitated using anti-SIPK antibodies, and the precipitate analyzed for MBP-phosphorylating activity with the in-gel kinase assay. A 46 kDa protein recovered with anti-SIPK displayed strong kinase activity following 10 minutes of ozone treatment (**Fig. 2.4**). The size and immuno-reactivity of the major ozone-activated protein kinase are thus both consistent with the properties of tobacco SIPK.

2.3.3 Ozone-induced activation of MAPK^{46} in tobacco suspension-cultured cells involves ROS

Pretreatment of tobacco suspension-cultured cells with the radical scavengers *N*-(2-mercaptopropionyl) glycine (MPG) and *N*-acetyl cysteine (NAC) completely interdicted the ozone-induced activation of MAPK^{46}. These data indicated that ozone induced activation of MAPK^{46} is reliant on the production of ROS (**Fig. 2.5, left**).

Ozone reacts very rapidly within aqueous environments to create reactive oxygen species, including hydrogen peroxide. In birch leaves, it has been shown that ozone-induced hydrogen peroxide initially accumulates around the perimeter, within the cytosol immediately adjacent to the plasmalemma (Pellinen et al., 1999). As described in Chapter 1, hydrogen peroxide can eventually produce additional ROS

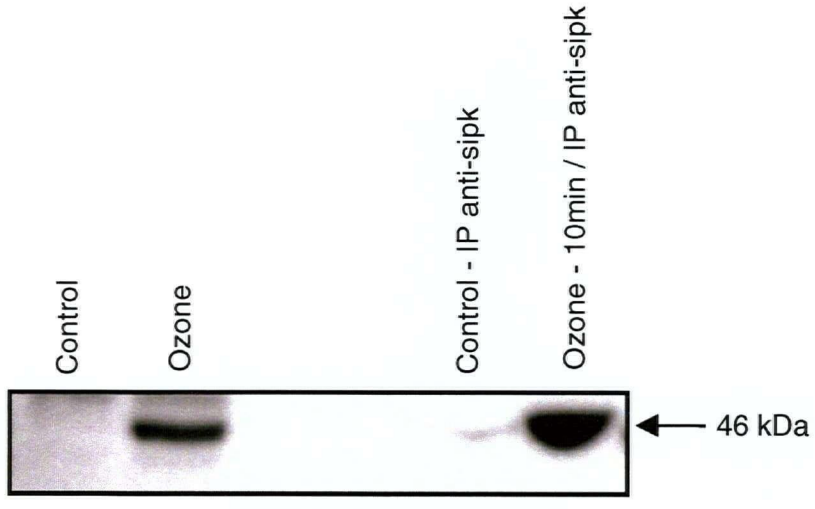

Figure 2.4 MAPK[46] in tobacco cells is related to SIPK. Extracted proteins (40 μg) from ozone-exposed (500 ppb) suspension-cultured cells were incubated with anti-SIPK (5 μg) antibodies. The immunoprecipitated proteins were subjected to an in-gel kinase assay, as described above for extracted total proteins from leaves. Total proteins from ozone-treated cells were used as positive control.

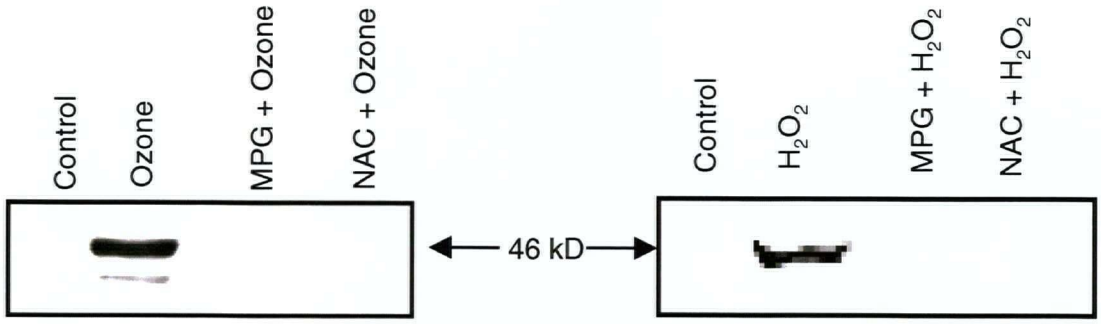

Figure 2.5 Ozone- and H_2O_2-activation of MAPK[46] is abrogated by pretreatment of suspesion-cultured cells with free radical scavengers. Total proteins (20 μg) from suspension-cultured cells from tobacco that had been treated with ozone (500 ppb) 10 minutes or 20 mM hydrogen peroxide for 15 minutes were analyzed by immunoblotting with anti-phospho ERK1&2 antibodies. Alternatively, cells were pretreated with NAC or MPG (20 mM) for 45 minutes, and then were either plated and exposed to ozone (500 ppb) for 10 minutes (**left**) or treated directly with 20 mM hydrogen peroxide for 15 minutes (**right**). Total proteins (20 μg) extracted from the treated cells were analyzed by immunoblotting with anti-phospho ERK1&2 antibodies.

such as •OH. The activation of the $MAPK^{46}$ by ozone could therefore involve one or more of these secondary oxidants, rather than ozone itself.

To determine if hydrogen peroxide has the ability to induce the activation of a MAPK in plants, cultured tobacco cells were treated for ten minutes with exogenous hydrogen peroxide (20 mM), followed by Western blotting analysis using anti-pERK 1&2 antibodies. Responding to this ROS challenge, tobacco suspension-cultured cells showed a rapid activation of the $MAPK^{46}$, directly analogous to the response induced by ozone (**Fig. 2.5, left**). Pretreatment of the cells with the free radical scavengers MPG and NAC completely interdicted the response of the $MAPK^{46}$ to hydrogen peroxide (**Fig. 2.5, right**). Poplar suspension-cultured cells showed similar results to that of tobacco cells (data not shown).

2.3.4 Activation of the $MAPK^{46}$ by ROS involves an upstream MAPKK and Ca^{2+} ions

Within canonical MAPK cascades, MAP kinases are normally activated by MAPK kinases (MAPKK). Mammalian MEK is one of the best characterized of the known MAPKKs, and its potential as a drug therapy target has led to the development of a highly specific MEK inhibitor, PD98059 (Alessi et al., 1995). When tobacco cells were pretreated with 100 μM PD98059 for one hour and then challenged with either ozone or hydrogen peroxide, the activation of the $MAPK^{46}$ in tobacco cells was strongly reduced (**Fig. 2.6**), indicating that the ROS-derived signal must be passing primarily through an upstream MAPKK rather than acting directly upon the MAPK itself. Pretreatment of the cells with lanthanum chloride (La^{3+}), a potent calcium

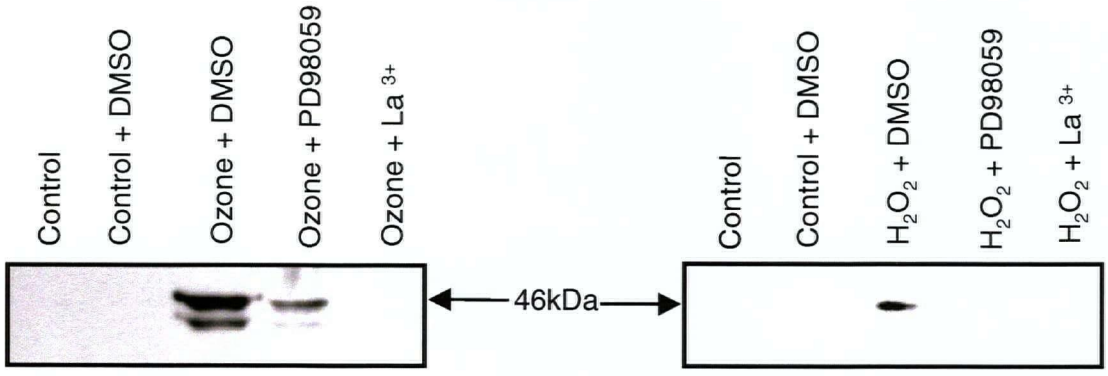

Figure 2.6 Activation of MAPK[46] is dependent on upstream MAPKK and calcium ion influx. Total proteins (20 μg) from suspension-cultured cells of tobacco that had been pre-treated with PD98059 (100 μM) or $LaCl_3$ (5 mM), followed by either plating and exposure to ozone (500 ppb) (**left**), or treatment with 20mM hydrogen peroxide (**right**) for 15 minutes, were analyzed by immunoblotting with anti-phospho ERK1&2 antibodies. Total proteins (20 μg) from poplar suspension-cultured cells that had been pre-treated with PD98059 (100 μM), followed by ozone fumigation (500 ppb) for 10 minutes and then analyzed by immunoblotting with anti-phospho ERK1&2 antibody.

channel blocker, also completely silenced the activation of the $MAPK^{46}$ by ROS (**Fig. 2.6**). In addition, pretreatment of tobacco (*Nicotiana tabacum* L. cv bright yellow 2) (BY-2) cells with the membrane-permeable calcium chelator 1, 2-bis (2-aminophenoxy)-ethane-N, N, N', N', - tetraacetic acid-tetrakis (acetoxy-methyl) ester (BAPTA-AM), resulted in a similar interdiction of the oxidant-induced activation of $MAPK^{46}$ (data not shown).

2.4 Discussion

Plant cells are bathed in a highly oxidizing milieu that arises from a combination of the atmospheric environment and their own metabolic activities. Plant survival therefore depends on possession of an array of effective antioxidant responses, coupled to mechanisms for sensing perturbations of their internal redox balance. Discrete redox sensors have been identified in a number of prokaryotic organisms (Demple, 1996), but the functional homologues of these gene products have not been reported from eukaryotic species. Nevertheless, it is clear that both mammals and plants are capable of detecting and rapidly responding to redox challenges such as hyperbaric oxygen, free radical generators (Ohlsson et al., 1995), nitric oxide (Nathan, 1995; Delladone et al.,1998), hydrogen peroxide (Levine et al., 1994; Abe et al., 1998), superoxide anion (Jabs et al., 1996; Graier et al., 1998) and ozone (Sharma and Davis,1997; Jaspers et al.,1998). In plant systems in particular, it has also been established that many biotic and abiotic stresses induce a rapid transient increase in

cellular ROS ("oxidative burst") as one of the earliest detectable metabolic responses (Lamb and Dixon, 1997).

While it is essential for plants to control the levels of potentially destructive ROS within their cells, it appears that they may also deploy these short-lived diffusible metabolites as direct signal transducers and/or generators of other systemic signal transduction components (Jabs, 1999). In this model, the oxidative burst induced in plant cells by non-oxidant stresses is envisioned as a critical step in recognition of the trauma and subsequent mobilization of an appropriate response (Mittler et al., 1999). However, the molecular targets of such ROS remain unknown.

Whether to respond to ROS signals or to prevent excess oxidative damage, plants must be capable of monitoring the level of oxidant species in and around their cells. By analogy to other organisms, the primary sensing mechanism(s) are likely to involve protein-associated redox centres such as thiol groups or metal ions (Demple, 1996). However, the initial perturbation of the oxidation state at these centres must ultimately be transmitted to other signal transduction components that are capable of amplifying and integrating the information. In metazoan organisms, MAP kinase cascades play a central role in such "midstream" signal transduction processes. In plants, an array of different MAP kinases have recently been found to be activated by treatments (wounding, fungal elicitors) that are also known to be capable of inducing an oxidative burst in the challenged tissues (Yaharus et al.,1995; Usami et al.,1995; Piedras et al., 1998; Romeis et al.,1999). However, in these reports the potential connection between MAPK activation and ROS generation has usually been examined from the perspective that kinases might be involved in regulating ROS

formation, rather than the converse. Likewise, the possible role of MAP kinase in response to direct oxidant stress has not been examined in plants, although a number of recent studies in animal cells have reported rapid changes in the phosphorylation status of protein kinases as a direct consequence of oxidant stress (Lander et al., 1995; Guyton et al., 1996; Abe et al., 1998).

There are many parallels between the responses induced in plants by exposure to atmospheric ozone and those resulting from other challenges to cellular integrity. Ozone-induced responses include elevated levels of antioxidant activity (Orvar et al., 1997), phenolic accumulation (Eckey-Kaltenbach et al., 1994), suppression of primary metabolic functions (Pell et al., 1992; Conklin and Last, 1995), salicylic acid accumulation, production of pathogenesis-related proteins (Yalpani et al., 1994), stimulation of ethylene (Tuomainene et al., 1997) callose biosynthesis, and local necrosis (Schraudner et al., 1992; 1998). Some or all of these same changes can also be observed following wounding, chilling, pathogen attack or elicitor treatment, indicating that ozone behaves as a volatile general elicitor of plant defense reactions (Sandermann et al., 1998). In this model, the parallelism in downstream responses could arise from the ability of ozone to create an oxidant stress which effectively mimics the ROS burst often induced in stressed cells. The intracellular signalling elicited in plant cells by ozone treatment would therefore be predicted to resemble the pathway(s) activated by other ROS-inducing stresses.

Since several plant MAP kinases were known to be stress-induced, I decided to explore the possibility of common signalling by first examining the influence of a brief exposure to ozone on the activity of MAP kinases in leaves of tobacco, poplar, and

Arabidopsis plants. In earlier studies in our lab, it had been established that exposure of tobacco to 250-500 ppb ozone for several hours was sufficient to induce phenolic accumulation and visible tissue damage within 48-72 hours (Orvar et al., 1997). Assays for MBP phosphorylation activity in ozone-treated leaves demonstrated, however, that induction of this hallmark reaction for MAPKs can be detected within 10 minutes of first contact with ozone. The protein kinase activity is associated with a single zone of protein (tobacco) migrating at a relative mobility of ~46 kDa, and two bands (*Arabidopsis*) ~44- and 46-kDa, sizes that are typical of many MAPKs. Immunological probing of this response with antibodies raised against a mammalian ERK-type MAPK, and with specific anti-phospho-ERK antibodies, confirmed that the ozone-activated kinase belongs to the ERK class of MAPKs, rather than to the SAPK or JNK classes that often participate in stress-induced in mammalian cells (Kyriakis et al., 1994). Interestingly, the majority of the MAPKs characterized from plants to date appear to belong to the ERK class (Kultz, 1998), which is a pattern of unkown significance.

A more experimentally tractable system for studying short-term responses to ozone was devised by establishing suspension cultures of tobacco cells which could be readily plated and uniformly challenged with various reagents. In this system, short-term exposure to ozone (200 to 500 ppb) not only induced an increase in cell mortality (Samuel et al., 2001), but the treatment also elicited a strong activation of two ERK-type MAP kinases, as had been seen with intact plants. Following a 10 minute challenge with ozone, the $MAPK^{46}$ remained activated for at least one hour before returning to its inactive state (or being destroyed). If the tobacco cells were

treated with calyculin A, an inhibitor of protein-serine / threonine phosphatases, a marked activation of the MAPK[46] was induced in the absence of any oxidative stress (Samuel et al., 2001). This is consistent with regular cycling of the kinase between its phosphorylated and de-phosphorylated states, whereby the relative activities of the cognate protein phosphatases and upstream kinase(s) would poise the MAPK at the appropriate level of activation.

Numerous recent reports have described the induction of MAPK activity in tobacco tissues by biotic and abiotic stimuli, but few of these kinases have been characterized in detail. The salicylate-induced protein kinase (SIPK) and wounding-induced protein kinase (WIPK) are not only the most extensively examined tobacco kinases, but they are notable for the range of stimuli to which they respond. Interestingly, these same stimuli are also associated with rapid ROS generation in the challenged tissue. It seems likely to us that it was likely SIPK, WIPK or both might be activated in response to a ROS burst, regardless of the nature of the intracellular ROS generator. This hypothesis was tested by using specific antibodies, which identified the ozone-induced ERK-type MAP kinases in tobacco as SIPK.

Since ozone itself is destroyed almost immediately upon contact with the apoplast, damage in ozone-treated cells is thought to be a consequence of the disposition of the resulting organic ozonides and associated ROS. Ozone has been shown to elicit accumulation of hydrogen peroxide (Schraudner et al.,1998; Pellinen et al.,1999), superoxide anion radical (Runeckles and Vaartnou, 1997) and hydroxyl radical (Grimes et al., 1983) in exposed plant tissues, but analysis of the physiological roles played by individual ROS species is complicated by both their intrinsic reactivity

and rapid inter-conversion. Thus, superoxide anion dismutation rapidly produces hydrogen peroxide, while superoxide and hydrogen peroxide together can undergo a Fe^{2+}-catalyzed reaction cycle that yields the highly destructive hydroxyl radical. Ozone can produce hydrogen peroxide directly by interacting with unsaturated membrane lipids. In view of this interplay, any process that induces a rapid increase in hydrogen peroxide levels will unleash a burst of oxidizing radicals within the cell.

When cultured tobacco cells were exposed to exogenous hydrogen peroxide, SIPK was activated within the same time frame as seen with ozone treatment. This activation was completely blocked by pre-incubation of the cells with free radical trapping reagents such as *N*-(2-mercaptopropionyl) glycine (MPG) or *N*-acetyl cysteine (NAC), implying that the MAPK activation is a consequence of the creation of ROS by ozone. Exogenous hydrogen peroxide has also recently been shown to activate ERK-type MAPKs in an MPG / NAC-sensitive manner in animal cells (Guyton et al., 1996; Abe et al., 1998). Some insight into the sequence of events underlying this effect was provided by a recent study in mouse striatal neuron cells, where the activation of ERK by H_2O_2 was found to be blocked by the specific MEK1&2 inhibitor PD98059 (Samanta et al., 1998). A similar effect of PD98059 was found in both tobacco and poplar cells treated with either ozone or H_2O_2 in this study, and activation of SIPK / WIPK during the Avr9 / Cf-9 interaction in transgenic tobacco plants was likewise abolished (Romeis et al., 1999). The activation of MAPKs by oxidants in both plant and animal cells therefore appears to result from an upstream redox event rather than from oxidative modification of the MAPK protein itself.

The ability of a Ca^{2+} channel blocker to completely inhibit SIPK activation by H_2O_2 or ozone indicates either that opening of Ca^{2+} channels is the critical redox-regulated upstream event, or that this upstream process has an absolute requirement for elevated Ca^{2+} concentrations. Lanthanum was similarly effective in blocking SIPK / WIPK activation during the hypersensitive response (Romeis et al., 1999). Ozone exposure leads to a rapid and transient increase in internal Ca^{2+} levels in transgenic aequorin-expressing *Arabidopsis* plants (Clayton et al., 1999). Similar increases in internal Ca^{2+} levels have also been directly observed in transgenic aequorin-expressing tobacco cells following treatments (oligogalacturonic acid elicitor or hypo-osmotic shock) that also induced an oxidative burst (Chandra and Low, 1997). Ca^{2+} channel blockers eliminated both the Ca^{2+} transient and the ROS burst elicited by each treatment.

Ca^{2+} fluxes also appear to be involved in activation of a number of other plant MAPKs. Activation of a p47 MAPK in tobacco cells by fungal elicitor (xylanase) treatment (Suzuki et al., 1999), and of two tobacco MAPKs (46- and 50-kDa) by cryptogein or oligogalacturonide elicitors (Lebrun-Garcia et al., 1998), was silenced by Ca^{2+} channel blockers. By contrast, activation of a 49 kDa tobacco protein kinase by harpin treatment (Adam et al., 1997) was not sensitive to these reagents, consistent with the observation that harpin also failed to induce a Ca^{2+} transient in aequorin-expressing tobacco cells (Chandra and Low, 1997).

The nature of other upstream events that link the ozone-induced ROS burst to rapid activation of SIPK in tobacco remain to be defined. Activation of SIPK in tobacco by calyculin A treatment (Samuel et al., 2001) implicates the involvement of

calyculin A-sensitive protein-serine / threonine phosphatases in down-regulation of the kinase, a phenomenon known to occur in animal cells, where PP2A down-regulates the ERK pathway by acting at multiple points in the cascade (Millward et al., 1999). In plants, the tobacco p47 MAPK induced by fungal xylanase was also shown to be activated by treatment with calyculin A (Suzuki et al., 1999), whereas the two tobacco MAPKs (46- and 50-kDa) activated by other elicitors were unaffected (Lebrun-Garcia et al., 1998).

The lack of influence of vanadate on SIPK activation by ozone / ROS argues against a central role for protein-tyrosine kinase between the primary oxidant species and SIPK (Samuel et al., 2001). The latter point stands in contrast to the function implied by the name "salicylate-induced protein kinase." However, it is worth noting that SIPK activation in tobacco requires high levels of exogenously applied salicylic acid (Zhang and Klessig, 1997), and the resulting induction is far weaker than that induced by either ozone / ROS treatments or the hypersensitive response (Romeis et al., 1999). In terms of physiological relevance, therefore, this kinase might appropriately be re-named as the "ROS-induced protein kinase" (RIPK). As has been pointed out earlier (Zhang and Klessig, 1998) there are grounds to suspect that at least some of the other plant MAPKs reported to be 45 - 50 kDa in size and to be elicitor- or wounding-induced represent orthologs of RIPK (SIPK). Taken together, the data point to a central and evolutionarily conserved role for RIPK (SIPK) in the transduction of signals generated by both biotic and abiotic stresses that trigger a burst of oxidant formation in plant cells.

Chapter 3

Suramin inhibits oxidant signalling in tobacco suspension-cultured cells.

3.1 Introduction

Like other eukaryotic organisms, plants require oxidant-sensing systems that ensure appropriate short-term and long-term responses to various oxidative stresses including photo-oxidation, ultraviolet radiation (UVR) or ozone (Lois 1994; Rao et al., 1996a; Sharma et al., 1996; Jansen et al., 1998). The cellular impacts of UVR and ozone range from direct DNA damage to protein oxidation and membrane lipid peroxidation, but a central element in the damage profile appears to be the generation of ROS within challenged plant cells (Rozema et al., 1997; Dai et al., 1997; and Jansen et al., 1998). In birch leaves, it has been shown that ozone-induced ROS initially accumulate around the cell perimeter, within the cytosol immediately adjacent to the plasmalemma (Pellinen et al., 1999).

The initial oxidant-induced signals are thought to be amplified through transduction networks but the nature of either the initial sensor or the related signalling pathway(s) remains unclear (Bolwell 1999; Kovtun et al., 2000; Stratmann et al., 2000a). One of the major signal transduction modules used by eukaryotic organisms consists of mitogen-activated protein kinases (MAPK). Several genes encoding MAPK homologues have been identified from plants (Mizoguchi et al., 1993; and Zang & Klessig, 1997; Hardie 1999), and some of these kinases are activated by oxidant stresses, including ozone, hydrogen peroxide and UVR (Kovtun et al., 2000; Stratmann et al., 2000a; Samuel et al., 2000). Since a common attribute of these

different oxidant stressors is their ability to trigger rapid accumulation of ROS in the affected tissue, it appears that one or more ROS sensors must operate on, or upstream of, plant MAPKs (Dai et al., 1997; Pellinen et al., 1999).

Based on work in animal systems, candidate oxidant sensors include protein kinase C (PKC), receptor tyrosine kinases, phospholipases, phosphoprotein phosphatases, and various transcription factors (Taher et al., 1993; Sachsenmaier et al., 1994; Guyton et al., 1996; Groß et al., 1999; Peus et al., 1999). While there is no firm evidence for the presence of receptor tyrosine kinases in plant cells, plant genomes do encode large numbers of receptor-like kinases, many of which contain structural motifs similar to mammalian receptor kinases (Hardie 1999).

In mammals, specific mammalian growth factor receptors and signalling cascades can become activated upon exposure to UVR or to hydrogen peroxide. For example, UVB induces the rapid activation of the epidermal growth factor receptor (EGFR) in human keratinocytes, leading to the downstream activation of the MAP kinase, ERK1&2 (Peus et al., 1999). This signalling response was blocked by pre-treatment of the cells with the externally-targeted reagent, EGFR-specific monoclonal antibody (Peus et al., 1999). Suramin (8,8'-[carbonyl-bis[imino-3,1-phenylenecarbonylimino(4-methyl-3,1-phenylene)carbonyl-imino]] bis-1,3,5-napthalenetrisulfonic acid hexasodium salt) is also a non-membrane permeable reagent, and is able to inhibit cytokine and growth factor receptor interactions as well as uncouple G proteins from their cognate receptors in mammalian cells (Hosang 1985; Oliver et al., 1990; Pollack & Richard, 1990; Chahdi et al., 1998). It is thought to block receptor activity by destabilizing or preventing the formation of the active

receptor conformation (Sachsenmaier et al., 1994; Chahdi et al., 1998), rather than by directly affecting other intracellular signalling components.

In plants, suramin was recently shown to inhibit intracellular defense signalling initiated by peptide or glycan elicitors in suspension-cultured tomato cells (Stratmann et al., 2000b). These elicitors are known to rapidly induce an intracellular "oxidative burst" in plant cells (Orozco-Cardenas & Ryan, 1999; Lee et al., 1999; and Bellincampi et al., 2000), but how this pulse of ROS production is linked to defense activation has not yet been established. However, it is noteworthy that ROS have recently been shown to immediately activate some plant MAPKs (Kovtun et al., 2000; Samuel et al., 2000), and that suramin pre-treatment of tomato cells also inhibited the activation of an unidentified 48 kDa MBP kinase by elicitors (Stratmann et al., 2000b).

In view of the presence in plant cells of candidate receptor species and protein phosphatases with potentially oxidizable cysteine residues (Hardie 1999; Satterlee & Sussman, 1998), and the fact that plant MAPKs can also be activated by oxidant stresses, I hypothesized that the initial step in oxidant detection in plant cells might involve an analogous, receptor-based, mechanism. I tested this hypothesis by examining the suramin sensitivity of MAPK activation induced in plants by a range of direct oxidant stresses.

3.2 Materials and Methods

3.2.1 Plant material and treatment

Tobacco (Xanthi nc) cell suspension cultures were established and maintained in Murashige and Skoog medium supplemented with 1 mg/l 2, 4-D and 0.1 mg/l of kinetin, subcultured at weekly intervals. Poplar suspension cultures (*Populus*

trichocarpa x deltoides clone H11) obtained from Dr. M. Gordon (U. Washington) were maintained using the same growth medium (no 2, 4-D or kinetin) and growth conditions as tobacco. The flasks (250 ml) were shaken at 110 rpm (gyratory shaker) in the dark at 25^{0}C. *Arabidopsis thaliana* (ecotype Columbia) and corn (*Zea mays* L.) plants were grown in soil, in greenhouse conditions with 25/20^{0}C (day/night) under 16 hr photoperiod, for five and three weeks, respectively. Moss (*Physcomitrella patens*) plants were grown in a minimal "BCD" medium in a growth room under controlled conditions 25/20^{0}C (day/night) under 16 hr photoperiod for 10 weeks. Embryogenic calli of white spruce (*Picea gluca*) were obtained from Dr. D. Ellis, Silvagen, Inc. Vancouver) and grown on agar-soliditied Linsmaier-Skoog maintenance medium.

One-week-old tobacco cell suspension cultures were plated onto a layer of Whatman 541 filter paper in petri plates drilled with multiple holes to allow the medium to flow through. The resulting thin cell layers were then exposed to UVC 10mj/cm^2 (total energy) or ozone (200 ppb) for a selected period of time, or hydrogen peroxide (20 mM) for 10 min. All samples were then immediately vacuum filtered and frozen in liquid nitrogen and stored at –80^{0}C to await further analysis. UVC irradiation was delivered from a Hoefer, UVC 500 crosslinker, emitting UVC at 254 nm. Ozone was generated with a Delzone ZO-300 ozone generating sterilizer (DEL industries) and monitored with a Dasibi 1003-AH ozone analyzer (Dasibi Envirinmental Corp.). Ozone samples were exposed in a flow-through chamber (3 L/min) while control plates were exposed to ambient air in a similar chamber. *Arabidopsis*, corn and *Physcomitrella* plants were exposed to UVC 500 mj/cm^2 and subsequently frozen in liquid nitrogen and stored at –80^{0}C to await further analysis. Poplar suspension cultures and spruce

callus were exposed to 10mj/cm^2 UVC, and frozen and stored as described above. Control plants and tissues were immediately frozen in liquid nitrogen so as to limit any potential handling-induced stress.

3.2.2 Protein extraction

Frozen tissue samples were pulverized in liquid nitrogen and the resulting powder was stirred into 1.5 volumes extraction buffer containing (50 mM Hepes pH 7.5, 5 mM EDTA, 5 mM EGTA, 10 mM DTT, 1 mM sodium orthovanadate, 10 mM sodium fluoride, 10% glycerol, 7.5% polyvinylpolyrolidone, and the protease inhibitor cocktail, (complete^{TM}, Boehringer Mannheim). The slurry was kept on a reciprocating shaker (100 oscillations / minute) for 10 minutes, at 4°C, followed by centrifugation (15,000 g; 30 minutes; 4°C). The soluble extracts were flash frozen immediately in liquid nitrogen and stored at –80°C for future analysis. The protein quantification was accomplished using the Bradford dye-binding assay.

3.2.3 Western blotting analysis

The Western blot analysis was performed in the same manner as in Chapter 2 (p44).

3.2.4 In-gel kinase assay

The in-gel kinase assay was performed in the same manner as in Chapter 2 (p45).

3.2.5 Immunoprecipitation and in-gel kinase assays

The immunoprecipitation and in-gel kinase assays were performed in the same manner as in Chapter 2 (p45).

3.2.6 Inhibitor treatments

Tobacco suspension cultures were pre-treated with the following inhibitors: MEK inhibitor PD98059 (100 μM) (New England Biolabs) for 1 hr, N-acetyl cysteine (20 mM) for 45 minutes, $LaCl_3$ (5 mM) for 15 minutes, or with suramin (1, 5, or 10 mM) for 1 hr. Unless otherwise noted, all reagents were obtained from Sigma. The inhibitor-treated suspension cells were plated and challenged with UVC or ozone as described, or treated in suspension with hydrogen peroxide, and subsequently extracted, for analysis.

3.3 Results and Discussion

3.3.1 Exposure to UVC rapidly activates a MAP kinase in plants

The chemical and structural complexity of whole plant tissues can make it difficult to detect the initial molecular events triggered by UVR. Cultured plant cells, on the other hand, provide a homogeneous tissue that is also free of UV-absorbing pigments. To examine the impact of UVR, freshly prepared thin layers of tobacco cells were irradiated with short bursts of UVC (10 J/m^2) and then either harvested or returned to liquid medium. Protein extracts from UV-treated and control cells were electrophoretically separated and assayed in-gel for protein kinase activity using MBP as a substrate. A single strong band of MBP-phosphorylating activity (~46 kDa) was detected in the extracts from UVC-treated cells, with no evidence of a corresponding band in the control lane (**Fig. 3.1a, top**). Exposure of tomato leaves to UVC radiation was recently reported to induce activation of a similar MBP kinase (~48 kDa) (Stratmann et al., 2000a). The size of these kinases, and their ability to use MBP as a

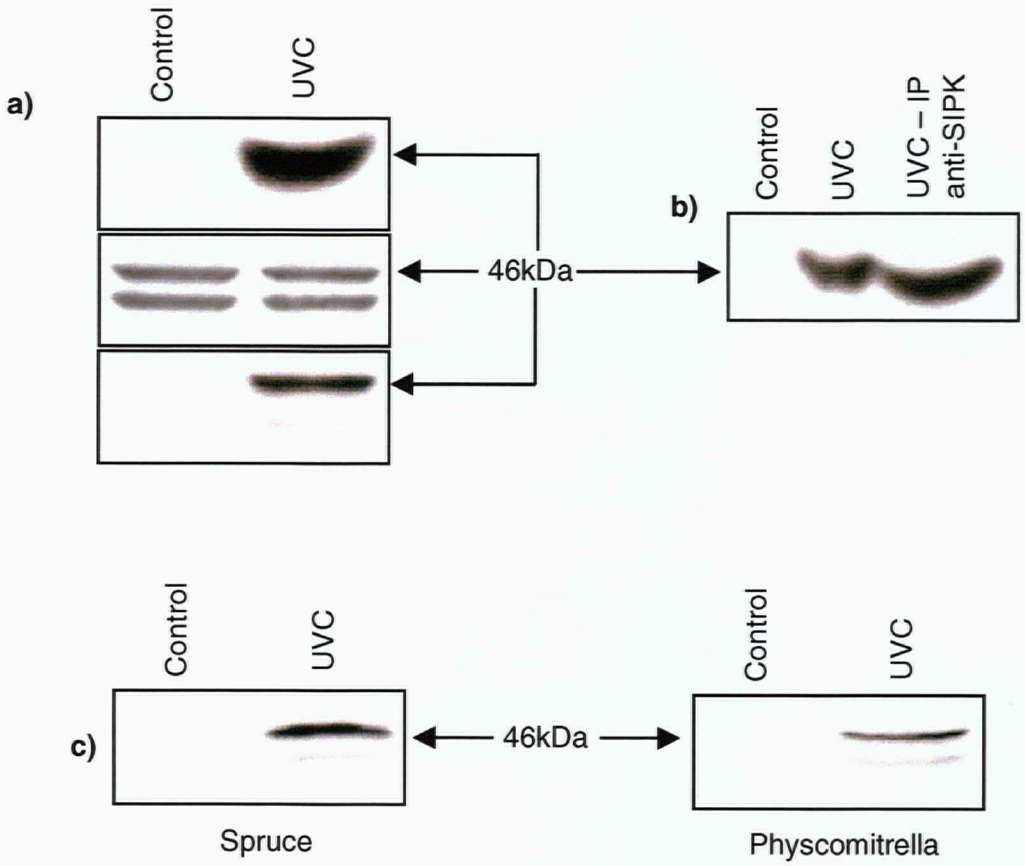

Figure 3.1 Exposure to UVC activates a MAP kinase in tobacco cells and other plants.
Figure legend on following page

Figure 3.1 Exposure to UVC activates a MAP kinase in tobacco cells and other plants. (**a, top**) MBP-phosphorylation activity was induced in UVC-challenged tobacco suspension-cultured cells (10 J/m^2). All UVC exposures involved a short burst equaling a total energy of (10 J/m^2), unless otherwise stated. Control cells were plated and exposed to ambient air for 10 min. Protein extracts from both UVC-challenged and control cells were fractionated in a SDS-polyacrylamide gel polymerized with MBP as a substrate for MAPK. After denaturation and renaturation of the gel, protein kinase activity on MBP was detected by incubating the gel with γ^{32}P-labelled ATP. Protein extracts (30 μg) from both control and UVC-challenged cells were also probed on western blots with anti-ERK 1&2 (**a, middle**) and anti-phospho-ERK 1&2 antibodies (**a, bottom**). (**b**) Extracted proteins from UVC-treated samples were immunoprecipitated using specific anti-SIPK antibodies (5 μg), and the precipitate was assayed for in-gel kinase activity as described above. (**c**) Extracted proteins (30 μg) from UVC-challenged spruce callus (10 J/m^2) and *Physcomitrella* (500 J/m^2) were subjected to immunoblotting using anti-phospho-ERK 1 & 2 antibody.

substrate, are both consistent with the properties of MAPK. As would be predicted for a MAPK, the tomato kinase was also recognized by a phospho-tyrosine monoclonal antibody (Stratmann et al., 2000a).

Since the majority of known plant MAPKs appear to belong to the ERK class, protein extracts from UVC-irradiated cells were probed on Western blots with anti-ERK 1&2 and anti-phospho-ERK 1&2 antibodies. Anti-ERK antibodies detected two proteins between (~46 and 44 kDa) in both the control and UVC-treated samples, with no apparent differences between the samples (**Fig. 3.1a, middle**). However, when these same samples were probed with anti-phospho-ERK antibodies which recognize only the doubly phosphorylated (-**TEY**-) motif located within the catalytic domain of MAPK, a distinct band (~46 kDa) was detected in the UVC-treated extract, while no signal appeared in the control lane (**Fig 3.1a, bottom**).

This pattern of MAPK activation is very similar to that recently reported in tobacco cells treated with another oxidant, ozone, where the specific kinase involved was identified as the 46 kDa SIPK (salicylic acid-induced protein kinase) (Samuel et al., 2000). Proteins from UVC-treated samples were therefore immunoprecipitated using specific anti-SIPK antibodies, and the precipitate was assayed for in-gel kinase activity. A ~46 kDa band with strong kinase activity could be precipitated from the UVC-treated cell extracts whereas no active kinase was recovered from the control cell extracts (**Fig. 3.1b**). Immunoprecipitation with anti-WIPK antibodies, which recognize a related stress-induced tobacco MAPK, failed to recover any active kinase from either the UVC-treated or control cell extracts (data not shown). These results

indicate that the UVC-activated protein kinase in tobacco cells was most probably SIPK.

The observed response is not restricted to tobacco and its relatives, since UVC treatment of plants as remotely related as conifers and moss (*Physcomitrella*) also resulted in rapid activation of a ~46 kDa kinase (**Fig. 3.1c**). Poplar, *Arabidopsis* and corn also show a rapid activation of a ~46 kDa kinase following UVC exposure (data not shown). The phylogenetic breadth of this UVC response implies that SIPK and its ortholoues in other species form part of a highly conserved oxidant stress-response signalling pathway in plants.

3.3.2 UVC-induced MAPK^{46} activation is dose-dependent, transient, and reliant on ROS and Ca^{2+} ions

When tobacco cells were treated with doses of UVC ranging from 0.5 J/m^2 to 500 J/m^2, there was a clear increase in the activation of the MAPK^{46}, as detected in immunoblots using anti-phospho ERK 1&2 (**Fig. 3.2a**). The time course of this activation is very rapid, with detectable accumulation of the phosphorylated MAPK^{46} within one minute after treatment and a maximal response after 10 min (**Fig. 3.2b**). This was followed by a somewhat slower inactivation process, which returned the MAPK^{46} to the non-phosphorylated state after 60 min.

The activation of MAPK in tobacco cells by UVC has essentially the same characteristics as that induced by exposure of the cells to ozone (Samuel et al., 2000). Since both ozone and UVC are believed to generate increased levels of ROS such as $^{\bullet}O_2^-$, $HO^{\bullet}$, $HO_2^{\bullet}$ and H_2O_2 when they enter living cells (Cerutti 1985; Dai et al., 1997;

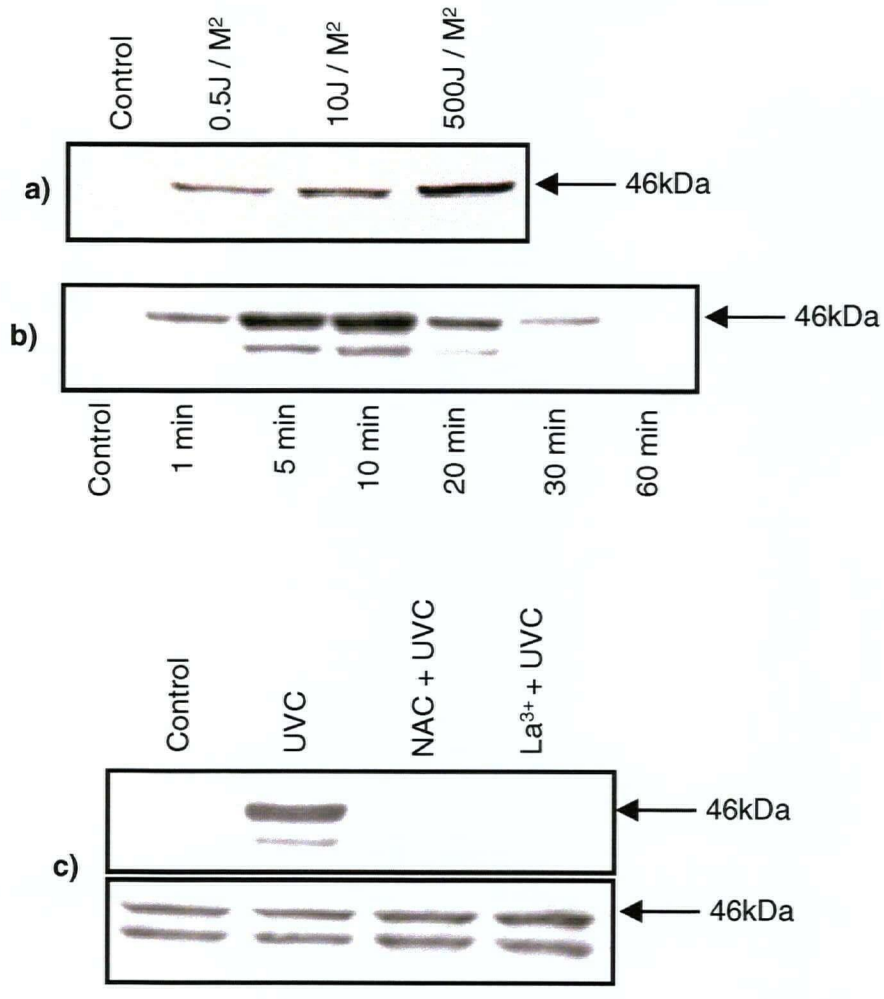

Figure 3.2 UVC-induced MAPK[46] activation is dose-dependent, transient, and reliant on ROS and Ca^{2+}. Figure legend on following page

Figure 3.2 UVC-induced MAPK[46] activation is dose-dependent, transient, and reliant on ROS and Ca^{2+}. (**a**) Extracted proteins (30 μg) from suspension-cultured cells of tobacco were challenged with doses of UVC ranging from 0.5 J/m^2 to 500 J/m^2 followed by immuno-blotting using anti-phospho-ERK 1 & 2 antibody. Control cells were plated and exposed to ambient air for 10 min. (**b**) Following UVC challenge (10 J/m^2), the treated cells were immediately returned to sterile liquid culture medium for up to 60 min, and the proteins extracted at different times post-treatment were immuno-blotted using anti-phospho-ERK 1 & 2 antibody. Extracted proteins (30μg) from suspension-cultured cells that had been pretreated with *N*-acetyl-cysteine (**c, top**) (20 mM, 45 min), $LaCl_3$ (**c, top**) (5mM, 15min) followed by challenge with UVC (10 J/m^2) were analyzed by immunoblotting using anti-phospho-ERK 1 & 2. The same samples were also probed with anti-ERK 1&2 antibodies (**c, bottom**).

Runeckles & Vaartnou, 1997; Pellinen et al., 1999), this indicates that activation of $MAPK^{46}$ may be a common early response to oxidant stress in plant cells. Consistent with this hypothesis, pretreatment of tobacco cells for 45 min with the free radical scavengers, N-acetyl-cysteine (NAC) (20 mM) (**Fig. 3.2c, top**) or N- (2-mercaptopropionyl)-glycine (data not shown) completely abolished the response of the $MAPK^{46}$ to UVC exposure.

In eukaryotic organisms, Ca^{2+} plays a pivotal role in regulation of signalling cascades (Lebrun-Garcia et al., 1998; Suzuki et al., 1999; Samuel et al., 2000). To determine whether the process of $MAPK^{46}$ activation by UVC requires Ca^{2+}, the tobacco cells were pre-treated for 15 minutes with the potent Ca^{2+} channel blocker, lanthanum (La^{3+}) (5mM). This greatly attenuated the subsequent activation of $MAPK^{46}$ by UVC (**Fig. 3.2c, top**), as did pretreatment with the membrane-permeable calcium chelator 1, 2-bis (2-aminophenoxy)- ethane-N, N, N', N',- tetraacetic acid-tetrakis (acetoxy-methyl) ester (BAPTA-AM) (data not shown) (**Fig. 3.2c, bottom**). These same protein extracts, were then blotted using anti-ERK 1 & 2 antibodies with no visual difference between control and pharmacologically treated samples.

3.3.3 Suramin blocks the activation of $MAPK^{46}$ by oxidants

Treatment with oxidants such as UVR or hydrogen peroxide have been shown to activate various signalling pathways in mammalian cells, including the associated MAPK cascades, but the mechanism of this oxidant stimulation has remained obscure (Sachsenmaier et al., 1994; Guyton et al., 1996). In one possible scenario, UVR-generated hydrogen peroxide could act as a source of hydroxyl radical production through metal-catalyzed Fenton reactions, followed by oxidation of accessible cysteine

residues on the receptor and/or cognate protein phosphatases. Both receptor activation (Sachsenmaier et al., 1994; Peus et al., 1999) and phosphatase inactivation (Groß et al., 1999) have been reported to result from oxidative modification in mammalian cells. The EGFR-mediated activation of ERK1&2 by UV in HeLa cells has been shown to be interdicted by treatment with catalase (Peus et al., 1999), consistent with a model in which hydrogen peroxide acts as a second messenger somewhere between the primary oxidative event and MAPK activation.

It has also been observed that activation of the EGFR-linked pathway by UVC in HeLa cells is sensitive to the mammalian growth factor antagonist, suramin (Sachsenmaier et al., 1994). Suramin is generally viewed as interfering with the extra-cellular ligand-binding of a number of growth factors to their cognate receptors, thus blocking receptor autophosphorylation and initiation of intracellular signalling (Betsholtz et al., 1986; Sachsenmaier et al., 1994). However, the ability of suramin to also block oxidant-induced activation of downstream signalling implies that these oxidants (or their derivatives) may be acting initially on membrane-associated receptors, either directly or through the inactivation of cognate protein phosphatases.

To determine whether the UVC-induced activation of plant MAPK[46] might be mediated through receptor phosphorylation, tobacco cells were pre- incubated with varying concentrations of suramin for one hour and then challenged with UVC (10 J/m^2). This treatment dramatically reduced the activation of MAPK[46] by UVC, as detected by anti-pERK 1&2 immunoblotting (**Fig. 3.3a**). When protein extracts from control cells, UVC-exposed cells and cells pretreated with suramin (10 mM) followed by UVC treatment, were

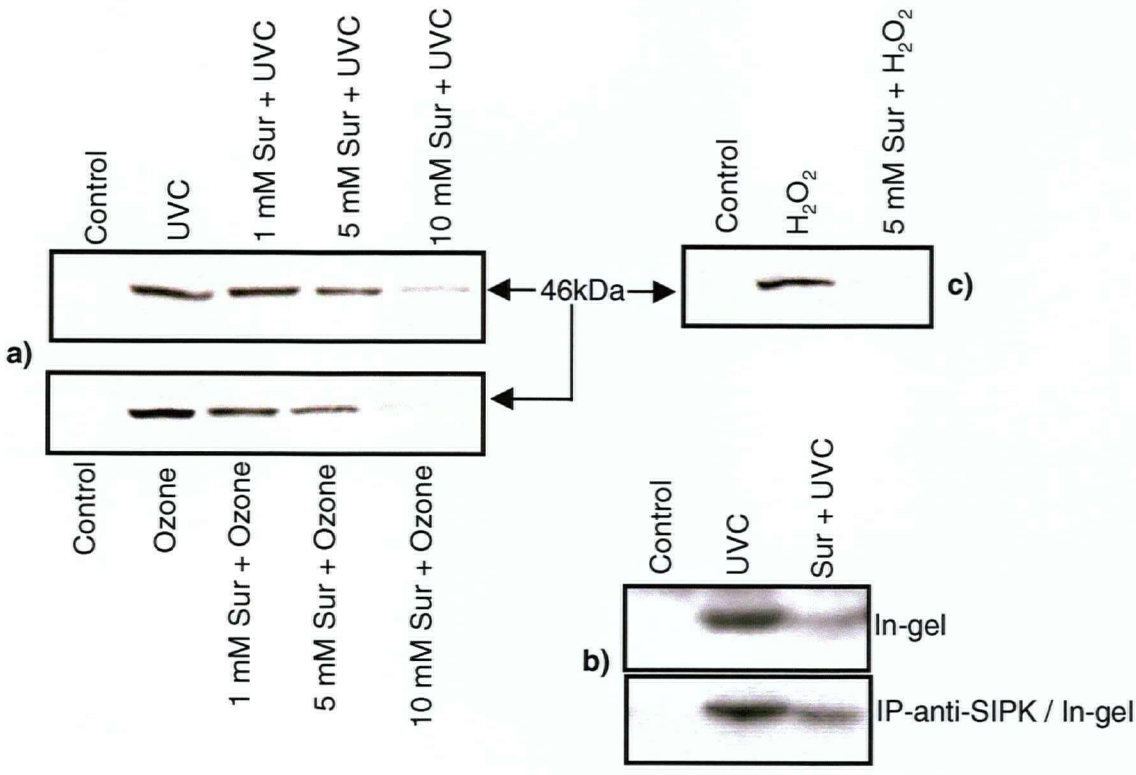

Figure 3.3 A growth factor receptor antagonist blocks the activation of MAPK[46].
Figure legend on following page

Figure 3.3 A growth factor receptor antagonist blocks the activation of MAPK[46]. (**a**) Extracted proteins (30 μg) from suspension-cultured tobacco cells that had been pre-incubated with different concentrations of suramin (0, 1, 5, or 10 mM) for 1 hr, and then plated and challenged with UVC (**top**) (10 J/m^2) or ozone (**bottom**) (200 ppb) for 10 minutes, were analyzed by immunoblotting with antiphospho-ERK 1 & 2. Protein extracts were fractionated in a SDS-PAGE polymerized with MBP as a substrate as in **Fig. 3.1**, (**top**). (**b, bottom**) Extracted proteins (40 μg) from control, UVC-challenged and suramin/UVC tobacco cells were immunoprecipitated using anti-SIPK antibodies and subjected to an in-gel kinase assay. Total proteins from UVC-treated cells were used as a positive control. (**c**) pre-incubated with suramin (5 mM) for 1hr, and treated with hydrogen peroxide (20 mM) for 15 min, were both immuno-probed using antiphospho-ERK 1&2 antibodies.

fractionated in a SDS-PAGE polymerized with MBP, reduced SIPK activation was also observed in the suramin-treated lane (**Fig. 3.3b, top**). A similar reduction in SIPK activity was observed when SIPK immunoprecipitated from the extracts was examined in the in-gel kinase assay (**Fig. 3.3b, bottom**).

We have previously demonstrated that both ozone and hydrogen peroxide induce the activation of a MAPK[46] (SIPK) in tobacco (Samuel et al., 2000), in a Ca^{2+}-dependent process that can be blocked by free radical quenchers. The activation profiles of tobacco MAPK[46] are thus very similar, whether the inducer is UVC, ozone, or hydrogen peroxide, suggesting that, in plant cells, all three oxidant stresses might induce a common signalling pathway leading to the MAPK module(s). This possibility was examined by pre-incubating tobacco cells with varying concentrations of suramin and subsequently challenging them with ozone (200 ppb) or hydrogen peroxide (20 mM). In both cases, the activation of MAPK[46] was clearly reduced in a manner similar to that observed in the UVC-treated cells (**Fig. 3.3a, bottom and 3.3c**).

Taken together, these data indicate that in plants, exposure to either UVC or ozone generates elevated local ROS concentrations in the cell periphery. These agents then activate redox-sensitive membrane-associated signalling mechanisms (e.g. membrane receptors) whose output leads to phosphorylation of a specific downstream MAPK[46].

Whether this transduction process is ultimately triggered by oxidative activation of a receptor or receptor-like kinase, or more indirectly through oxidative inactivation of a protein phosphatase, remains to be established. UVR- and ozone-induced redox stresses in plant cells can activate a number of defense-related genes similar to those

activated by pathogens and wounding (Rao et al., 2000b), and protein phosphorylation is required as part of this activation process (Lois 1994; Mehdy 1994; Greene & Fluhr, 1995; Rao et al., 1996a; Dai et al., 1997; Jansen et al., 1998; Kovtun et al., 2000). The fact that stresses other than UVR and ozone also initiate ROS accumulation, and that UVR and ozone share overlapping patterns of defense-related gene expression with these other stresses, makes it likely that these stimuli share at least part of the subsequent signal transduction cascades. The ability of suramin to block the activation of MAPK[46] by UVC, ozone or hydrogen peroxide indicates that these oxidants act initially at the cell periphery, possibly through a receptor-based pathway, rather than further downstream. This model identifies cell surface receptors as possible mediators of oxidant-induced signalling, and helps to explain the overlapping patterns of abiotic and biotic stress responses.

Mastoparan rapidly activates plant MAP kinase signalling independent of heterotrimeric G proteins

4.1 Introduction

It has long been known that mastoparan (MP), a cationic, amphiphilic tetradecapeptide isolated from wasp venom, is capable of directly stimulating the guanine nucleotide exchange reaction of the α-subunit of animal heterotrimeric G-proteins via a mechanism analogous to that of G protein-coupled receptors (GPCR). This leads to a myriad of downstream events including the activation of mitogen-activated protein kinases (MAPKs). Here, we show that the induction of plant MAPK signalling by MP does not require the participation of either the Gα- or Gβ-subunits of the plant heterotrimeric G proteins, but is reliant on reactive oxygen species (ROS), a cognate MAPKK, and influx of extra-cellular Ca^{2+} ions. While this does not preclude a role for a heterotrimeric G protein in MAPK signalling, it raises concern about the conclusions drawn from published experiments using MP.

Gα-, Gβ-, and Gγ-homologues have been identified in *Arabidopsis* and other plant species (Ma et al., 1990; Gotor et al., 1996; Lee and Assmann, 1999; Saalbach, et al., 1999; Mason and Botella, 2000). In *Arabidopsis*, a single prototypical Gα (*Arabidopsis* G PROTEIN, ALPHA SUBUNIT1 (GPA1)) and one prototypical Gβ (*Arabidopsis* G PROTEIN, BETA SUBUNIT1 (AGB1)) subunit and potentially, two Gγ subunits (*Arabidopsis* G PROTEIN, GAMMA SUBUNIT1 (AGG1 and AGG2)), are found. Interaction has been detected between the *Arabidopsis* Gγ and Gβ subunits (Mason and Botella, 2000; reviewed in Jones, 2002), and evidence has been obtained

for *in vitro* and *in vivo* interaction of GPA1 and Gβ (J-G Chen, J.S. Liang and A.M. Jones, unpublished data).

Mutational and pharmacological studies have implicated plant heterotrimeric G-protein subunits in numerous physiological processes and phenotypic changes, including auxin and gibberellin signalling, K^+ channel regulation, Ca^{2+} regulation, cell division, and stomatal function (Aharon et al., 1998; Jones et al., 1998; Saalbach et al., 1999; Ullah et al., 2001; Wang et al., 2001).

MP has been widely used to implicate G protein regulated processes in both plants and animals (Higashijima et al., 1988; Legendre et al., 1992; Legendre et al., 1993; Wise et al., 1993; Höller et al., 1999). For example, short-term responses to MP treatment reported for plants include increases in cellular Ca^{2+} ions, induction of an oxidative burst, stimulation of 1, 4, 5-inositol triphosphate (IP3) turnover, and activation of phospholipase C, phospholipase D2 and MBP kinases (Scherer, 1992; Kauss and Jeblick, 1996; Chahdi et al., 1998; Takahashi et al., 1998; Chahdi et al., 2003). Although it is generally assumed that these responses are mediated by the initial activation of heterotrimeric G proteins, there is limited direct evidence for this, particularly in plants.

4. 2. Materials and Methods

4. 2.1 Chemicals and reagents

Mastoparan [I-N-L-K-A-**L**-A-A-L-A-K-K-**I**-L-NH_2] was purchased from Biomol. Research Laboratories Inc. (Plymouth, PA., USA) (synthetic peptide) or Sigma (St. Louis, MO., USA) (peptide purified from wasp venom). Mas-17, an inactive analog of

mastoparan, [I-N-L-K-A-**K**-A-A-L-A-K-K-**L**-L-NH_2] was purchased from Biomol Research Laboratories Inc. (Plymouth, PA., USA). (Amino acid residues changed to produce the inactive analog are shown in boldface type). Myelin basic protein (MBP), γ-^{32}P-labeled ATP, N-acetyl cysteine (NAC), N-(2-mercaptopropionyl)-glycine (MPG), lanthanum chloride ($LaCl_3$), MEK 1&2 inhibitor, PD98059 (PD), Bradford protein assay reagent, and Murashige and Skoog (MS) cell culture medium were purchased from Sigma (St. Louis, MO., USA). Complete^{TM} protease inhibitor cocktail was purchased from (Boehringer Mannheim, Canada). Anti-pERK 1&2 and anti-pMEK 1&2 were purchased from New England Biolabs, (Beverly, MA, USA), and peroxidase-conjugated goat anti-rabbit IgG from Dako Corp. (Carpinteria, CA, USA). Enhanced Chemiluminescence Detection reagents (ECL) were purchased from Amersham Corp. (Quebec, Canada). Anti-AtMPK6 antibodies (Miles et al., 2004) raised against the N-terminal portion of the MPK6 polypeptide, were used for IP work.

4.2.2 Plant material and treatments

Tobacco (Xanthi nc) cell suspension cultures were established from aseptic seedlings, maintained in Murashige and Skoog medium supplemented with 1 mg/l 2, 4-D and 0.1 mg/l of kinetin, and subcultured at weekly intervals. The flasks (250 ml) were shaken at 110 rpm (gyratory shaker) in the dark at 25^0 C. One-week-old tobacco suspension-cultured cells were incubated with various reagents, immediately harvested, frozen in liquid nitrogen and stored at -80^0 C until analyzed. For pharmacological pre-treatments, the following regimes were used: $LaCl_3$ (5 mM) for 15 minutes, N-acetyl cysteine (NAC) and N-(2-mercaptopropionyl)-glycine (MPG) for 45

minutes, and PD98059 (100 μM) for 60 minutes. After the appropriate pre-treatment, cultures were treated with mastoparan (1 or 5 μM) for 1 or 5 minutes. It has been reported that mastoparan concentrations above 10 μM can affect membrane integrity through pore formation and destabilize cell homeostasis. To minimize these possible toxicological complications, only concentrations of 5 μM or lower were used. All experiments were performed in triplicate.

For UVC exposure, one-week-old tobacco cell suspension cultures were plated onto a layer of Whatman 541 filter paper in Petri plates drilled with multiple holes to allow the medium to flow through. The resulting thin cell layers were then exposed to UVC (10 J m^{-2}, total energy) delivered from a UVC 500 crosslinker (Hoefer Pharmacia Biotech., San Francisco, CA, USA). Control plates were exposed to ambient air for 10 minutes. All samples were then immediately harvested, frozen in liquid nitrogen and stored at -80^0 C until further analysis.

Wild type (Wassilewskija, WS and Columbia, Col) and transgenic *Arabidopsis* seeds (WS and Columbia ecotypes: *gpa1-2* and *agb1-2*, respectively) were surface-sterilized, placed into sterile 12-well, serological plates containing liquid media, (1/2 strength MS salts, pH 5.7, plus 1% sucrose) for 3 days at 4^o C in the dark without shaking. After 3 days, the plates containing the germinated seeds were transferred to growth chambers and held at $25/20^0$C (day/night) under a 16-h photoperiod, for 2 weeks without shaking. At the appropriate time, all plates were drained of media and re-filled with 950 μl of fresh growth media and allowed to sit for six hours, after which mastoparan solution (50 μl) was added to each well, yielding a 5 μM final concentration. The seedlings were allowed to incubate for five minutes, followed by

harvesting, freezing in liquid nitrogen and storage at -80°C. Tobacco seedlings, both wild type and transgenic, were prepared in a similar manner, except that the seeds were plated onto solid medium. Two-week-old tobacco seedlings were treated with mastoparan by flooding the seedlings with a 5 μM mastoparan solution, and allowing these to stand for 5 minutes. They were then harvested and stored as described above. Seedlings flooded with distilled water served as a control.

For ozone treatments, 2-week-old tobacco and *Arabidopsis* seedlings were exposed to the indicated concentrations of ozone for various times in a flow-through chamber (3 L/min). Ozone was generated with a Delzone ZO-300 ozone generating sterilizer (DEL industries) and monitored with a Dasibi 1003-AH ozone analyzer (Dasibi Environmental Corp.). The seedlings were then harvested and stored as described as above.

4.2.3 Protein extraction

The protein extraction method was performed in the same manner as in Chapter 3 (p70).

4.2.4 Immunoblot analysis

The immunoblot analysis was performed in the same manner as in Chapter 2 (p44).

4.2.5 In-gel kinase assay

The in-gel kinase assay was performed in the same manner as in Chapter 2 (p45).

4.2.6 Immunoprecipitation and in-gel kinase assays

The immunoprecipitation and in-gel kinase assays were performed in the same manner as in Chapter 3 (p71).

4.3 Results

4.3.1 Mastoparan-induced activation of MAPKs in *Arabidopsis* heterotrimeric Gα and Gβ loss-of-function genotypes

Since the Gα-subunit is the classical target of MP in animal cells, I anticipated that loss of Gα function would interfere with its ability to activate downstream effectors such as terminal MAPKs. To test this, I employed both wild-type and loss-of-function mutant lines of *Arabidopsis* in which the genes encoding the prototypical heterotrimeric Gα (*gpa-1*) and Gβ (*agb-1*) proteins were disrupted. These well-characterized lines have provided insight into the role of plant G proteins in control of other plant processes such as cell division (Ullah et al., 2001; 2003) and stomate closure (Wang et al., 2001).

To determine if MP had the ability to induce the activation of an *Arabidopsis* protein kinase capable of phosphorylating MBP, a known substrate of eukaryotic MAPKs, I treated *Arabidopsis* wild-type seedlings (Columbia ecotype) with MP (5 μM) for 5 min, followed by in-gel analysis. As shown in (**4.1a**), MP treatment led to strong MBP-phosphorylating activity by two proteins (approximately 44 and 46 kDa). Anti-AtMPK6 antibodies (raised against the N-terminal peptide of AtMPK6)

immunoprecipitated the 46-kDa MBP-phosphorylating activity, indicating that the 46kDa MAPK was most likely AtMPK6, the orthologue of salicylic acid-induced protein kinase (SIPK) from tobacco (*Nicotiana tabacum*). The lower band has an activation profile that is similar to that of AtMPK3, the orthologue of the wound-induced protein kinase (WIPK) from tobacco. Treatment of *gpa-1*, *agb-1*, and WT seedlings with MP (5 μM) for 5 min, followed by immunoblotting of the extracted proteins, revealed that neither loss of the Gα-subunit, nor loss of the Gβ-subunit, interfered with the ability of MP to activate AtMPK6 (**Fig. 4.1b, top**). Neither the control nor treatment with Mas-17, the largely inactive analog of MP, was able to elicit a signalling response in these *Arabidopsis* seedlings (**Fig. 4.1b, bottom**).

ROS-induced modifications of animal heterotrimeric Gα proteins lead to their dissociation, followed by subsequent MAPK activation (Nishida et al., 2002). In light of our previous results, we hypothesized that G proteins might not be required for ROS-induced MAPK signalling in plants. To test this, we examined the ability of direct oxidant stress (ozone; 200 ppb) and indirect oxidant stress from ultraviolet C radiation (UVC; 10 J M^{-2} [at 254 nm] total energy) to activate AtMPK6 in the *gpa-1* and *gpb-1* backgrounds. Immunoblot analysis of the proteins from the treated tissues was performed using anti-phospho-ERK 1& 2 antibodies, which identify the dual-phosphorylated, active form of SIPK (Samuel et al., 2000; Miles et al., 2002). As predicted, ROS-induced activation of the SIPK ortholoue, AtMPK6, was unaffected by loss of either GPA1 or AGB1 (**Fig. 4.1c**).

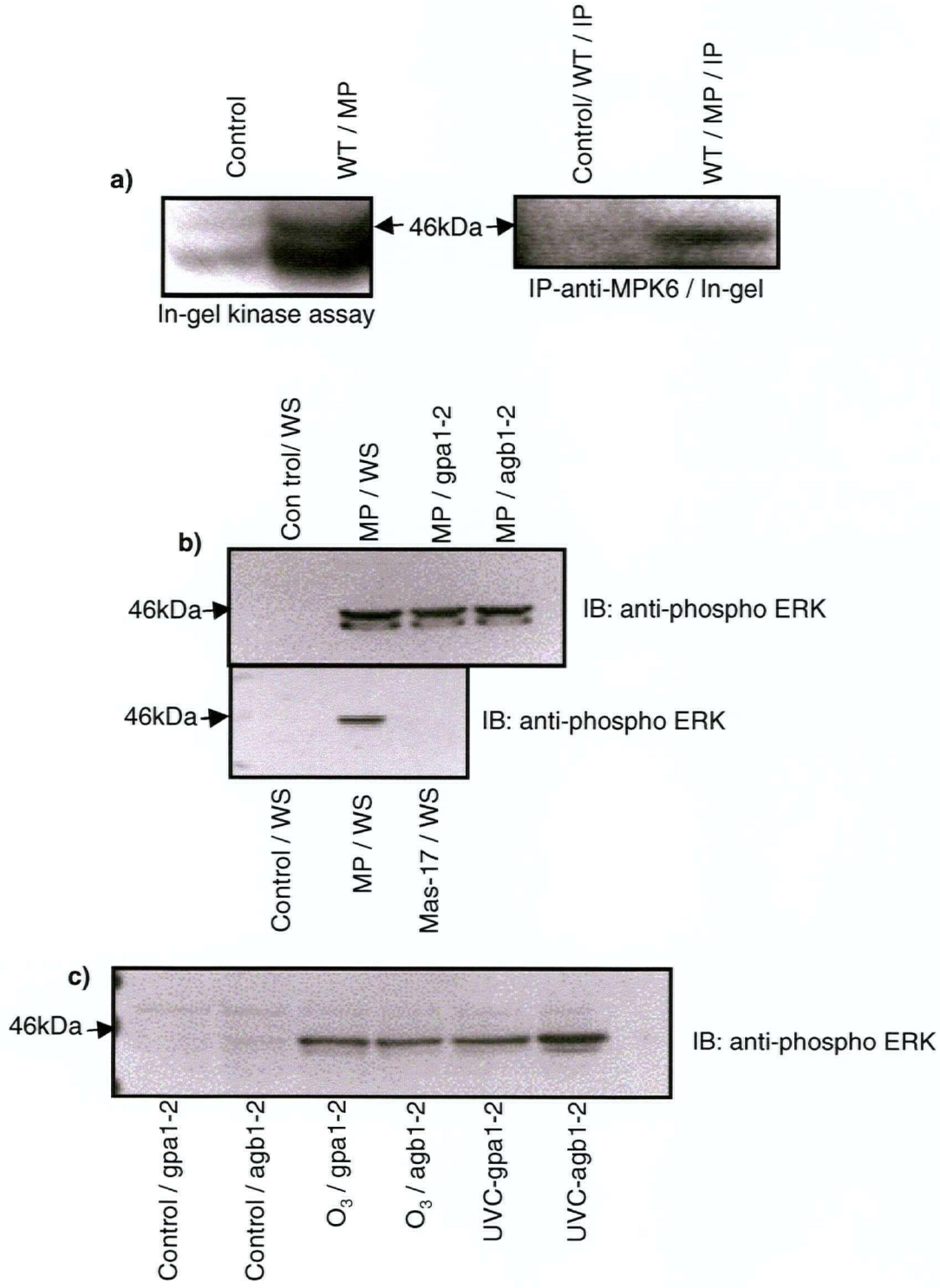

Figure 4.1 MP, ozone, and UVC induced the activation of MAPKs in WT and heterotrimeric (Gα, *gpa1-2* and Gβ, *agb1-2*) loss-of-function *Arabidopsis* seedlings. Figure legend on following page.

Figure 4.1 MP, ozone, and UVC induced the activation of MAPKs in WT and heterotrimeric (Gα, *gpa1-2* and Gβ, *agb1-2*) loss-of-function *Arabidopsis* seedlings. (**a**), To ascertain if MP is capable of inducing the activation of an Arabidopsis MAPK, extracted proteins (40 µg) from MP-treated (5 μM for 5 min) samples, both crude and immunoprecipitated (using specific anti-AtMPK6 antibodies) were assayed for in-gel kinase activity. MBP-phosphorylation was detected in both the crude and immunoprecipitated samples but absent from the control cells. (**b** and **c**), Seedlings were treated with MP or Mas-17 (5 µM, 5 min), ozone (200 ppb, 10 min), or UVC (10 J M^{-2}, total energy) and harvested as described earlier. Control tissue was from seedlings exposed to ambient air (ozone or UVC) or treated with water, the vehicle used for the MP solution. Protein (40 µg) extracts prepared from 2-week-old leaf tissue, isolated from MP-, ozone-, and UVC- exposed WT and heterotrimeric G protein loss-of-function seedlings, were resolved on a 10% SDS-polyacrylamide gel, blotted and probed with anti-pERK 1&2 antibodies (primary antibodies). Columbia wild-type seedlings, when treated with MP (5 µM, 5 min), ozone (200 ppb, 10 min), or UVC (10 J M^{-2}, total energy), gave the same results as the parental (WT) ecotype Wassilewskija seedlings (data not shown). All experiments were performed in triplicate.

4.3.2 Mastoparan-induced MAPK phosphorylation in Tobacco (Xanthi nc) suspension-cultured cells requires Ca^{2+} ions, a cognate MAPKK, and ROS

On the other hand, the chemical and structural complexity of whole plant tissues can make it difficult to employ pharmacological probes. Cultured plant cells, on the other hand, provide a relatively homogeneous and dispersed tissue that is more easily manipulated and amenable to pharmacological studies.

To address the impact of MP on plant MAPK signalling, tobacco cv Xanthi nc suspension-cultured cells were employed. MP treatment of tobacco cells was previously reported to activate protein kinases (Takahashi et al., 1998). Although the kinases involved were not identified, examination of the published data indicated that two of the main species might be SIPK and WIPK, two MAPKs known to be activated by various environmental stresses, including ozone, wounding, and microbial elicitors (Samuel et al., 2000; for review, see Jonak et al., 2002; Miles et al., 2002).

To test this hypothesis, 1-week-old suspension-cultured tobacco cells were incubated for 1 min with either 5 µM MP or 5 µM mas-17, the inactive analogue of MP. When protein extracts from treated cells were assayed in-gel for protein kinase activity, two bands (~44- and 46 kDa) displaying MBP-phosphorylating activity were detected in the extracts from MP-treated cells, but were absent from untreated or mas-17-treated cells (**Fig. 4.2a**). The position of these MBP kinases, and their ability to phosphorylate MBP, are consistent with the properties of MAPKs, while comigration with the 46-kDa phosphorylation activity in UVC-irradiated tobacco cells (Miles et al., 2002) indicated that the upper band activity might be SIPK. Consistent with this, anti-SIPK antibodies were able to immunoprecipitate a 46-kDa MBP-phosphorylating

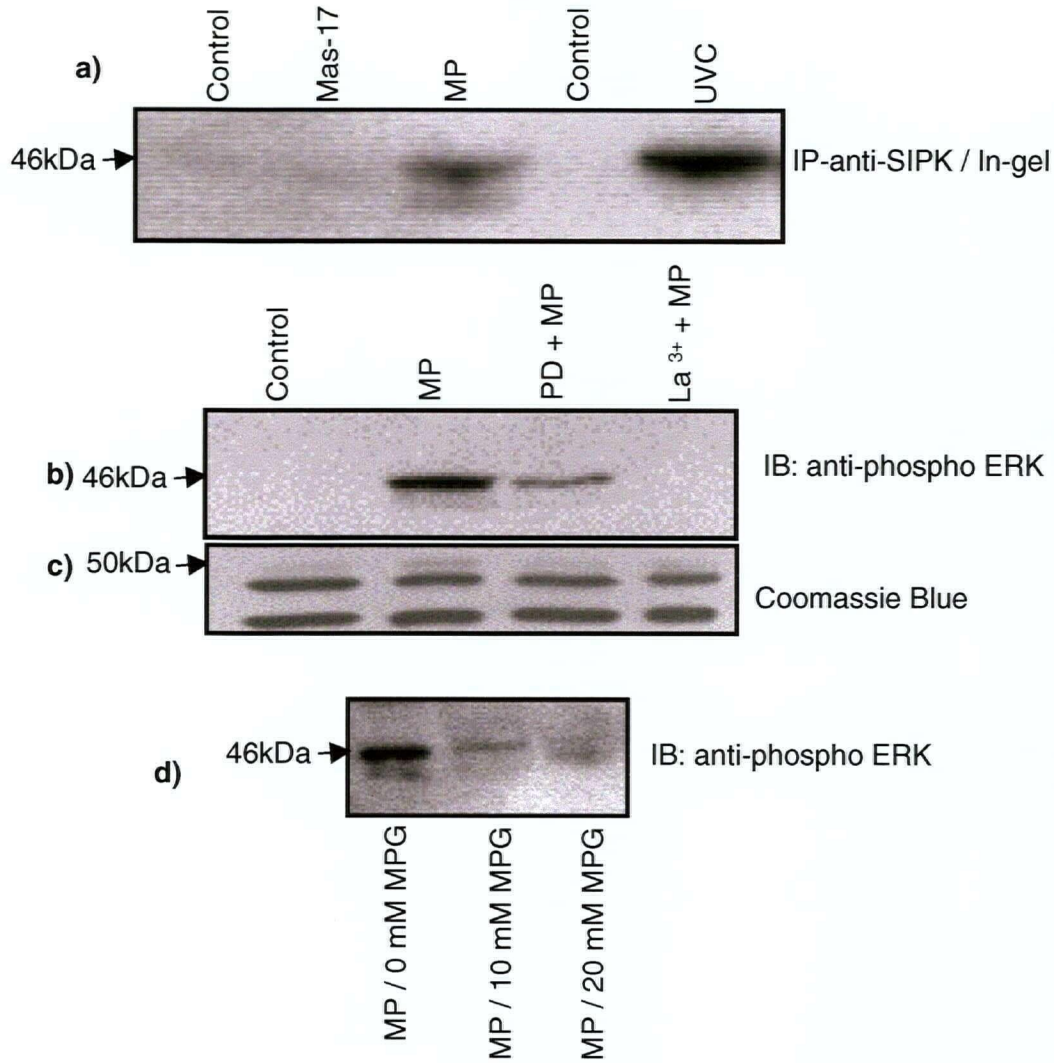

Figure 4. 2 MP, but not the less active analog (Mas-17), rapidly activates an MAP kinase in WT tobacco suspension-cultured cells. Figure legend on following page.

Figure 4. 2 MP, but not the less active analog (Mas-17), rapidly activates an MAP kinase in WT tobacco suspension-cultured cells. (**a**), Extracted proteins (40 µg) from these same samples were immunoprecipitated using specific anti-SIPK antibodies (5 µg), and the precipitate was assayed for in-gel kinase activity. MBP-phosphorylation was evident in MP-treated (5 μM for 1 min) tobacco cells, but absent from Mas-17 treated cells. Control cells were treated with water, the vehicle for MP treatment. UVC-irradiated tobacco cells also displayed MBP-phosphorylation activity and extracts of these cells were used as an in-gel size standard. Protein extracts from both controls, MP- and UVC-exposed cells, were analyzed by the MAPK phosphorylation assay. (**b**), MP-induced activation of SIPK is dependent on Ca^{2+} ions, and an upstream MAPKK. Protein extracts (20 µg) from suspension-cultured tobacco cells that had been pretreated with either La^{3+} (5 mM, 15 min), or the MEK 1&2 inhibitor, PD98059 (100 µM, 60 min) or followed by MP treatment (5 µM, 1 min) were analyzed via immunoblotting using anti-pERK 1&2 antibodies. Pretreatment of tobacco suspension cultured cells with either La^{3+} or PD interdicted the ability of MP to induce the activation of SIPK. (**c**), The Coomassie Brilliant Blue-stained membrane is used as a loading control. (**d**), MP-induced activation of SIPK was also inhibited by pretreatment of the tobacco suspension-cultured cells with MPG (10 or 20 mM, 60 min) as detected by anti-pERK1&2 antibodies. All experiments were performed in triplicate with similar results.

activity (**Fig. 4.2a**). Taken together, these results indicate that SIPK is activated by MP treatment in tobacco cells.

In eukaryotic organisms, Ca^{2+} ions play important regulatory roles in a multitude of physiological processes (Lebrun-Garcia et al., 1998; Suzuki et al., 1999; Samuel et al., 2000; Miles et al., 2002). It has been shown that MP is able to induce a rapid intracellular increase in Ca^{2+} ion levels in both plants and animals (Okano et al., 1985; Franklin-Tong et al., 1996; Tucker and Boss, 1996; Takahashi et al., 1998). Ca^{2+} ions are also important in protein kinase signalling. We previously showed that oxidant-induced activation of SIPK in tobacco cells is strongly attenuated by pretreatment of the cells with either the Ca^{2+} channel blocker, La^{3+}, or the membrane-permeable Ca^{2+} chelator 1,2-bis(2-aminophenoxy)ethane-N,N,N',N'-tetraacetic acid-tetrakis (acetoxy-methyl) ester (Samuel et al., 2000; Miles et al., 2002). The report that MP induced activation of MAPK activity in tobacco is calcium-dependent (Takahashi et al., 1998) was confirmed in this study. When tobacco cells were pretreated with $LaCl_3$ (5 mM) for 15 min followed by incubation with MP (5 μM) for 1 min, immunoblot analysis revealed that La^{3+} blocked the MP-induced activation of SIPK (**Fig. 4.2b**). Since MP has been previously reported to induce a rapid influx of extracellular Ca^{2+} ions, our present data imply that this influx of extracellular Ca^{2+} ions mediates some of the downstream effects induced by the peptide, including MAPK activation.

While these results establish the importance of Ca^{2+} fluxes for signal transmission from MP to SIPK, the nature of the intervening steps remains to be defined. In canonical MAPK signalling modules, activation of a terminal MAPK is catalyzed by a cognate MAPKK. We previously reported that oxidant-induced

activation of SIPK can be blocked by PD98059, a potent and specific MAPKK inhibitor (Samuel et al., 2000). Tobacco cells pretreated with PD98059 (100 μM) for 60 min followed by MP (5 μM) for 1 min had significantly reduced MP-induced SIPK activation, indicating that this activation involves one or more MAPKK (**Fig. 4.2b**). The Coomassie Brilliant Blue-stained membrane (**Fig 4.2c**) was used as a representative loading control.

It has been reported that MP can induce a rapid and transient accumulation of ROS in plant cells (Kauss and Jeblick, 1996), mimic an elicitor-induced oxidative burst in cultured soybean (*Glycine max*) cells (Legendre et al., 1992), induce the production of superoxide-anion formation in intact mammalian HL-60 cells (Klinker et al., 1994), and elicit a hypersensitive response in isolated *Asparagus sprengeri* mesophyll cells (Allen et al., 1999). Since it is well established that H_2O_2 and $^{\bullet}O_2$ can induce the activation of MAPKs in both plants and animals, we investigated the possibility that MP-induced ROS production might be involved in its ability to activate SIPK.

Extracted proteins (20 μg) from suspension-cultured tobacco cells that had been pretreated with the free radical scavenger, *N*-(2-mercaptopropionyl)-glycine (MPG; 10 or 20 mM) for 60 min, followed by MP (5 μM) for 1 min, were analyzed by immunoblotting using anti-pERK 1&2 antibodies. The control cells were treated only with MP (5 μM) for 1 min. MPG-treated cells showed a marked suppression of SIPK activation compared to control cells (**Fig 4.2d**). The use of a different free radical scavenger, *N*-acetyl cysteine, gave similar results (data not shown).

4.4 Discussion

Our findings indicate, at least with respect to the canonical heterotrimeric Gα and Gβ species in *Arabidopsis*, that neither MP action nor oxidant-induced activation of AtMPK6 requires a functional heterotrimeric G protein. While *Arabidopsis* has a single canonical Gα-subunit gene, there are three other genes (*XLGPA1-3*) that share some deduced amino acid sequence identity to GPA1 in their carboxy-terminal halves (Lee and Assmann, 1999; Assmann, 2002). By extending our current understanding of G protein action from metazoans to *Arabidopsis*, we conclude that it is unlikely that the MP effects we observe here are dependent on one of these other unusual putative Gα-subunits. Since Gβ-subunits are required for Gα function, and there is a single G-β gene in *Arabidopsis*, the observed MP effects in the absence of AGB1 (**Fig. 4.1b**), infer a mode of action independent of a heterotrimeric G protein complex, regardless of the Gα-subunit composition. However, we emphasize that the results do not preclude a role for a heterotrimeric complex in MAPK signalling.

In addition, we have demonstrated in tobacco suspension-cultured cells that an influx of extracellular Ca^{2+} ions plays an essential role in the activation of SIPK, the AtMPK6 orthologue by both MP and ROS. However, the calcium-dependent step has not been identified. Plants contain many calcium-dependent protein kinases whose roles remain undefined, so it is possible that activation of one or more of these is required in order for the input signal to reach the MAPK module(s). It is also possible that an MP-induced Ca^{2+} influx could affect the intracellular redox environment by stimulating ROS formation through the calcium-regulated NADPH oxidases.

In aequorin-transformed tobacco cells, the MP-induced oxidative burst was inhibited by Ca^{2+} chelators or Ca^{2+} channel blockers (Chandra and Low, 1997), and movement of exogenous Ca^{2+} into the same cells initiated an oxidative burst in the absence of MP. Since addition of catalase had no effect on the influx of Ca^{2+} in these same tobacco cells, the Ca^{2+} ion influx was placed upstream of the ROS burst. By extension, this model would place the ROS signal generation, whether MP- or oxidant-induced, upstream of MAPK activation, which is fully consistent with the suppressive effect of free radical trapping reagents.

MP and its active analogs have been extensively employed in studies of both plant and animal signalling networks. The work reported here demonstrates that, at least in plants, MP clearly has the ability to activate a central signal pathway without requiring the involvement of a canonical heterotrimeric G protein. Hence, use of MP in studies of plant cells should consider other modes of signal transmission than the prototypical Gα protein.

Chapter 5

Protein-level analysis of RNA interference-based (RNAi) suppression of AtMPK6 and AtMKK5 in *Arabidopsis thaliana*

5.1 Introduction

As described previously, ozone challenge has been shown to rapidly activate MAPK signalling in plants through a process which requires ROS accumulation, receptor activation, calcium influx and activation of one or more upstream MAPKKs (Samuel et al., 2000; Miles et al., 2002). However, while several studies have demonstrated that ozone and other oxidizing agents induce MAPK activation, very little information is known as to the roles of these individual MAPKs in response to oxidative stress.

Dessikan et al. (1999) was the first to demonstrate that treatment of *Arabidopsis* suspension-cultured cells with hydrogen peroxide could induce the activation of a MAPK. Kovtun et al. (2000) through transient expression studies in protoplasts, provided evidence for specific activation of MPK6 and MPK3 by hydrogen peroxide. Hydrogen peroxide has also been shown to induce the activation of the upstream *Arabidopsis* MAPKKK, ANP1 (Kovtun et al., 1999), which led to the subsequent activation of both MPK6 and MPK3. Ectopic expression of a constitutively active ANP1 was able to mimic this hydrogen peroxide effect, inducing expression of a reporter gene under the control of the GST6 promoter, which is an oxidant stress-response gene (Kovtun et al., 1999). MPK6 thus appears to be central to oxidant-

induced signalling making it a prime candidate for further analysis. Recently, it was shown that OXI1, a serine/threonine kinase is needed for full activation of MPK3 and MPK6 by hydrogen peroxide (Rentel et al., 2004) in *Arabidopsis thaliana*.

To obtain a better understanding of the role played by MPK6 in mediating cellular responses to oxidant signalling, I used RNAi technology to produce a MPK6, loss-of-function genotype in *Arabidopsis* (Columbia). The RNAi-MPK6 plants were found to be more sensitive to ozone than WT plants. When examined at the MAPK-level following treatment to ozone, the RNAi-MPK6 genotype displayed a more intense and prolonged activation of MPK3, indicating that MPK6 may be involved in the regulation of this related MAPK, at least in an oxidant-response context.

In contrast to what is known about the structure of the MAPK cascades connecting pathogen/elicitor recognition to activation of MPK3 and MPK6, which has been more fully examined, the identification of the cognate MAPKK(s) involved in the oxidant-induced activation of MPK3 and MPK6, remains unclear. In *Arabidopsis*, activation of MPK3/MPK6 by elicitor treatment with a flagellin peptide (flg22) appears to involve two closely-related upstream MAPKKs, MKK4 and MKK5, that form part of a signalling module consisting of MEKK1, MKK4/MKK5, and MPK3/MPK6 (Asai et al., 2002). Flagellin-22, like other elicitors, elicits both rapid changes in protein phosphorylation and an oxidative burst in challenged cells, indicating a logical link between elicitor-induced signalling and oxidant-induced signalling. Consistent with this, stable over-expression of constitutively activated forms of either MKK4 or MKK5 led to increased activation of MPK3 and MPK6, with an associated oxidative burst and lesion formation (Ren et al., 2002). While both MKK4 and MKK5 thus have the ability

to serve as upstream activators of MPK3 and MPK6 in the context of elicitor response it is not known whether they also control activation of these MAPKs in response to direct oxidant challenge. In addition, since their role in transducing pathogen-related signals was only tested by ectopic over-expression, it is uncertain whether these two closely-related MKKs are functionally fully redundant, or whether they possess some differentiated properties that only become apparent under physiological conditions.

To examine this question, I utilized an RNAi-MKK5, loss-of-function genotype, which was produced in the same manner as the RNAi-MPK6, to specifically manipulate the expression of MKK5 in *Arabidopsis*. My preliminary data shows that even partial silencing of MKK5 is sufficient to render the transgenic genotype highly susceptible to ozone damage, as determined by visible leaf damage and abnormally high levels of hydrogen peroxide accumulation in leaf tissue. MKK5 suppression also interfered with ozone-induced activation of the downstream MAPKs, MPK3 and MPK6. These data point to a possible non-redundant role for MKK5 in the overall response to oxidant-induced stress.

Physiologically, it is well established that oxidant stress triggers a wide range of remedial responses in plant cells, including enhancement of the anti-oxidant capacity and suppression of primary metabolic functions such as photosynthesis (Rao et al., 1996; Saitanis, et al., 2001). These responses are frequently associated with changes in the transcriptional activity of the relevant genes (Conklin and Last, 1995; Sharma and Davies, 1997) changes which may, in turn, impact the abundance of the encoded proteins. Protein phosphorylation often plays an integral role in eukaryotic transcriptional regulation (Johnson and Lapadar, 2002; Yang et al., 2004), and

activation of mammalian MAPKs, in particular, has been shown to rapidly modify the function of a variety of transcription factors and associated proteins (Chong, et al., 2003; Tanoue and Nishida, 2003). Activation of MPK6 by oxidant challenge would therefore be anticipated to result in rapid phosphorylation of MPK6 targets in the cell, and these modifications are likely to effect changes in both the cell's transcriptome and proteome. However, the identity of those putative MPK6 targets remains unknown.

To gain additional insight into the role of AtMPK6 in transducing ozone derived signals, I made a transcriptional and proteomic profile comparison of WT and RNAi-MPK6, plants both before and after (2 h and 8 h) treatment with 500 ppb ozone. The transcript profiling data is still undergoing analysis, and will be reported elsewhere. For proteomics profiling, I employed isotope-coded affinity tagging (ICAT) analysis (Gygi et al., 1999; Li et al., 2003), a method which enabled me to both identify and quantify alterations in protein expression between WT and AtMPK6-RNAi genotypes in response to ozone challenge.

5.2 Materials and Methods

5.2.1 RNA extraction and RT-PCR

RNA was extracted from leaf tissue of five-week-old *Arabidopsis thaliana* cv Columbia plants using the RNeasy Plant Mini Kit (Qiagen) according to the manufacturer's protocol (leaf tissue ~100 mg). Reverse transcription-polymerase chain reaction (RT-PCR) was accomplished by using a First-strand cDNA Synthesis

Kit (Amersham Pharmacia Biotech). A total of 0.2 μg RNA was used in a 15 μl first-strand cDNA reaction.

5.2.2 RNAi construct

The open reading frames of both MPK6 and MKK5 were amplified using the reverse transcriptase-mediated PCR method with gene-specific primers and RNA isolated from non-treated 5-week-old *Arabidopsis thaliana* cv Columbia leaves. The double-stranded RNA interference (dsRNA) constructs were produced via a PCR-mediated approach using the amplification products from a unique N-terminal region (300 bps for MPK6 and 307 bps for MKK5) spanning a portion of the 5'- untranslated region and adjacent coding region of the MPK6 and MKK5 genes respectively. A minimal intron based on the splice junctions and flanking regions belonging to the fourth intron of MPK6 was integrated into the sense strand primer. The sense strand was then amplified using a primer combination that generated an *Xho1* restriction site and an intron-*Xba1* sequence on the opposed ends of the product, whereas the anti-sense strand was amplified using a primer combination that added *BamH1* and *Xba1* restriction sites on the opposite ends of the product. These two products were cloned into Xho1/BamH1-cut Bin19/pRT101 by means of a triple ligation to place the RNAi construct under the control of the CaMV 35S promoter in a pRT101-MKK5RNAi or pRT101-MPK6RNAi plasmid. For a schematic representation of the construction of both MPK6- and MKK5-RNAi constructs, see **Fig 5.1.**

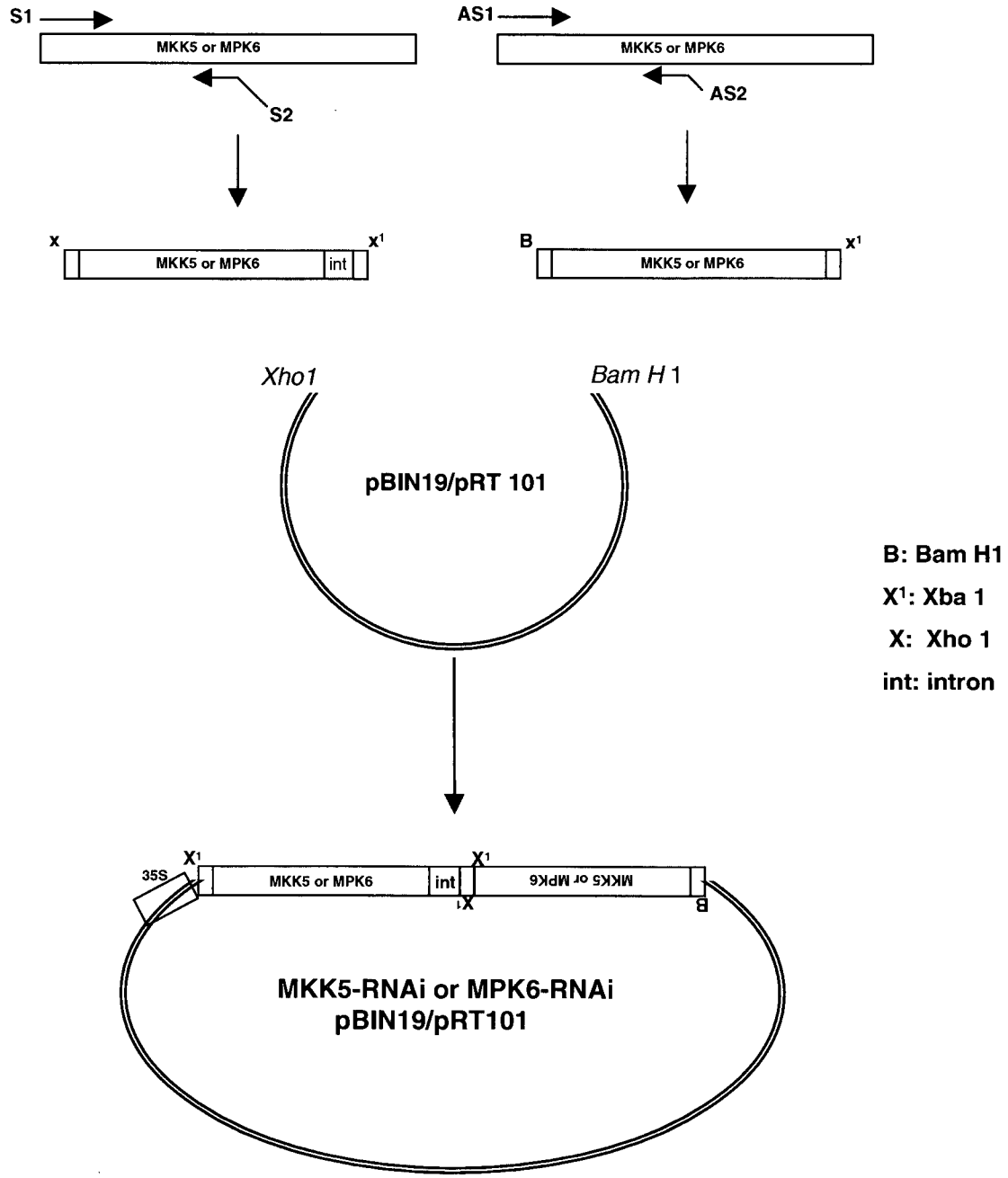

Fig. 5.1 Schematic diagram describing construction of the MKK5 / MPK6-RNAi constructs.

The following primer sets were used for the RNAi constructs:

MKK5 (**At3g21220**) (f)	5'- ccctcgagaaagccatgaaaccgattcaatctccttctgga-3'
MKK5 (r)	5'- gctctagactaagaggcagaaggaagaggacg-3'
MKK5-RNAi S1 (sense-f)	5'- ccctcgagaaagccatgaaaccgattcaatctccttctgga-3'
MKK5-RNAi S2 (sense-intron-r)	5'-gctctagactatgaagctgcaaaaac tacttacctccactttgagaaaaggacgtgacgt-3'
MKK5-RNAi AS1 (anti-sense f)	5'- cgggatccaaagccatgaaaccgattcaatctccttctgga-3'
MKK5-RNAi AS2 (anti-sense-r)	5' - gctctagacactttgagagcgaaaggacgtgacgt-3'
MKK4 (**At1g51660**) (f)	5' - gaagaacgaatcaatttaagcctg - 3'
MKK4 (r)	5' - tggggatacatgcaccatcataag - 3'
35S (f)	5'- atgacgcacaatcccact-3'
Arabidopsis histone H1 (AtH1)	5'- ggttaaagtcaaagcttcttttaaga-3'
AtH1 (r)	5'- gagtgaagaaaccatcacattata-3'
AtMPK6 **(At3g43790)** (f)	5'- ccctcgagaaagccatgaaaccgattcaatctccttctgga-3'
AtMPK6 (r)	5'- cgggatccctattgctgatattctggattgaa-3'
AtMPK6-RNAi S1 (sense-f)	5'- ccctcgagttaccggtcatggacggtggttcaggtcaa-3'
AtMPK6-RNAi S2 (sense-intron-r)	5'- gctctagactatgagctgcaaaaactacttacctcgtt agcaattttcttaatcgcaacgct-3'
AtMPK6-RNAi AS1 (anti-sense-f)	5'- cgggatccttaccggtcatggacggtggttcaggtcaa-3'
AtMPK6-RNAi AS2 (anti-sense-r)	5'-gctctagagttagcaattttcttaatcgcaacgct-3'
AtMPK4 (**At4g01370**) (f)	5'- atgtcggcggagagttgtttcg-3'
AtMPK4 (r)	5'- tcacactgagtcttgaggattg-3'
AtMPK10 (**At3g59790**) (f)	5'- atggagccaactaacgatgctg-3'
AtMPK10 (r)	5'- agc tcc aga agc aaa cga agc -3'

Fig. 5.2 List of primers used for both the construction of the RNAi (MKK5 and MPK6) constructs and for RT-PCR screening.

5.2.3 The AtMPK3 loss-of-function genotype

The AtMPK3 loss-of-function genotype (which was a gift from Dr. Yuelin Zhang, UBC) was produced using the Deleteagene method (Li et al., 2002) that utilizes fast neutron mutagenesis to produce random deletion libraries which can be screened for the loss of a specific gene via polymerase chain reaction (PCR), using primers flanking our target gene. The AtMPK3 gene spans 99407-100965 in the BAC F9K21 and the deletion removes bases between nucleotides 100505 and 106782 (6.3kb). These MPK3-DG plants were grown under greenhouse conditions.

5.2.4 *Arabidopsis thaliana* transformation

Arabidopsis thaliana cv Columbia plants that were used for inoculation with *Agrobacterium tumefaciens* were grown under greenhouse conditions. Transformation was carried out by the floral-dip method (Clough and Bent, 1998). When the primary inflorescence reached a height of 5 to 10 centimeters, the bolting stems were clipped to enhance the growth of multiple secondary bolts. Within 6 to 8 days following clipping, the plants had ~25% of their floral clusters open and were ready for floral dipping.

Competent *Agrobacterium tumefaciens* (EAH105) cells were transformed by a freeze-thaw transformation method (Holsters et. al., 1978). Cultures carrying either the AtMPK6-RNAi or AtMKK5-RNAi construct were grown overnight at 25-28°C in LB medium containing 50 μg/ml each of kanamycin and rifamycin. Cultures were typically started from a 1:1000 dilution of a smaller overnight culture and grown for roughly 18 to 24 hours. The cells were harvested by centrifugation (30 min at 4000 rpm) and

resuspended to an OD_{600} of approximately 0.8 in LB containing 50 g/L sucrose. Immediately before dipping, the culture was supplemented with Silwet L-77 (500 µl/L), a surfactant which aids in the transformation process by wetting the tissue and allowing better access by the bacteria.

For the floral dipping, the inoculum culture was transferred to a 300 ml breaker, and the plants were inverted and flowers held in the culture suspension for 3 to 4 seconds, with gentle agitation. The dipped plants were then placed in boxes and covered with black plastic bags for approximately 24 hours to maintain high humidity and protect them from direct sunlight. The plants were then watered and returned to normal growth conditions. To help increase the transformation rate, previously dipped plants were sometimes re-dipped (7 days after this first dipping) into a freshly prepared *Agrobacterium tumefaciens* suspension, in the same manner as previously described.

The (T_1) seeds from these dipped plants (T_0) were collected, surface sterilized (chapter 2, p41) and placed in the dark at 4°C for three days. They were then spread on selection plates containing 0.5 strength MS salts (pH 5.6) with 50 µg/ml kanamycin, and 1% sucrose, solidified with 0.8% tissue culture agar. Transformants were identified as kanamycin-resistant seedlings that produced normal green leaves on this medium (**Fig 5.3**). These putative transformants (T_1) were transferred into heavily moistened soil at the 4- to 6-leaf stage (usually 3 - 4 weeks post-germination). The seedlings were then grown under a clear plastic cover (sprayed with water on its inside surface) to increase the relative humidity, for three days post-transplantation.

On the fourth day, the cover was lifted approximately one centimeter, to allow the seedlings to adjust to greenhouse or growth chamber conditions. (T_1)

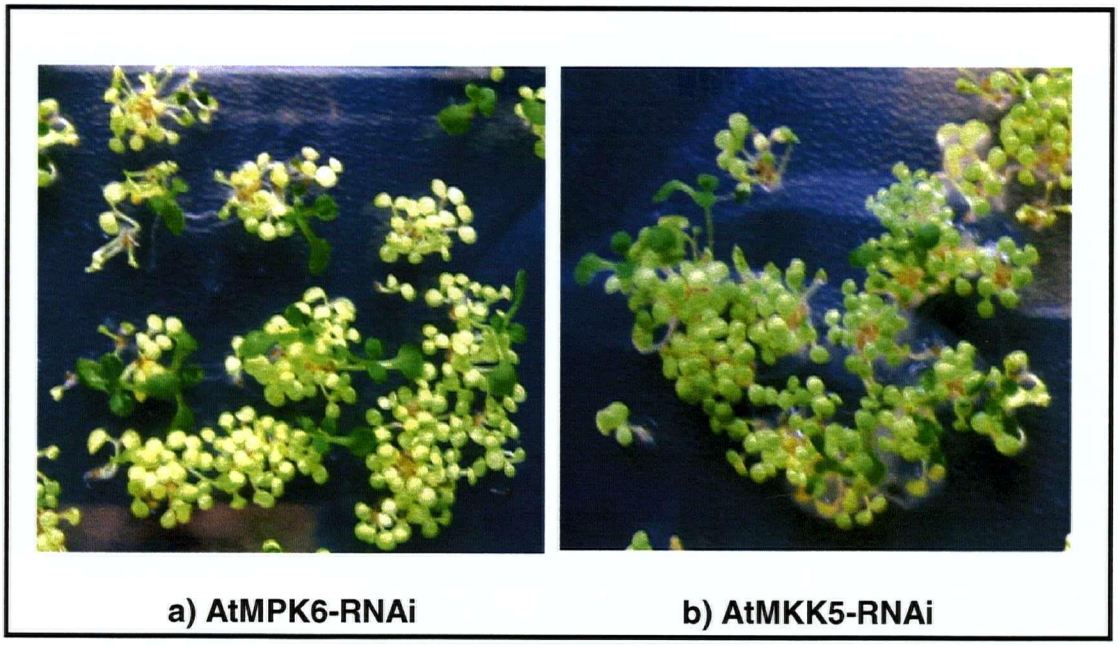

Fig. 5.3 T_1 generation of AtMPK6-RNAi (a) and AtMKK5 (b) seedlings on selective plates. Putative transformants have green leaves and a developing root mass.

5.2.5 Ozone fumigation

Arabidopsis thaliana cv Columbia plants (WT, MPK6-RNAi, MKK5-RNAi and MPK3-DG) were grown either on selection plates or in soil, under environmentally controlled conditions (25/20°C, 16 hr light / 8 hr dark cycle), or under greenhouse conditions. Three or five-week-old plants were fumigated with ozone in a flow-through chamber for different times as previously described for tobacco (*Nicotiana tabacum*) plants (Samuel et al., 2000) and foliage was then harvested, frozen in liquid nitrogen and stored at -80°C. Ozone was generated with a Delzone ZO-300 ozone generating

sterilizer (DEL industries) and monitored with a Dasibi 1003-AH ozone analyzer (Dasibi Environmental Corp.).

5.2.6 Protein extraction

Protein extraction was performed in the same manner as in Cchapter 3 (p70).

5.2.7 In-gel kinase assay

The in-gel kinase assay was performed in the same manner as in Chapter 2 (p45).

5.2.8 Immunoprecipitation and in-gel kinase assays

The immunoprecipitation and in-gel kinase assays were performed in the same manner as in Chapter 2 (p45).

5.2.9 Western blotting analysis

Western blotting analysis was performed in the same manner as in Chapter 2 (p44). The amount of crude protein used was 20 or 40 μg.

5.2.10 3, 3'- Diaminobenzidine (DAB) staining for H_2O_2

The presence of H_2O_2 was visualized *in situ* via DAB staining. *Arabidopsis* rosette leaves were collected 4 hr post-ozone fumigation (500 ppb) from five-week-old *Arabidopsis* WT, MPK6-RNAi, MKK5, and MPK3-DG genotypes. The leaves were vacuum infiltrated with DAB (1 mg/ml) solution, held in the light for 4 hr under high humidity, and then fixed in a solution of ethanol/lactic acid/glycerol (3:1:1 v/v) for two days. Finally, the stained leaves were cleared in 100% methanol and the results recorded photographically.

5.2.11 Chemicals and reagents

Bradford protein assay reagent, 3, 3'-diaminobenzidine, and Murashige and Skoog (MS) cell culture medium were obtained from Sigma (St. Louis, MO., USA). Complete^{TM} protease inhibitor cocktail was purchased from Boehringer Mannheim, (Montreal Canada). Anti-pERK 1&2 antibodies were purchased from New England Biolabs (Beverly, MA, USA), and peroxidase-conjugated goat anti-rabbit IgG from Dako Corp. (Carpinteria, CA, USA). Enhanced Chemiluminescence (ECL) detection reagents were purchased from Amersham Corp. (Quebec, Canada).

5.2.12 ICAT Protocol

The ICAT work was carried out at the Institute for Systems Biology, Seattle WA with the cooperation of G. Sperrazzo (assisted me with the labeling step), S. Donohoe (ran the MS/MS runs for my samples), Dr. J. Ranish (showed me how to interpret my ICAT results), and Dr. R. Aebersold (the work was accomplished in Dr. A.'s lab). WT and AtMPK6 sample proteins (750 μg each) were dissolved separately in 300 μL ICAT™ labeling buffer (6 M urea, 0.05% SDS, 200 mM Tris pH 8.3, 5 mM EDTA). Tris (2-carboxyethyl) phosphine hydrochloride (Pierce, Rockford, IL) was added at a final concentration of 5 mM to both solutions, which were then incubated at 37°C for 30 minutes to promote disulfide reduction. In darkness, 1.225 μmol d_0 (light, ^{12}C) ICAT™ label (Applied Biosystems) was added to the WT samples and 1.225 μmol of d_9 (heavy, ^{13}C) ICAT™ label was added to AtMPK6 samples. The samples were then agitated in darkness at room temperature for 90 minutes to promote labeling. A 10-fold excess of DTT (12.25 μmol) was then added to the labeled protein samples followed by a further incubation at room temperature for 5 minutes to quench the

labeling reaction. The "light" and "heavy" samples were combined in a single tube and the combined sample was diluted six-fold to achieve a final urea concentration of 1 M. Trypsin was added to the solution at a 1:50 trypsin : protein ratio and digestion was allowed to proceed overnight at 37°C.

The resulting peptide solution was passed over a PolysulfoethylA™ column (PolyLC, Columbia, MD), which was washed with solvent A (5 mM monobasic potassium phosphate, 25% acetonitrile, pH 3). The peptides were then eluted with a 50 minute biphasic gradient of 0-25 % solvent B (solvent A + 600 mM potassium chloride) in 0-30 minutes followed by 25-100 % solvent B in 30-50 minutes, at a constant flow rate of 0.44 ml/min. Eluent fractions (0.44 ml) were collected and neutralized with 44 μl of sodium phosphate, pH 10. They were subsequently passed over an immobilized avidin cartridge (Applied Biosystems, Framingham, MA), washed with 2X phosphate-buffered saline, then washed with water, and finally washed with 50 mM ammonium bicarbonate in 20 % methanol pH 8.3. Biotinylated peptides were eluted from the avidin matrix with a 30 % aqueous acetonitrile, 0.4 % trifluoroacetic acid solution and dried down. All of the preceding peptide chromatography steps were performed automatically on a Vision™ multidimensional high-performance liquid chromatography instrument (Applied Biosystems).

The dried sample pellets were dissolved in cleavage buffer (Applied Biosystems) in order to remove the biotin portion of the ICAT™ tag. The samples were again dried down and then re-dissolved in 0.2 % acetic acid and transferred to autosampler vials for LC-MS/MS analysis. An LCQ DECA ion trap mass spectrometer (Thermo Finnigan, San Jose, CA) was used with an in-house fabricated micro-

electrospray source and an HP1100 solvent delivery system (Agilent, Palo Alto, CA). Samples were automatically delivered by a FAMOS autosampler (LC Packings, San Francisco, CA) to a 100 µm internal diameter fused silica capillary pre-column packed with 2 cm of 200 Å pore-size Magic C18AQ™ material (Michrom Bioresources, Auburn, CA) as described in Yi et al., (2003). The samples were washed with solvent A (0.1 % formic acid, 5 % acetonitrile) on the pre-column and then eluted with a gradient of 10-35% solvent B (100% acetonitrile) over 128.5 minutes that resolve the peptide mixture on a 75 µm x 14 cm fused silica capillary column packed with 100 Å pore-size Magic C18AQ™ material (Michrom). The eluate from this column was fed into the mass-spectrometer at a constant column-tip flow rate of ~300 nl/min. Eluting peptides were analyzed by µLC-MS and µLC-MS/MS techniques as described previously (Gygi et al., 1999).

The MS/MS peptide sequences were identified by searching the collision-induced dissociation (CID) spectra against the TIGR *Arabidopsis* Annotation: ATH1.pep database using SEQUEST™ (Keller et al., 2002). The results of the database search were validated using the PeptideProphet software program (Keller et al., 2002; and von Haller et al., 2003). PeptideProphet assigns to each peptide identified a probability that it has been correctly identified based upon its SEQUEST scores and the features of the designated peptide, including the number of tryptic termini. A total of 1948 0 hr-air, and 5611 8 hr-O_3 individual spectra were retained. There were more 8hr proteins identified, which may have been due to more efficient labeling with the 8hr samples. ProteinProphet software (von Haller et al., 2003; and Nesvizhskii et al., 2003) was used to group the peptides and to compute the correct

protein assignment of each peptide. Proteins which were represented by high percent coverage, numerous peptides, or very strong single ion elution profiles were classified as abundant. ASAPRatio (Li et al., 2003) software was used to perform relative quantification between heavy and light ICAT tagged proteins.

Evaluation of the significance of abundance change for each identified protein was carried out in the following manner. A major application of quantitative proteomics is the identification of changes of protein expression in different cell states by accurately measuring the relative abundance of a large number of proteins present in two or more samples (Aebersold and Mann, 2003). In the absence of suitable software tools, protein abundance ratios are typically used to identify differentially expressed proteins without considering the effect of the confidence level of the protein abundance ratios (Han, et al., 2001; Ranish, et al., 2003; Blagoev, et al., 2003). The ASAPRatio program adopts a more sophisticated statistical approach to improve this analysis. It is valid if the expression level of a large number of identified proteins does not change between the two cell states. In this case, a distribution of the logarithm (base 10) of all unique peptide ratios in an LC-ESI-MS/MS experiment is first generated. Assuming the dominant peak in the distribution is attributed to proteins of unchanged abundance, the ASAPRatio program fits the peak automatically with a normal distribution.

$$n(r;A,r_0,\sigma) = A \times \exp[-(\log(r/r_0))^2/2\sigma^2] \qquad (1)$$

Here r_0 is the most likely abundance ratio of a protein of unchanged abundance. The validity of using a normal distribution to model the data is justified by the following consideration: Due to natural variation in labeling efficiency, the logarithm (base 10) of

unique peptide ratios belonging to proteins of unchanged abundance spreads into a distribution. On the basis of the central limit theorem, (Taylar, 1997) this distribution is approximately normal as long as the data set is large. The r_0 value can be used to normalize protein abundance ratios to correct for any systematic errors introduced during sample handling (Von Haller et al., 2003). For a protein abundance ratio r_P and its error Δr_P, the normalized ratio is given by $\hat{r}_P = r_P/r_0$, and its associated error is given by $\Delta\hat{r}_P = \hat{r}_P\sqrt{(\Delta r_P/r_P)^2+(\Delta r_0/r_0)^2}$, where Δr_0 is the fitting error of r_0. The probability of the protein not changing in abundance is described statistically by the p value, which is given by

$$p = \mathrm{erfc}[|\log(r_P/r_0)|/\sqrt{2((\Delta\log r_P)^2 + (\Delta\log r_0)^2 + \sigma^2)}] \quad (2)$$

where erfc(x) is the complementary error function (Teukolsky, 1997), $\Delta\log_{10} r_P = 0.4343\Delta r_P/r_P$ and $\Delta\log r_0 = 0.4343\Delta r_0/r_0$. This formula is derived from the normal distribution in eq 1. Its accuracy in describing a particular protein depends on how well the normal distribution in eq 1 fits the overall data of unchanged proteins. Certain p values can be chosen as significant in assessing protein abundance changes. Besides the protein abundance ratio, the error of the protein abundance ratio and the background distribution all affect the p value. A protein with a large ratio may still be considered as not significantly distinguished from the background if its ratio error is too large or if the background distribution is too wide. The evaluation of p values provides a reliable method for assessing the significance of protein abundance changes in large-scale protein profiling experiments and for making data in different quantitative

data sets transparently comparable. The result of this final step of the process is a calculated significance of abundance change for each identified protein.

5.3 Results

5.3.1 MPK6

Ozone has the ability to activate *Arabidopsis* protein kinases (approximately 44- and 46-kDa) capable of phosphorylating MBP, a known substrate eukaryotic MAPK (**Fig 5.4, left**). Using anti-AtMPK6 antibodies (Miles et al., 2004) raised against the N-terminal portion of the AtMPK6 polypeptide, I was able to immunoprecipitate the 46kDa MBP-phosphorylating band (**Fig. 5.4, right**), indicating that this kinase is most likely AtMPK6, the ortholoue of SIPK from tobacco (*Nicotiana tabacum*).

Arabidopsis plants transformed with the MPK6-RNAi construct (**Fig. 5.5a**) yielded ~3% putative transformants (determined by kanamycin-resistant seedlings devided by the non-kanamycin-resistant seedlings) (**Fig. 5.3**), which were transferred to soil and allowed to grow for an additional three weeks. The transplanted MPK6 (T_1) seedlings had a survival rate of ~30%, which is markedly lower than the survival rate of WT seedlings.

To determine the success of MPK6 silencing, two rosette leaves were then excised from each of the (T_1) plants after brief (10 minute) ozone fumigation (200ppb) and the extracted proteins were subjected to Western blot analysis using anti-pERK antibodies. We decided to use a lower concentration of ozone to gas these (T_1) seedlings so as to lessen the chance of killing the plants. A number of putative MPK6-silenced plants showed loss of the 46kDa MPK6 protein band on the Western blots.

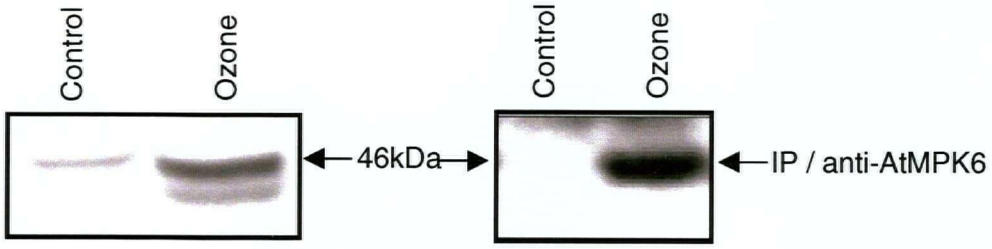

Fig. 5.4 Ozone is able to induce the activation of two MBP-kinases in *Arabidopsis* seedlings. left, MBP-phosphorylation was evident in ozone-treated WT *Arabidopsis* seedlings, but was largely absent in untreated plants. **right,** Extracted proteins (40 µg) from these same samples were immunoprecipitated using specific anti-AtMPK6 antibodies (5 µg) (Miles et al. 2004), and the precipitate was assayed for in-gel kinase activity as described in the Materials and Methods section. This is the same picture as Fig. 2.1.

The results for the two MPK6-RNAi parental lines R (6-7) and R (6-8), which were the main lines used for this study, are shown in (**Fig. 5.5b**). T_3 progeny from the (T_1) MPK6-suppressed parental lines R(6-7,-8) retained the same level of MPK6 suppression (**Figs. 5.6a and 5.7a**) respectively. MPK4 is very closely related to MPK6, sharing 68% identity at the nucleotide level. The double-stranded RNA interference (dsRNAi) construct directed at MPK6 targeted a unique N-terminal region of the gene which possesses only 66% identity to MPK4 in the same region. To confirm that the RNAi construct specifically targets MPK6, the expression levels of MPK6 and MPK4 were analyzed in the transgenic line MPK6-7 (T_3) (the central parental line of this study). RT-PCR analysis showed that the expression of MPK6 appears to be completely abolished (**Fig. 5.5c**), while the expression of MPK4 was unaffected in this background **(Fig. 5.5d)**.

In addition to the MPK6- and MKK5-RNAi genotypes, I attempted to make an empty vector (pRT101) line, without success. I screened ~5,000 T_1 seeds, from 25 T_0 plants, without seeing a single successful transformation. However, I did have available primary (T_1) transformants which carried the MPK6-RNAi construct, but did not show any MPK6 suppression (for example, line R(6-2)), as determined by Western blotting analysis (**Fig. 5.5b**) and RT-PCR (**Fig. 5.5e**).

5.3.2 MPK6 is important in the activation of MPK3

Samuel & Ellis (2002) recently showed that the activation of WIPK, the tobacco orthologue of MPK3, is radically altered in a SIPK-suppressed background when the SIPK-suppressed plants are exposed to ozone. To determine if a similar response

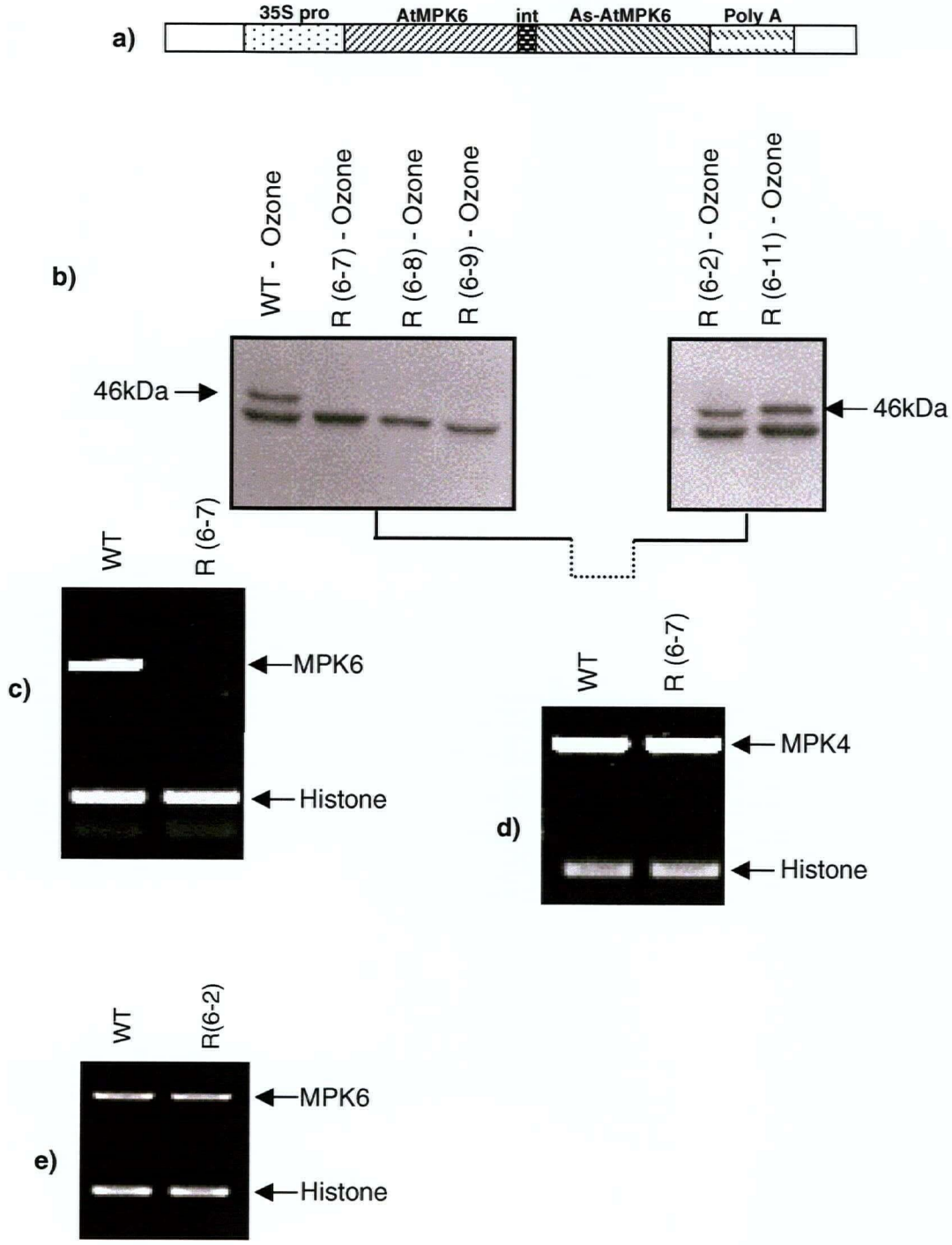

Fig. 5.5 MPK6-RNAi R(6-7) construct and loss-of-function genotype selection.
Figure legend on following page.

Fig. 5.5 MPK6-RNAi R(6-7) construct and loss-of-function genotype selection. (**a**) The MPK6-RNAi construct under the control of the 35S promoter of the *Cauliflower mosaic* virus. (**b**) Extracted proteins (30 μg) from ozone-fumigated (500ppb, 10minutes), 5-week-old (T_1) seedlings (WT and parental lines: R(2,7,8,9, and 11), and were fractionated by 10% SDS-PAGE, and transferred onto PVDF membranes. The resulting PVDF membranes were incubated using anti-phospho-ERK 1&2 antibodies. Control plants (ozone) were harvested at the same time as the ozone-treated transgenic plants. (**c**) RT-PCR of R(6-7) (T_3) shows MPK6 suppression. (**d**) The closely related MAPK, MPK4 was not suppressed in the MPK6-RNAi line R (6-7). (**e**) R(6-2) (T_2) line showed no MPK6 silencing.

could be observed in *Arabidopsis*, WT and R(6-7) plants were exposed to continuous ozone (500ppb) followed by Western blot analysis using anti-pERK antibodies. Protracted fumigation with ozone produced strong and prolonged activation of MPK3 in the R(6-7) genotype compared with that of WT plants (**Fig. 5.6a**). MPK3 remained active up to 4 hr in the MPK6-RNAi genotype, compared to only 1 hr in WT plants. The same result was observed in the R (6-8) parental line (**Fig. 5.7a**). By contrast, MPK3 and MPK6 showed WT activation profiles in non-suppressed R(6-2) plants continuously exposed to ozone (**Fig. 5.7b**).

Given the fact MPK6 plays an important role in the activation/regulation of MPK3, I wanted to next determine if MPK3 played any role in the activation/regulation of MPK6. To accomplish this, loss-of-function (MPK3)-Deleteagene (DG) (MPK3)-DG plants were exposed to continuous ozone (500ppb) for 4 hr followed by Western blotting analysis using anti-pERK antibodies. Continuous ozone exposure produced an MPK6 prolonged and heightened activation profile analogous to the response of MPK3 in the MPK6-RNAi genotype (**Fig. 5.6b**).

5.3.3 MPK6-RNAi and MPK3-DG transgenic genotypes both exhibit enhanced ozone sensitivity

To examine the impact of MAPK loss-of-function modifications on control of redox capacity, MPK6-suppressed transgenic plants (MPK6-7) from the T_3 generation, along with WT plants, were exposed to continuous ozone fumigation (500 ppb). Leaf damage was consistently observed in leaves of MPK6-RNAi (6-7) plants by 24 hr,

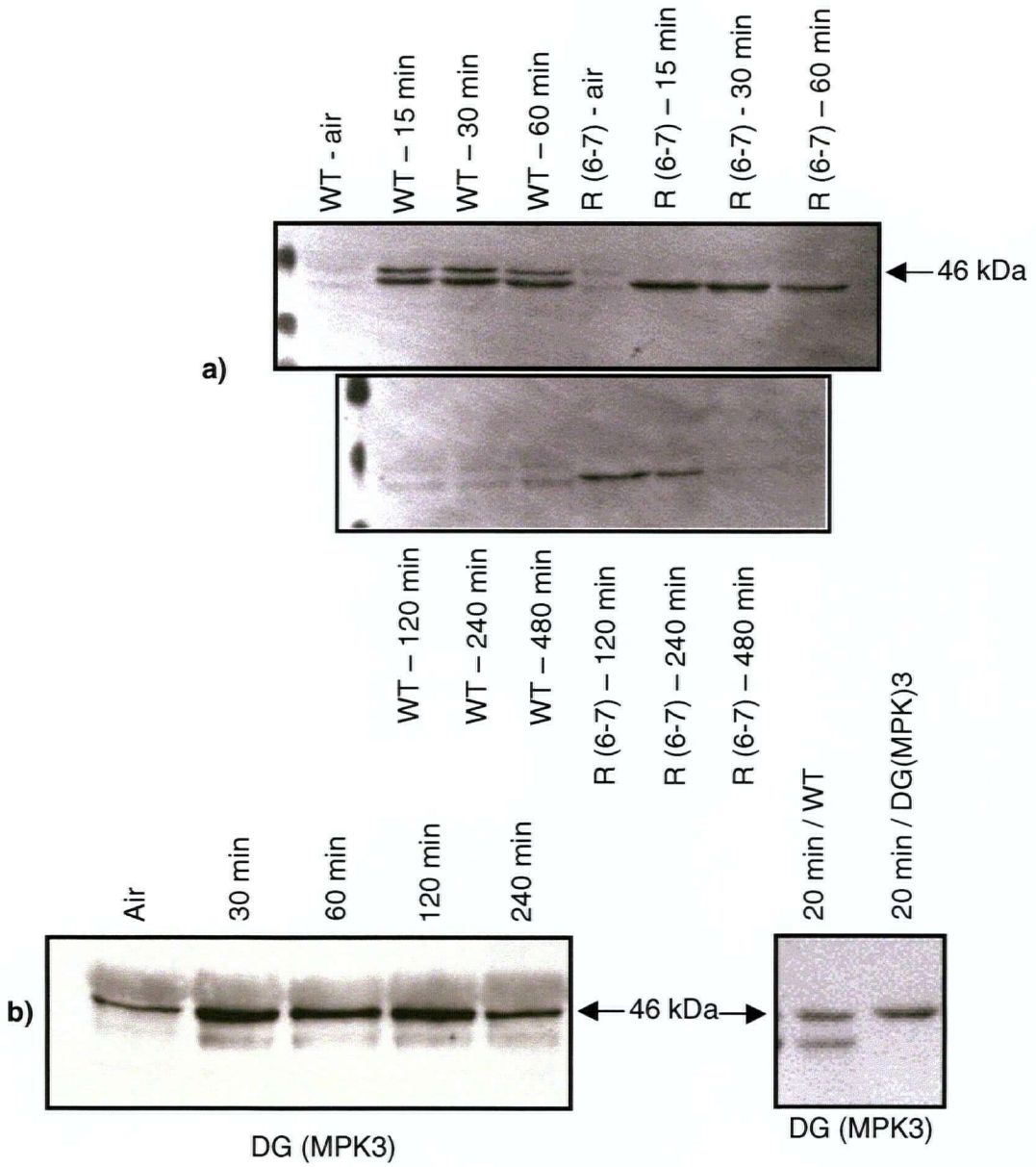

Fig. 5.6 RNAi-mediated silencing of MPK6 leads to enhanced and protracted activation of MPK3. Figure legend on following page.

Fig. 5.6 RNAi-mediated silencing of MPK6 leads to enhanced and protracted activation of MPK3. (**a**) Extracted proteins (30 µg) from ozone-treated (500 ppb, continuous) 5-week-old (T_3) seedlings (parental line: R (6-7) were fractionated by 10% SDS-PAGE, and transferred onto PVDF membranes. The resulting PVDF membranes were incubated using anti-pERK 1&2 antibodies. Control plants were harvested at the same time as the ozone-treated plants. MPK3 activation was more intense and prolonged in a MPK6-RNAi background. (**b**) Extracted proteins (30 µg) from ozone-treated DG (MPK3) plants were assayed via Western blot in the same manner as the MPK6 proteins. Activation of MPK6 was stronger and more prolonged in a MPK3- (Deleteagene)-DG loss-of-function genotype.

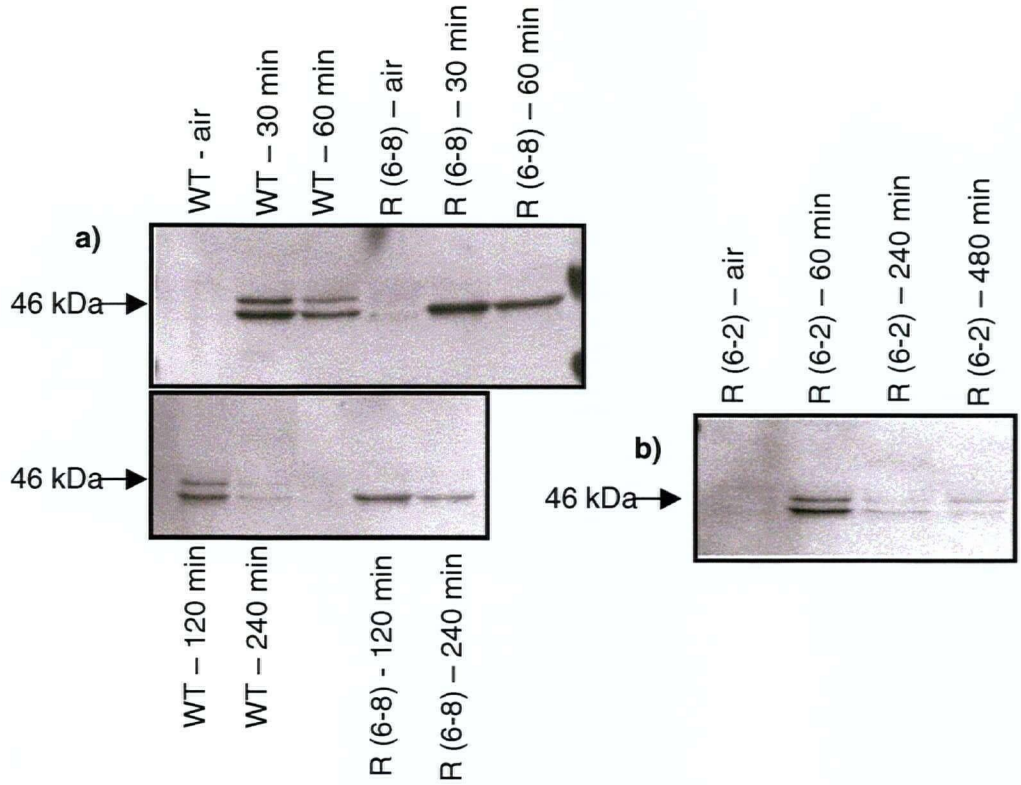

Fig. 5.7 RNAi-mediated silencing of MPK6 leads to enhanced and protracted activation of MPK3 (second parental line), but not in non-suppressed MPK6-RNAi line. (**a**) Extracted proteins (30 µg) from ozone-treated (500 ppb, continuous) 5-week-old (T_3) seedlings (parental line: R (6-8) were fractionated by 10% SDS-PAGE, and transferred onto PVDF membranes. The resulting PVDF membranes were incubated using anti-pERK 1&2 antibodies. Control plants were harvested at the same time as the ozone-treated plants. (**b**) Ozone time-course of parental line R(6-2) which did not show any MPK6 suppression in the T_2 screen.

whereas no damage was seen on WT or R(6-2) leaves (**Fig. 5.8c,d,e,f**). Only MPK6-RNAi lines that showed MPK6 silencing showed this visible leaf damage.

Interestingly, the ozone-damaged leaves on the MPK6-RNAi became very brittle, but maintained their green colour throughout their life span. This process of rapid dehydration appears analogous to the response of leaves displaying hypersensitive response (HR) cell death elicited by incompatible pathogens. Rapid dehydration is thought to play an important role in limiting the multiplication of pathogens by depriving them of water (Goormachtig et al., 2004). The ability of WT plants to withstand ozone challenge is not unlimited; when exposed to continuous fumigation at higher ozone levels (650ppb), both the RNAi and WT genotypes showed leaf damage (data not shown). Unlike the WT leaves, which became yellow and died over time as a result of this higher ozone level, the leaves of the MPK6-RNAi plants again maintained their green colour throughout their life span. I only tested this higher level of ozone treatment on WT and R(6-7) plants.

When, MPK3-DG transgenic plants were exposed to continuous ozone fumigation (500 ppb) leaf damage was again consistently observed as early as 2 hr, whereas no damage was seen on WT leaves at 4 hr or at any subsequent time (**Fig. 5.8 i,j**). Like the MPK6-RNAi plants, the damaged leaves on the MPK3-DG plants became very brittle and maintained their green colour throughout the plant's life. However, only around 80% of the MPK3-DG plants survived to produce seeds, compared to 100% for the MPK6-RNAi plants, indicating that the impact of losing MPK3 function was perhaps more severe than the loss of MPK6. Alternatively, the

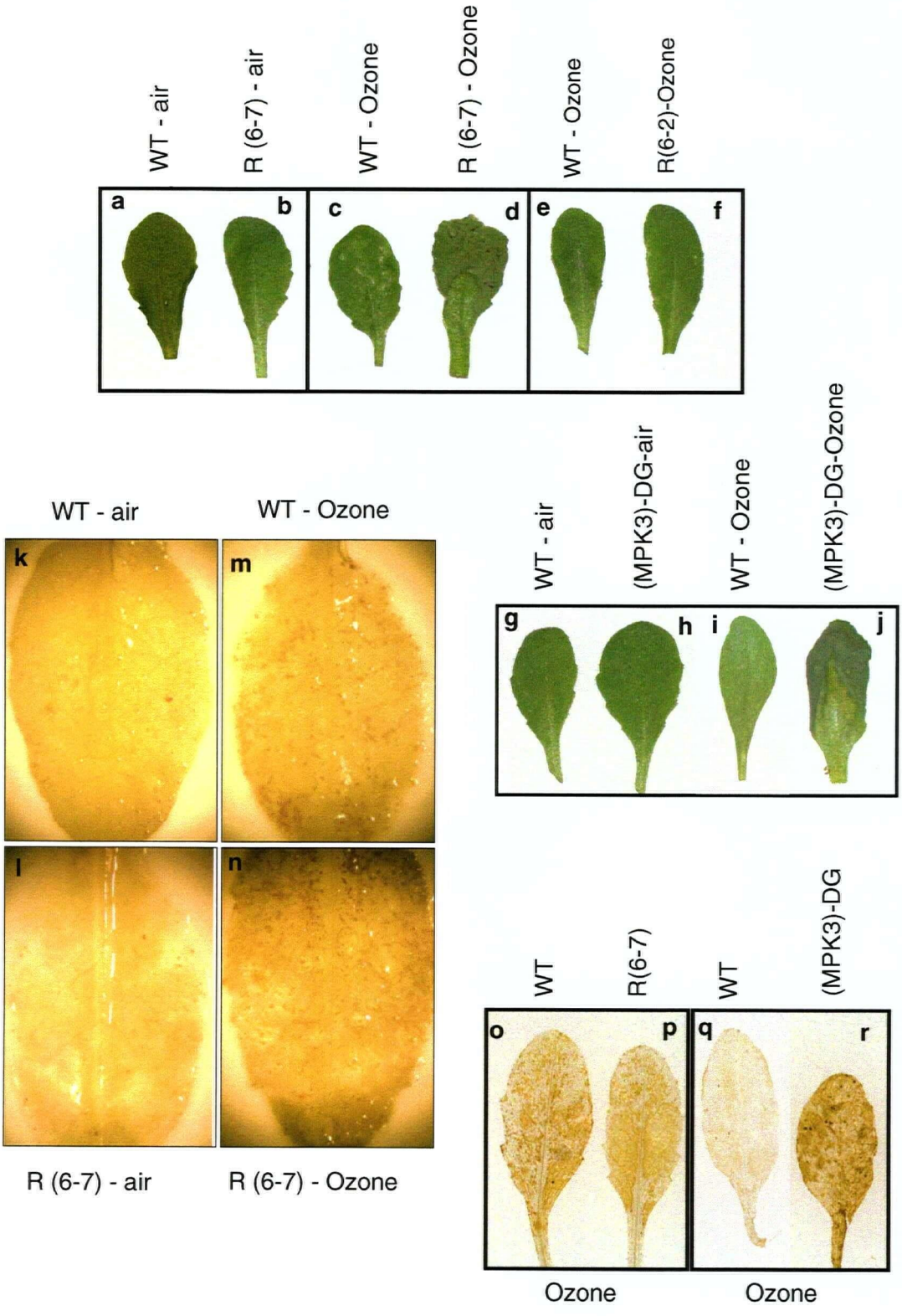

Fig. 5.8 Ozone treatment of WT and transgenic plants. Figure legend is on following page

Fig. 5.8 Ozone treatment of WT and transgenic plants (**a,c,e,g,i**) = WT, (**b,d**) = R (6-7), (**f**) = R(6-2), and (**h,j**) = (MPK3)-DG. Plants were fumigated with ozone (500ppb) for 24 hr (WT and R(6-7) or 4 hr (WT and MPK3-DG plants). All leaves were photographed immediately after ozone fumigation. 3, 3'- Diaminobenzidine staining was used to detect hydrogen peroxide accumulation in ozone-treated leaf tissue. (**k,m,o,q**) = WT, (**l,n,p**) = R(6-7), and (**r**) = (MPK3)-DG plants.

residual MPK6 activity in the RNAi plants may have buffered the impact of the MPK6 suppression. Air controls are seen in (**Fig. 5.8 g,h**).

5.3.4 Hydrogen peroxide accumulation in both MPK6-RNAi and MPK3-DG leaf tissue

Since the MPK6-RNAi and MPK3-DG transgenic plants displayed increased sensitivity to ozone, I asked whether this represented an inability of the ozone-challenged tissue to control the build-up of ROS. To examine this, I compared the patterns of hydrogen peroxide accumulation in WT, MPK6-RNAi, and MPK3-DG leaves following continuous ozone exposure.

There was little to no hydrogen peroxide detectable in untreated leaves from either WT or transgenic plants (**fig. 5.8 k,l**). However, with 8 hr of continuous ozone-fumigation (500ppb), there was an increase in DAB staining in both the MPK6 plants and the WT plants (**Fig. 5.8 m,n**), After 24 hr of ozone fumigation, the same time point that visible leaf damage started to appear on the MPK6-RNAi plants, both WT and MPK6 leaves were infiltrated with 3,3'–diaminobenzidine (DAB) solution (**fig. 5.8 o,p**). The staining patterns showed a similar level of DAB staining in both genotypes; even though, only the MPK6 leaves showed signs of visible leaf damage. It would appear from these results that the WT plants were able to maintain their cellular integrity in the face of this level of oxidant stress whereas the MPK6 plants were not.

Since the MPK3-DG plants are much more sensitive to ozone than either the WT or MPK6 plants, I selected a 4 hr time point for DAB staining. After 2 hr of ozone exposure (500 ppb) a number of the MPK3-DG plants already showed signs of visible leaf damage. And after four hours, the majority of MPK3-DG plants showed extensive

leaf damage. To determine if this leaf damage was coincident with hydrogen peroxide accumulation, I assayed ozone-treated (500 ppb, 4 hr) leaves from WT and the MPK3-DG genotype (**Fig. 5.8 q,r**). As evident in the picture shown in **Fig. 5.8**, the MPK3-DG leaves showed a greatly elevated level of DAB staining as a result of ozone exposure. A total of six whole plants per time point / per genotype were used for the DAB and ozone-sensitivity work. This was the same for the MKK5 work described below.

5.3.5 MKK5-RNAi plants, preliminary results.

Arabidopsis plants transformed with the MKK5-RNAi construct (**Fig. 5.9a**) yielded ~1% putative transformants (**Fig. 5.3**), which were transferred to soil and allowed to grow for an additional two weeks. To determine the success of suppression of MKK5, two rosette leaves were then excised from each of 46 (T_1) plants and analyzed by RT-PCR using gene-specific primers (**Fig. 5.9b**). Varying degrees of suppression were observed, but in none of the recovered lines was MKK5 expression completely silenced. Progeny (T_2) from the (T_1) MKK5-suppressed parental lines retained the same modest level of MKK5 suppression (**Fig. 5.9c**).

MKK5 and MKK4 are the two most closely related *Arabidopsis* MKKs, sharing 78% identity at the nucleotide level. The double-stranded RNA interference (dsRNA) construct directed at MKK5 targeted a unique N-terminal region of the gene which possesses only 61.8% identity to MKK4 in the same region. To confirm that the RNAi construct specifically targeted MKK5, the expression of MKK4 was analyzed in the transgenic line MKK5-2 that showed the strongest MKK5 suppression. The expression of MKK4 is not reduced in this background **(Fig 5.9c)**. It appears from this preliminary RT, that the expression level of MKK4 is greater in the R(5-2) genotype compared to

that of the WT, but this possibility, along with the MKK5 reduction in the MKK5-RNAi lines, needs to be evaluated using quantitative PCR. If MKK4 is up-regulated in the MKK5 background, it would indicate that MKK4 might have the ability to compensate for the loss of MKK5. This possibility could be assessed by use of MKK4- and MKK5-specific antibodies.

5.3.6 MKK5 plays a role in the ozone-induced activation of MAPKs

Since ozone strongly induces activation of MPK6 in WT *Arabidopsis* (**Fig. 5.4**), and MKK5 has been proposed to be an upstream activator of MPK3 and MPK6, I next evaluated the impact of MKK5 suppression on ozone-induced MAPK activation. When the transgenic (T_1) and WT genotypes were exposed to ozone (500 ppb, 10 minutes), followed by Western blotting analysis using anti-pERK antibodies, a marked decrease in the activation of these two MAPKs was observed in the more strongly MKK5-suppressed lines (**Fig. 5.10**), indicating that this particular MAPKK is necessary for full signal transmission to the target MAPKs in response to oxidant stress. The activation of these MAPKs by ozone was unaffected in lines that did not show any suppression of MKK5.

5.3.7 MKK5-RNAi transgenic plants exhibit enhanced ozone sensitivity

MKK5-2 RNAi transgenic plants from the (T_2) generation, along with WT plants, were exposed to continuous ozone fumigation (500 ppb) for four hours and examined 4 hr post-fumigation (8 hrs total response time). Extensive leaf damage was consistently observed in leaves of MKK5-RNAi plants at the 8 hr time-point, whereas no damage was seen on WT leaves (**Fig. 5.11a, b**). Even at the 4 hr time-point (i.e.

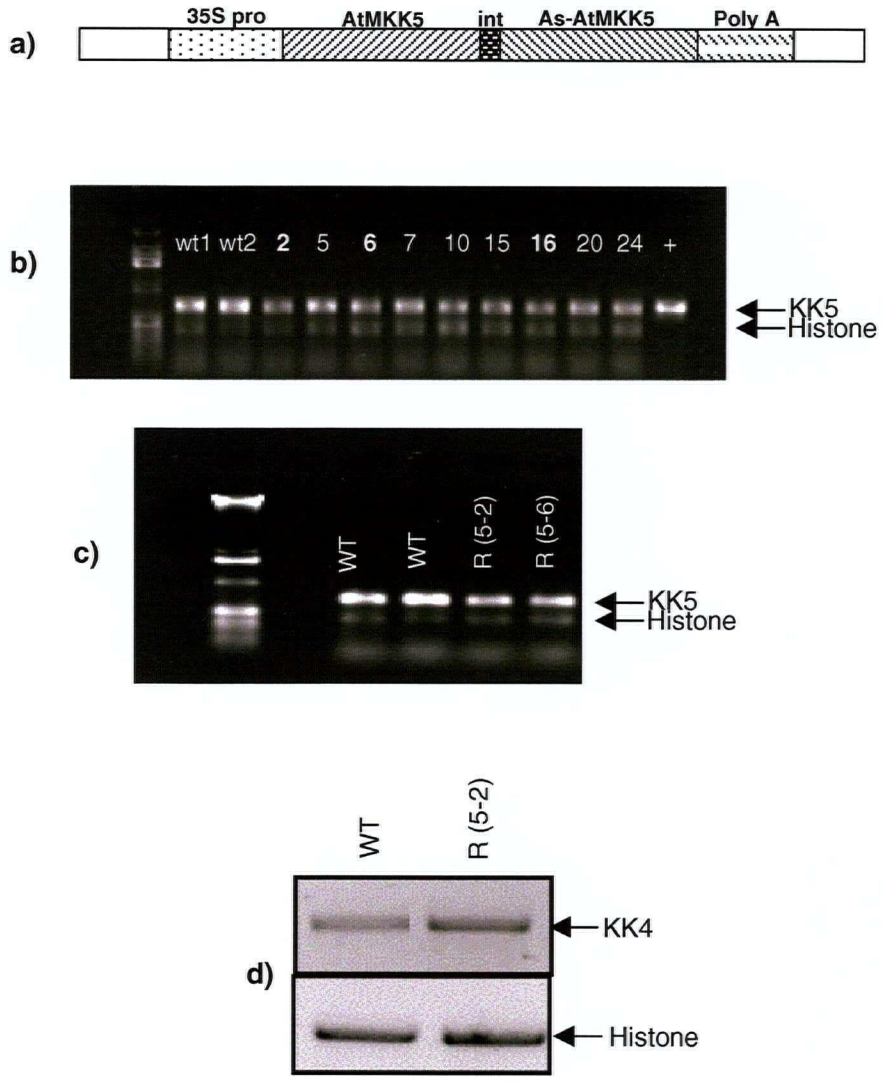

Fig. 5.9 MKK5-RNAi construct and loss-of-function genotype selection. (**a**) The MKK5-RNAi construct under the control of the 35S promoter of the *Cauliflower mosaic* virus. (**b**) Initial RT-PCR of numerous putative (T_1) MKK5 lines. (**c**) Selected (T_2) lines showed the same level of MKK5 suppression as their (T_1) parental lines, demonstrating multiple-generation suppression. (**d**) The closely related MAPKK, MKK4, was not suppressed in the MKK5-RNAi (MKK5-2).

immediately after fumigation), some of the MKK5-RNAi plants already showed visible leaf damage. After 24 hours of continuous acute ozone exposure (500 ppb), 100% of the MKK5-RNAi test plants showed visible leaf damage while WT plants showed none (data not shown).

Interestingly, just like the MPK6 and MPK3-DG plants, the ozone-damaged leaves on the MKK5-RNAi plants became very brittle, but maintained their green colour.

5.3.8 Hydrogen peroxide accumulation in MKK5-RNAi leaf tissue

Since the MKK5-RNAi transgenic plants displayed increased sensitivity to ozone, I wanted to determine whether this represented an inability of the ozone-challenged tissue to control the build-up of ROS. To examine this, I compared the patterns of hydrogen peroxide accumulation in both WT and MKK5-RNAi- suppressed leaves following ozone exposure.

When control and ozone-treated leaves from both WT and the MKK5-RNAi plants were infiltrated with 3,3'–diaminobenzidine (DAB) solution, the staining patterns revealed no detectable hydrogen peroxide in untreated leaves from either WT or transgenic plants (data not shown). However, within four hours of ozone-fumigation (500ppb), there was a marked increase in DAB staining in the MKK5-suppressed plants compared to the WT plants (**Fig. 5.11c,d**), demonstrating that the MKK5-suppressed plants were less effective at controlling the redox environment within their tissues.

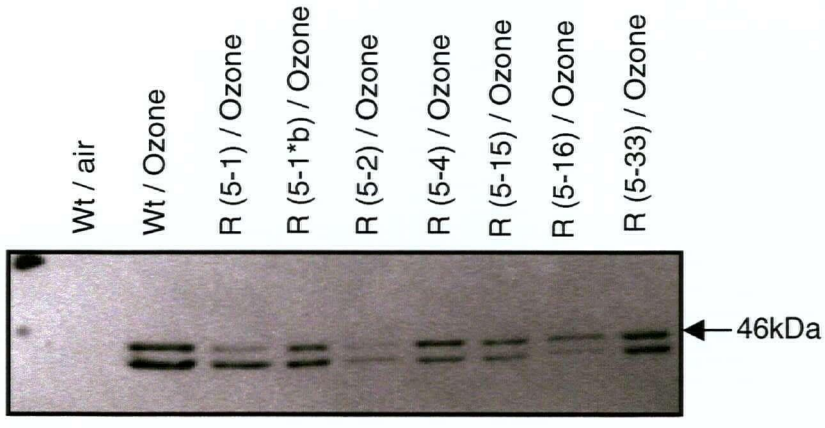

Fig. 5.10 Ozone-induced activation of two MAPKs is interdicted in MKK5-RNAi plants. Extracted proteins (20 μg) from ozone-fumigated (200 ppb, 10 min), 5-week-old (T_1) seedlings (parental lines: MKK5-1, MKK5-1b, MKK5-2, MKK5-4, MKK5-15, MKK5-16, and MKK5-33) were fractionated by 10% SDS-PAGE, and transferred onto PVDF membranes. The resulting PVDF membranes were incubated using anti-phospho-ERK 1&2 antibodies. Control plants exposed to ambient air were harvested at the same time as the ozone-treated plants. There was a mix-up with the numbering and this is why I have two MKK5-1 (MKK5-1 and MKK5-1b) lines. They were two different T_1 plants.

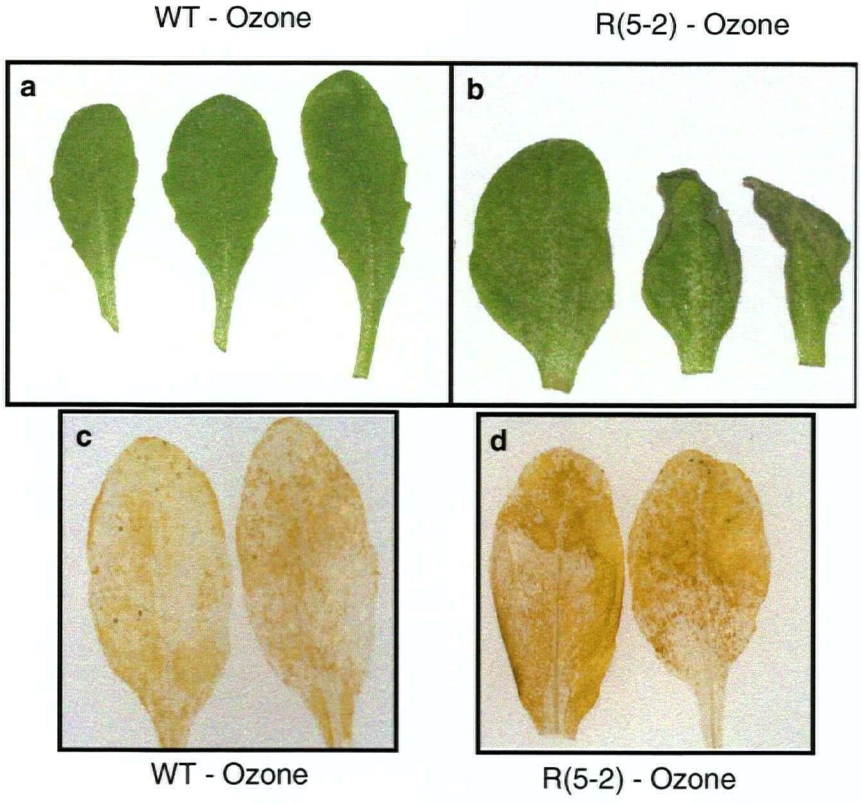

Fig. 5.11 MKK5-RNAi (T_2) plants show an increased susceptibility to ozone and concomitant hydrogen peroxide accumulation. (**a, c**) = WT leaves; (**b, d**) = MKK5-suppressed leaves. (**a, b**) MKK5-RNAi lines, together with WT plants, were fumigated with ozone (500 ppb) for 4 hr. The treated leaves were photographed 4 hr after the end of this exposure. (**c, d**) 3, 3'- Diaminobenzidine staining to detect hydrogen peroxide accumulation in ozone-treated MKK5-RNAi (T_2) and WT leaves.

5.3.9 Isotope-coded affinity-tag-based protein profiling (ICAT)

The use of ICAT permits the quantification of protein expression levels through stable isotopic labeling. These reagents consist of four functional parts (**1**) a protein (iodoacetamide) group which reacts with the free sulfhydryl group of a reduced cysteine side-chain, (**2**) a biotin moiety to help isolate the modified peptides via avidin affinity chromatography, (**3**) a linker group containing either a heavy or light (normal) isotope, and (**4**) an acid cleavable site. I used the ICAT reagent (Applied Biosystems), that contains either [^{12}C] or [^{13}C] atoms - thus resulting in a mass difference of 9 daltons between the control versus the corresponding experimental version of the same tryptic peptide. For a diagram of the ICAT reagent, see **Fig. 5.12**.

A central feature of ICAT is that the *in vitro* incorporation of a different stable isotope into each of the two samples being compared obviates the need to analyze by mass spectrometry the control and experimental samples separately. ICAT technology thus provides information on the relative abundances of individual proteins under two experimental conditions. It should be noted that sub-population of proteins that do not contain cysteines will not be detected with this method. In addition, ICAT is not able to provide absolute protein concentrations nor does it provide the ratio of the relative concentration of one protein to another protein in a single condition (Greenbaum et al., 2003). Furthermore, it is difficult to evaluate changes in abundances of proteins that are undergoing phosphorylation.

Both WT and R(6-7) genotype plants were exposed to continuous ozone (500 ppb) for 8 hr. Control plants for both genotypes were exposed to ambient air and harvested at the same time as the ozone-treated plants. A total

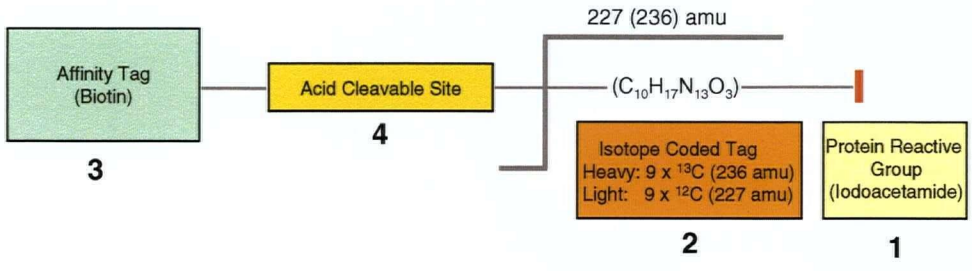

Fig. 5.12 Cleavable ICAT reagent structure. The cleavable ICAT reagent is composed of four main segments: **1**) a protein reactive group, **2**) an affinity tag (biotin), **3**) an isotopically labeled linker ($C_{10}H_{17}N_3O_3$), and **4**) an acid cleavable site. Structure taken from Applied Biosystems.

of 150 five-week-old plants of each genotype were extracted at each time point. ICAT derivatization ([R (6-7) = ^{13}C and WT = ^{12}C]) and tandem mass spectrometry, then provided a large-scale picture of protein expression in both air control and ozone-exposed plants. For a schematic flow-chart of the ICAT procedure, see **Fig. 5.13**.

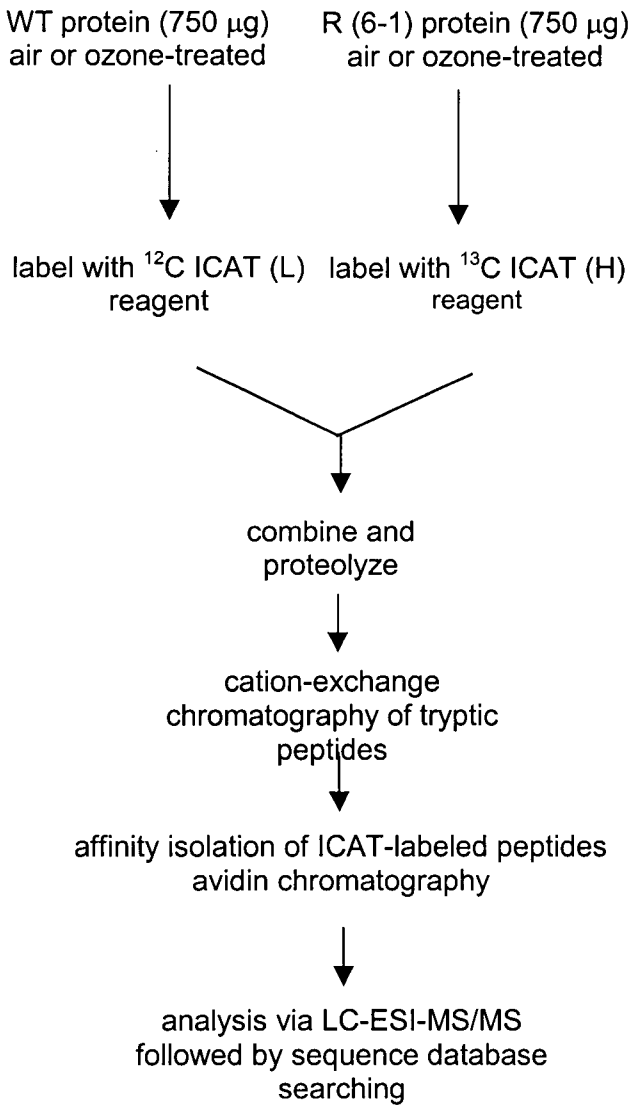

Fig. 5.13 Schematic representation of the quantitative proteomics (ICAT) analysis employed to identify relative expression ratios of individual proteins between WT and R (6-7) genotypes

Each time point was processed in duplicate. To increase the robustness of the data, the mass spectrometry data from both the replicates at both time points (0 hr and 8 hr) were combined, producing a 0 hr_combined (0 hr-air) and a 8 hr_combined (8 hr-O_3) data set.

A breakdown of the results from the ICAT experiment is given in **Table 5.1**. For the 0 hr-air samples, a total of 609 proteins were automatically quantified by ASAPRatio. After filtering this set with a probability cut off of 0.99, a list of 211 proteins was acquired. Next, I examined the list of proteins which had a probability cut-off of 0.90, where I found 2 additional proteins, making a total of 213 identified 0 hr-air proteins. From this set of 213 proteins, 132 were determined to be unquantifiable by manual re-interpretation of the ASAPRatio output, leaving a final 0hr-air list of 81 proteins (13.3% of the original 609 entries). Human intervention is needed to make sure that the peak integration is correct. The values for this final set of 81 entries were then normalized (**Table 5.2**) and the 0 hr-air proteins with a significant change in H/L abundance ratio are listed (**Table 5.3**). There were 5 proteins in the 0 hr-air set whose abundance was greater in the R(6-7) genotype than in the WT, and 10 proteins whose abundance was lower than in the WT genotype, reflecting changes in the protein composition of the plants that have MPK6 constitutively suppressed.

For the 8 hr-O_3 proteins, a total of 1309 proteins were quantified by ASAPRatio (**Table 5.1**). The 0.99 probability cut off produced a list of 264 candidate proteins. As with the 0 hr-air proteins, I examined the 8 hr-O_3 protein list with a probability cut off of 0.90, and found an additional 2 proteins, making a final list of 266 proteins. Of these, 115 were determined to be unquantifiable via

	0 hr_combined
Entries	609
0.99 prob.	211
Manual investigation	81 (13.3%)
0 hr_up_sign	**5**
0 hr_down_sign	**10**
	8 hr_combined
Entries	1309
0.99 prob.	264
Manual investigation	151 (11.5%)
8 hr_up_sign	**14**
8 hr_down_sign	**18**

Table 5.1 This table represents an overview of the data generated from the ICAT experiment.

manual re-interpretation of the ASAPRatio output, leaving 151 proteins (11.5%) of the original 1309 entries for further analysis. After normalizing the data for these 151 proteins (**Table 5.2**), I identified 14 proteins whose abundance was greater in the R(6-7) genotype compared to WT, and 18 proteins whose abundance was lower than in the WT genotype (**Table 5.3**). A differential of +/- 1.5 and a p-value of ~ 0.2 were used as the criteria for defining differentially expressed proteins with significant differences.

Functional classification of the differentially expressed proteins from ozone treated tissue (R(6-7) / WT), was conducted based on the cellular component, and biological process with which they are associated in the GO ontology system (**Table 5.4, and assorted pie charts, 5.1 to 5.4**). For the cellular component classifications, both the 0 hr-air and 8 hr-O_3 lists are very similar in their overall distribution indicating that there was no bias during the protein extraction step. The majority of both the 0 hr-air and 8 hr-O_3 proteins are annotated as being located in the chloroplast, while the rest are associated with the mitochondria, nucleus, and cytosol. In terms of biological process, the categories of "other metabolic processes" and "electron transport" or "energy pathways" make up the bulk of the 0 hr-air and 8 hr-O_3 protein entries, with an assortment of other categories covering the rest of the protein entries.

Table 5.2 The complete list of both 0 hr and 8 hr normalized proteins from ICAT experimentation. Columns indicate protein identification, number of total peptides, normalized expression ratio [R (6-7-1) / WT, ^{13}C / ^{12}C] derived from all sequenced peptides for that particular protein entry (protein data base: ATH1.pep), error and p-value. All values were generated from the normalized data.

0 hr_proteins	#peps	ratio	error	p-value
At1g42970.1 glyceraldehyde-3-phosphate dehydrogenase	16	0.364	0.062	0.087
At2g26080.1 glycine dehydrogenase [decarboxylating]	20	0.566	0.163	0.370
At5g09810.1 ACTIN 2/7 (sp|P53492)	9	0.607	0.345	0.532
At2g16600.1 cytosolic cyclophilin (ROC3)	7	0.566	0.065	0.324
At2g05710.1 aconitate hydratase [cytoplasmic]	3	0.849	0.053	0.774
At4g38970.1 fructose-bisphosphate aldolase	15	0.465	0.045	0.181
At4g13930.1 hydroxymethyltransferase	10	1.254	0.871	0.800
At5g63570.1 glutamate-1-semialdehyde 2,1-aminomutase	3	0.465	0.063	0.188
At1g19570.1 dehydroascorbate reductase, putative	13	1.132	0.407	0.852
At5g38480.1 14-3-3 protein GF14	5	1.274	0.096	0.671
At2g03680.1 68409.m00292 nitrilase-associated protein related	4	1.031	0.109	0.957
At5g66570.1 photosystem II oxygen-evolving complex 33 (OEC33)	5	0.566	0.03	0.316
At1g23310.1 alanine aminotransferase -related	11	0.546	0.183	0.357
At5g19820.1 expressed protein	2	0.768	0.165	0.663
At3g55440.1 triosephosphate isomerase, cytosolic, putative	7	0.789	0.305	0.728
At1g56070.1 elongation factor	17	1.436	0.509	0.587
At5g14740.1 CARBONIC ANHYDRASE 2	40	0.465	0.123	0.219
At2g24270.1 NADP glyceraldehyde-3-phosphate dehydrogenase	12	1.092	0.649	0.914
At1g16080.1 expressed protein	3	2.164	0.277	0.182
At4g33010.1 glycine dehydrogenase [decarboxylating]	27	0.688	0.264	0.583
At2g21330.1 fructose-bisphosphate aldolase, putative	19	0.93	0.166	0.902
At1g20340.1 plastocyanin	11	0.991	0.406	0.989
At2g13360.1 alanine-glyoxylate aminotransferase	22	1.274	1.093	0.813
At5g61410.1 ribulose-5-phosphate-3-epimerase	3	1.011	0.226	0.985
At5g66530.1 aldose 1-epimerase family	3	1.355	0.972	0.739
At1g23190.1 phosphoglucomutase -related	6	1.132	0.149	0.830
At5g25980.2 glycosyl hydrolase family 1	43	0.849	0.87	0.889
At2g30970.1 aspartate aminotransferase, mitochondrial	2	3.883	0.323	0.017
At5g17920.1 5-methyltetrahydropteroyltriglutamate	58	0.627	0.066	0.416
At1g23740.1 oxidoreductase, zinc-binding dehydrogenase family	4	0.445	0.063	0.164
At4g11010.1 nucleoside diphosphate kinase 3 (ndpk3)	2	0.586	0.031	0.347
At4g35630.1 phosphoserine aminotransferase	5	0.728	0.145	0.596

Table 5.2 - *continued*

0 hr_proteins	#peps	ratio	error	p-value
At3g19170.1 metalloprotease -related	7	0.708	0.648	0.747
At1g09340.1 RNA-binding protein -related	2	0.688	0.085	0.517
At4g20360.1 elongation factor Tu (EF-Tu)	3	0.586	0.031	0.347
At2g47940.1 DegP2 protease	2	0.728	0.105	0.586
At3g60750.1 transketolase - like protein	9	0.607	0.607	0.663
At1g59900.1 pyruvate dehydrogenase E1 alpha subunit -related	4	0.303	0.024	0.036
At1g67090.1 ribulose-bisphosphate carboxylase small unit	19	1.416	0.368	0.576
At5g17990.1 anthranilate phosphoribosyltransferase precursor	4	0.89	0.245	0.852
At5g50920.1 ATP-dependent Clp protease ATP-binding subunit	4	0.546	0.143	0.331
At4g31990.2 aspartate aminotransferase, chloroplast	3	0.91	0.467	0.901
AtCg00490 rbcL riblose 1	506	1.234	0.113	0.713
At1g24510.1 T-complex protein 1	3	0.506	0.045	0.233
At1g17290.1 alanine aminotransferase, putative	3	2.083	0.295	0.208
At1g60950.1 ferrodoxin, chloroplast	30	0.364	0.082	0.096
At1g70730.1 phosphoglucomutase -related	6	1.132	0.149	0.830
AtCg00480 ATP synthase CF1 beta chain (atpB)	3	0.952	0.089	0929
At1g72370.1 40S ribosomal protein SA (RPSaA)	4	0.728	0.086	0.582
At3g47520.1 malate dehydrogenase [NAD], chloroplast, putative	7	0.566	0.244	0.423
At4g35090.1 catalase 2	27	1.173	0.871	0.864
At3g24170.1 glutathione reductase, putative	4	1.072	0.092	0.903
At4g29060.1 expressed protein	5	0.87	0.487	0.860
At1g32060.1 phosphoribulokinase precursor	24	0.546	0.304	0.445
At5g03290.1 isocitrate dehydrogenase [NAD+], putative	2	2.123	0.086	0.184
At3g09820.1 adenosine kinase 1 (ADK1)	23	0.627	0.244	0.496
At5g38430.1 ribulose bisphosphate carboxylase small chain 1b	2	0.91	0.346	0.890
At4g26530.1 fructose-bisphosphate aldolase, putative	12	0.93	0.326	0.913
At4g33680.1 aminotransferase	2	0.728	0.036	0.576
At4g21580.1 oxidoreductase	1	0.95	0.108	0.929
At3g15730.1 phospholipase D, putative	1	1.719	0.123	0.342
At1g03475.1 coproporphyrinogen III oxidase	3	0.829	0.039	0.741
At4g23600.1 aminotransferase family	2	0.809	0.106	0.714
AtCg00160 ribosomal protein S2 (rps2)	3	1.314	0.097	0.631
At1g06000.1 glycosyltransferase family	1	0.991	0.09	0.987
At4g24220.1 expressed protein induced upon wounding	2	0.971	0.072	0.958
At3g02520.1 14-3-3 protein GF14 nu (grf7)	1	0.991	0.057	0.987
At2g47390.1 expressed protein	2	0.789	0.125	0.686

Table 5.2 - *continued*

0 hr_proteins	#peps	ratio	error	p-value
At3g48990.1 AMP-dependent synthetase and ligase family	2	0.425	0.026	0.132
At2g01140.1 fructose-bisphosphate aldolase, putative	1	1.719	0.158	0.344
At1g13280.1 allene oxide cyclase family similar to ERD12	1	1.031	0.074	0.956
At5g20890.1 chaperonin, putative	1	1.052	0.148	0.931
At2g25080.1 glutathione peroxidase, putative	1	0.829	0.145	0.751
At3g54660.1 gluthatione reductase, chloroplast	1	0.748	0.106	0.618
At1g50200.1 alanine--tRNA ligase -related	1	1.618	0.12	0.398
At1g76730.1 5-formyltetrahydrofolate cyclo-ligase family	1	0.243	0.022	0.013
At2g20580.1 26S proteasome regulatory subunit S2 (RPN1)	1	0.627	0.025	0.409
At4g19410.1 pectinacetylesterase, putative	2	0.768	0.037	0.642
At3g52880.1 monodehydroascorbate reductase, putative	1	1.355	0.209	0.604
At5g52810.1 expressed protein	1	0.667	0.085	0.485
At1g24180.1 pyruvate dehydrogenase E1 alpha subunit	1	2.042	0.147	0.210

Table 5.2 - *continued*

8 hr_proteins	#peps	ratio	error	p-value
At4g16330.1 oxidoreductase, 2OG-Fe(II) oxygenase family	3	0.622	0.109	0.223
At2g28000.1 RuBisCO subunit binding-protein alpha subunit	3	0.576	0.078	0.139
At1g23190.1 phosphoglucomutase -related	6	0.98	0.126	0.957
At5g09810.1 actin 2/7	21	0.996	0.095	0.990
At1g78900.1 ATPase 70 kDa subunit –related	5	0.934	0.203	0.867
At3g51800.1 nuclear DNA-binding protein G2p -related	11	1.136	0.188	0.740
At3g48990.1 AMP-dependent synthetase and ligase family	11	0.778	0.296	0.626
At1g67090.1 ribulose-bisphosphate carboxylase small unit	52	0.949	0.064	0.883
At1g11860.1 aminomethyltransferase-related	16	1.198	0.358	0.693
At2g31790.1 UDP-glycosyltransferase family	4	0.731	0.02	0.369
At5g38430.1 ribulose bisphosphate carboxylase small chain 1b	6	1.058	0.05	0.872
At1g76010.1 expressed protein	2	1.167	0.08	0.663
At1g24510.1 T-complex protein 1 protein	7	0.825	0.389	0.742
At5g16110.1 expressed protein	14	0.949	0.156	0.892
At4g26690.1 expressed protein	2	0.965	0.035	0.918
At3g17810.1 dehydrogenase -related protein	5	1.385	0.25	0.406
At3g28940.1 AIG2-related protein	11	0.7	0.11	0.350
At4g13940.1 adenosylhomocysteinase	62	0.949	0.079	0.884
At1g53240.1 malate dehydrogenase [NAD], mitochondrial, putative	8	0.778	0.064	0.482
At4g34870.1 peptidylprolyl isomerase (cyclophilin)	6	1.229	0.096	0.562
At3g54050.1 fructose-bisphosphatase precursor	17	0.762	0.141	0.490
At1g05010.1 1-aminocyclopropane-1-carboxylate oxidase	7	1.54	0.068	0.217
At1g65930.1 isocitrate dehydrogenase [NADP+], putative	9	0.56	0.063	0.112
At1g07140.1 Ran-binding protein (atranbp1a)	6	1.167	0.095	0.665
At1g60950.1 ferrodoxin, chloroplast	106	1.151	0.126	0.698
At1g03475.1 coproporphyrinogen III oxidase (coproporphyrinogenase)	4	0.591	0.019	0.132
At3g47520.1 malate dehydrogenase [NAD], chloroplast, putative	7	0.622	0.296	0.420
At4g33010.1 glycine dehydrogenase [decarboxylating]	54	1.089	0.126	0.815
At1g17100.1 SOUL-related protein	2	1.432	0.157	0.325
At2g26080.1 glycine dehydrogenase [decarboxylating]	39	0.84	0.965	0.884
At2g01140.1 fructose-bisphosphate aldolase, putative	9	0.685	0.156	0.362
At1g26630.1 initiation factor 5A-4 -related	5	2.583	0.268	$8.94E^{-3}$
At3g01480.1 thylakoid lumen rotamase	3	1.214	0.126	0.593
At2g39730.1 auxin-regulated protein	66	0.903	0.095	0.777

Table 5.2 - *continued*

8 hr_proteins	#peps	ratio	error	p-value
At4g25130.1 protein-methionine-S-oxide reductase	2	1.183	0.312	0.700
At1g63770.1 aminopeptidase -related	5	1.276	0.483	0.635
At3g55440.1 triosephosphate isomerase, cytosolic, putative	25	0.762	0.203	0.535
At5g14740.1 carbonic anhydrase 2	119	0.856	0.079	0.665
At4g10320.1 isoleucine-tRNA ligase	5	0.996	0.187	0.991
At1g32060.1 phosphoribulokinase precursor	30	0.903	0.187	0.800
At5g26000.1 glycosyl hydrolase family 1, myrosinase precursor	27	1.26	0.234	0.557
At3g23990.1 chaperonin (HSP60) [Arabidopsis thaliana]	3	0.903	0.079	0.774
At5g15650.1 reversibly glycosylated polypeptide-3	10	0.965	0.064	0.919
At3g55800.1 sedoheptulose-bisphosphatase precursor	13	0.607	0.171	0.265
At5g16050.1 14-3-3 protein GF14 upsilon (grf5)	3	1.4	0.173	0.361
At5g17990.1 anthranilate phosphoribosyltransferase	3	0.98	0.095	0.956
At1g72370.1 40S ribosomal protein SA (RPSaA)	12	1.323	0.111	0.434
At1g20620.1 catalase 3	39	1.043	0.126	0.909
At4g26530.1 fructose-bisphosphate aldolase, putative	21	0.747	0.125	0.449
At1g52400.1 glycosyl hydrolase family 1, beta-glucosidase (BG1)	5	3.859	0.141	$1.12E^{-4}$
At1g16080.1 expressed protein	8	0.794	0.141	0.553
At1g47128.1 cysteine proteinase RD21A	3	0.794	0.56	0.768
At5g26360.1 chaperonin, putative	7	0.903	0.079	0.774
At2g21170.1 triosephosphate isomerase, chloroplast, putative	3	1.074	0.219	0.860
At4g11150.1 H+-transporting ATPase chain E, vacuolar	7	1.26	0.467	0.648
At5g66570.1 photosystem II oxygen-evolving complex 33 (OEC33)	17	1.556	0.545	0.370
At5g25980.2 glycosyl hydrolase family	158	0.949	0.064	0.883
At2g24270.1 NADP-dependent glyceraldehyde-3-phosphate dehydrogenase	30	0.747	0.125	0.449
At5g49910.1 heat shock protein cpHsc70-2 (hsc70-7)	7	0.809	0.529	0.774
At5g11670.1 NADP dependent malic enzyme - like protein	33	1.26	0.234	0.557
At2g41790.1 zinc protease -related to insulinase protein family	5	1.043	0.065	0.906
At2g05710.1 aconitate hydratase [cytoplasmic]	14	1.183	0.25	0.680
At4g24620.1 glucose-6-phosphate isomerase	2	0.529	0.156	0.162
At5g17920.1 homocysteine S-methyltransferase	127	1.074	0.126	0.846
At5g61410.2 ribulose-5-phosphate-3-epimerase	5	1.447	0.374	0.393
At5g48300.1 glucose-1-phosphate adenylyltransferase, small subunit	3	0.591	0.01	0.131
At4g13930.1 hydroxymethyltransferase	28	0.934	0.483	0.912
At3g12290.1 tetrahydrofolate dehydrogenase/cyclohydrolase, putative	2	1.027	0.065	0.939
At1g70730.1 phosphoglucomutase -related	8	1.011	0.157	0.976
At4g31990.1 aspartate aminotransferase, chloroplast	13	1.214	0.281	0.642

Table 5.2 - *continued*

8 hr_proteins	#peps	ratio	error	p-value
At4g38970.1 fructose-bisphosphate aldolase, putative	65	0.716	0.11	0.378
At4g09000.1 14-3-3 protein GF14 chi (grf1)	21	0.856	0.11	0.674
At5g54160.1 O-methyltransferase 1	6	1.385	0.53	0.528
At5g63570.1 glutamate-1-semialdehyde 2,1-aminomutase 1 (GSA 1)	10	0.669	0.11	0.295
At3g49120.1 peroxidase, putative	13	1.338	0.173	0.432
At5g35630.1 glutamate-ammonia ligase	15	1.027	0.141	0.943
At3g24170.1 glutathione reductase, putative	4	1.945	0.174	0.064
At1g17290.1 alanine aminotransferase, putative	9	0.84	0.234	0.696
At3g26650.1 glyceraldehyde 3-phosphate dehydrogenase A subunit	44	0.84	0.11	0.639
At4g35830.1 aconitate hydratase	15	1.229	0.203	0.592
At3g09820.1 adenosine kinase 1 (ADK1)	45	0.84	0.172	0.666
At2g21250.1 mannose 6-phosphate reductase (NADPH-dependent)	6	1.54	0.173	0.237
At1g24180.1 pyruvate dehydrogenase E1 alpha subunit	3	0.513	0.094	0.089
At2g43910.1 thiol methyltransferase	2	0.871	0.218	0.748
At1g66970.1 expressed protein	7	0.731	0.203	0.481
At4g20850.1 expressed protein tripeptidyl-peptidase II	2	1.183	0.111	0.641
At3g11830.1 chaperonin, putative	5	0.918	0.11	0.816
At5g35360.1 acetyl-CoA carboxylase	9	0.794	0.11	0.536
At4g35090.1 catalase 2	35	0.934	0.11	0.851
At1g72610.1 germin-like protein (AtGER1)	6	2.178	0.221	0.031
At5g38480.1 14-3-3 protein GF14 psi (grf3/RCI1)	10	1.074	0.05	0.839
At4g19410.1 pectinacetylesterase, putative	3	1.26	0.081	0.512
At3g48730.1 glutamate-1-semialdehyde 2,1-aminomutase 2	9	0.669	0.11	0.295
At1g09340.1 RNA-binding protein -related	26	1.089	0.08	0.810
At2g25080.1 glutathione peroxidase, putative	9	0.965	0.141	0.924
At4g39280.1 phenylalanyl-trna synthetase - like	2	1.789	0.044	0.095
At5g10450.1 14-3-3 protein GF14 lambda (grf6/AFT1)	14	0.903	0.125	0.784
At3g62030.1 peptidylprolyl isomerase ROC4	4	1.338	0.111	0.415
At1g23310.1 alanine aminotransferase -related	33	0.98	0.141	0.957
At1g56070.1 elongation factor	44	0.731	0.11	0.408
At1g20340.1 plastocyanin	47	2.147	1.603	0.353
At3g48870.1 ATP-dependent Clp protease ATP-binding subunit	23	0.669	0.094	0.284
At5g43940.1 alcohol dehydrogenase class III	14	0.934	0.125	0.853
At1g33670.1 leucine rich repeat protein	6	1.011	0.265	0.979
At4g23100.1 gamma-glutamylcysteine synthetase	5	0.996	0.187	0.991

Table 5.2 - *continued*

8 hr_proteins	#peps	ratio	error	p-value
At2g21330.1 fructose-bisphosphate aldolase, putative	29	0.778	0.125	0.512
At5g09660.1 malate dehydrogenase, glyoxysomal	15	1.151	0.436	0.783
At2g47400.1 chloroplast protein CP12 -related	11	2.287	0.546	0.049
At2g47390.1 expressed protein	5	1.634	0.042	0.159
At2g23350.1 polyadenylate-binding protein (PABP), putative	11	1.4	0.081	0.339
At3g48420.1 haloacid dehalogenase-like	2	0.56	0.063	0.112
At4g24280.1 heat shock protein cpHsc70-1 heat shock 70 protein	9	0.622	0.094	0.211
At3g52880.1 monodehydroascorbate reductase, putative	4	1.976	0.099	0.052
At1g42970.1 glyceraldehyde-3-phosphate dehydrogenase	72	1.105	0.05	0.776
At5g51820.1 phosphoglucomutase	18	0.545	0.048	0.090
At1g09310.1 expressed protein	5	1.307	0.219	0.487
At3g58610.1 ketol-acid reductoisomerase	7	0.778	0.156	0.531
At3g61440.1 cysteine synthase	10	0.84	0.049	0.621
At4g38740.1 peptidylprolyl isomerase ROC1	27	1.509	0.654	0.458
At1g78300.1 14-3-3 protein GF14 omega (grf2)	10	0.794	0.156	0.562
At3g19170.1 metalloprotease -related	11	0.856	0.094	0.669
At4g20360.1 elongation factor Tu (EF-Tu)	7	1.26	0.157	0.531
At3g60750.1 transketolase - like	37	0.576	0.063	0.130
At2g13360.1 alanine-glyoxylate aminotransferase	21	0.903	0.218	0.808
At5g20890.1 chaperonin, putative	2	1.011	0.126	0.975
At5g19440.1 cinnamyl-alcohol dehydrogenase (CAD), putative	6	0.809	0.28	0.666
At1g55480.1 expressed protein	5	0.576	0.094	0.150
At1g80360.1 aminotransferase family	2	1.416	0.096	0.326
At2g37760.1 aldo/keto reductase family	3	1.26	0.026	0.506
At2g14170.1 methylmalonate-semialdehyde dehydrogenase	2	0.529	0.032	0.071
At4g18810.1 expressed protein	2	0.7	0.033	0.310
At1g80380.2 auxin-regulated protein	1	0.638	0.063	0.213
At5g49810.1 methionine S-methyltransferase	1	1.183	0.111	0.641
At5g27470.1 seryl-tRNA synthetase	2	0.685	0.048	0.285
At4g09320.1 nucleoside-diphosphate kinase	3	0.762	0.358	0.642
At3g26060.1 peroxiredoxin -related	1	2.552	0.237	$9.27E^{-3}$
At2g18230.1 inorganic pyrophosphatase -related	3	0.545	0.018	0.082
At1g01090.1 pyruvate dehydrogenase E1 alpha subunit	1	1.307	0.142	0.462
At2g03680.1 nitrilase-associated protein -related	2	0.607	0.033	0.155
At4g18480.1 magnesium-chelatase, subunit chll,	2	2.35	0.074	0.014
At3g07720.1 Kelch repeats protein family	1	0.762	0.094	0.462

Table 5.2 - *continued*

8 hr_proteins	#peps	ratio	error	p-value
At5g24300.1 starch synthase, putative	1	0.731	0.063	0.382
At1g09780.1 2, 3-bisphosphoglycerate-independent phosphoglycerate	1	0.871	0.095	0.705
At5g23010.1 MAM1, methylthioalkylmalate synthase	1	7.609	1.128	$8.01E^{-8}$
At2g39940.1 coronatine-insensitive 1 (COI1)	1	1.183	0.037	0.631
At5g40450.1 expressed protein microtubule-associated homolog	1	0.903	0.125	0.784
At5g36210.1 acyl-peptide hydrolase-related	1	0.778	0.064	0.482
At1g67280.1 glyoxalase I, putative (lactoylglutathione lyase)	1	1.043	0.024	0.904
At3g25530.1 gamma hydroxybutyrate dehydrogenase	2	0.731	0.063	0.382
At2g40290.1 eukaryotic translation initiation factor 2 alpha subunit	1	1.12	0.126	0.755
At1g62750.1 elongation factor Tu family protein	1	0.498	0.047	0.053
At1g18080.1 WD-40 repeat auxin-dependent protein ARCA	1	1.898	0.045	0.065

Table 5.3 Differentially regulated proteins generated from both 0 hr and 8hr normalized protein lists (≥ 1.5-fold and p-value of around 0.2 or <). Columns indicate protein identification, number of total peptides, normalized expression ratio [R (6-7-1) / WT, ^{13}C / ^{12}C] derived from all sequenced peptides for that particular protein entry (protein data base: ATH1.pep), error and p-value. All values were generated from the normalized data.

0 hr_proteins_up	#peps	ratio	error	p-value
At2g30970.1 aspartate aminotransferase, mitochondrial	2	3.883	0.323	0.017
At1g16080.1 expressed protein	3	2.164	0.277	0.182
At5g03290.1 isocitrate dehydrogenase [NAD+], putative	2	2.123	0.086	0.184
At1g17290.1 alanine aminotransferase, putative	3	2.083	0.295	0.208
At1g24180.1 pyruvate dehydrogenase E1 alpha subunit	1	2.042	0.147	0.210
0 hr_proteins_down	**#peps**	**ratio**	**error**	**p-value**
At1g76730.1 5-formyltetrahydrofolate cyclo-ligase family	1	0.243	0.022	0.013
At1g59900.1 pyruvate dehydrogenase e1 alpha subunit -related	4	0.303	0.024	0.036
At1g60950.1 ferrodoxin, chloroplast	30	0.364	0.082	0.096
At1g42970.1 glyceraldehyde-3-phosphate dehydrogenase	16	0.364	0.062	0.087
At3g48990.1 AMP-dependent synthetase and ligase family	2	0.425	0.026	0.132
At1g23740.1 oxidoreductase, zinc-binding dehydrogenase family	4	0.445	0.063	0.164
At4g38970.1 fructose-bisphosphate aldolase	15	0.465	0.045	0.181
At5g63570.1 glutamate-1-semialdehyde 2,1-aminomutase	3	0.465	0.063	0.188
At5g14740.1 CARBONIC ANHYDRASE 2	40	0.465	0.123	0.219
At1g24510.1 T-complex protein 1	3	0.506	0.045	0.233

Table 5.3 - *continued*

8 hr_proteins_up	#peps	ratio	error	p-value
At5g23010.1 MAM1, methylthioalkylmalate synthase	1	7.609	1.128	$8.01E^{-8}$
At1g52400.1 glycosyl hydrolase family 1, beta-glucosidase (BG1)	5	3.859	0.141	$1.12E^{-4}$
At1g26630.1 initiation factor 5A-4 -related	5	2.583	0.268	$8.94E^{-3}$
At3g26060.1 peroxiredoxin -related (chl)	1	2.552	0.237	$9.27E^{-3}$
At4g18480.1 magnesium-chelatase, subunit chlI,	2	2.35	0.074	0.014
At1g72610.1 germin-like protein (AtGER1)	6	2.178	0.221	0.031
At2g47400.1 chloroplast protein CP12 -related	11	2.287	0.546	0.049
At3g52880.1 monodehydroascorbate reductase, putative (cyt)	4	1.976	0.099	0.052
At3g24170.1 glutathione reductase, putative (cyt)	4	1.945	0.174	0.064
At1g18080.1 WD-40 repeat auxin-dependent protein ARCA	1	1.898	0.045	0.065
At4g39280.1 phenylalanyl-trna synthetase - like	2	1.789	0.044	0.095
At2g47390.1 expressed protein	5	1.634	0.042	0.159
At1g05010.1 1-aminocyclopropane-1-carboxylate oxidase	7	1.54	0.068	0.217
At2g21250.1 mannose 6-phosphate reductase (NADPH-dependent)	6	1.54	0.173	0.237

8 hr_proteins_down	#peps	ratio	error	p-value
At1g62750.1 elongation factor Tu family protein	1	0.498	0.047	0.053
At2g14170.1 methylmalonate-semialdehyde dehydrogenase	2	0.529	0.032	0.071
At2g18230.1 inorganic pyrophosphatase -related	3	0.545	0.018	0.082
At1g24180.1 pyruvate dehydrogenase E1 alpha subunit	3	0.513	0.094	0.089
At5g51820.1 phosphoglucomutase	18	0.545	0.048	0.090
At1g65930.1 isocitrate dehydrogenase [NADP+], putative	9	0.56	0.063	0.112
At3g48420.1 haloacid dehalogenase-like	2	0.56	0.063	0.112
At3g60750.1 transketolase - like	37	0.576	0.063	0.130
At5g48300.1 glucose-1-phosphate adenylyltransferase, small subunit	3	0.591	0.01	0.131
At1g03475.1 coproporphyrinogen III oxidase	3	0.591	0.019	0.013
At2g28000.1 RuBisCO subunit binding-protein alpha subunit	3	0.576	0.078	0.139
At1g55480.1 expressed protein	5	0.576	0.094	0.150
At2g03680.1 nitrilase-associated protein -related	2	0.607	0.033	0.155
At4g24620.1 glucose-6-phosphate isomerase	2	0.529	0.156	0.162
At4g24280.1 heat shock protein cpHsc70-1 heat shock 70 protein	9	0.622	0.094	0.211
At1g80380.2 auxin-regulated protein	1	0.638	0.063	0.213
At4g16330.1 oxidoreductase, 2OG-Fe (II) oxygenase family	3	0.622	0.109	0.223

Functional Categorization for:
Cellular Component

	0 hr_proteins	0 hr_up_sign	0 hr_down_sign
Chloroplast	**41%**	**16.70%**	**80%**
Other cytoplasmic components	**13.40%**	**16.70%**	
Cellular component unknown	**9.70%**	**16.70%**	**20%**
Other membranes	8.20%		
Other intracellular components	7.50%		
Mitochondria	**6.70%**	**50%**	
Cytosol	3.70%		
Nucleus	3.70%		
Ribosome	2.20%		
Plasma Membrane	2.20%		
ER	0.70%		
Other cellular components	0.70%		

Functional Categorization for:
Cellular Component

	8 hr_proteins	8 hr_up_sign	8 hr_down_sign
Chloroplast	**39.3%**	**42.1%**	**57%**
Cellular component unknown	**16.80%**	**10.50%**	**4.30%**
Other cytoplasmic components	**12.60%**	**21.10%**	**8.70%**
Other membranes	**10.50%**	**15.80%**	**4.30%**
Mitochondrion	**7.90%**		**13%**
Other intracellular components	**3.70%**		**4.30%**
Cytosol	3.10%		
Nucleus	**2.60%**		**8.70%**
Plasma Membrane	**1.60%**	**5.30%**	
Other cellular components	1.00%		
Ribosome	0.50%		
Extracellular	**0.50%**	**5.30%**	

Table 5.4 Functional categorization " Cellular Component" of 0 hr-air and 8 hr-O_3 protein lists.

Table 5.4, cont.

Functional Categorization for:
Biological Process

	0 hr_proteins	0 hr_up_sign	0 hr_down_sign
Other metabolic processes	**55.20%**	**82.40%**	**50%**
Electron transport or energy pathways	**13.80%**	**11.80%**	**23.30%**
Protein metabolism	6.50%		
Other physiological processes	**5.20%**		**6.70%**
Response to abiotic or biotic stimulus	**5.20%**		**6.70%**
Response to stress	3.00%		
Other cellular processes	3.00%		**6.70%**
Transport	**2.60%**	**5.90%**	**3.30%**
Signal transduction	2.20%		
Biological process unknown	**2.20%**		**3.30%**
Developmental processes	0.40%		
Other biological processes	0.40%		
Cell organization and biogenesis	0.40%		

Functional Categorization for:
Biological Process

	8 hr_proteins	8 hr_up_sign	8 hr_down_sign
Other metabolic processes	**53.80%**	**48.40%**	**49.50%**
Electron transport or energy pathways	**12.70%**	**12.90%**	**3%**
Protein metabolism	**9%**	**6.50%**	**12.10%**
Biological process unknown	**5%**	**12.90%**	**3%**
Response to abiotic or biotic stimulus	**3.70%**	**3.20%**	
Transport	**2.90%**	**3.20%**	
Signal transduction	**2.90%**	**3.20%**	
Other physiological processes	**2.70%**	**3.20%**	
Response to stress	**1.90%**	**3.20%**	
Developmental processes	**1.90%**	**3.20%**	**9.10%**
Other cellular processes	**1.90%**		**6.10%**
Transcription	**0.50%**		**3%**
Cell organization and biogenesis	**0.50%**		**6.10%**
DNA and RNA metabilism	0.30%		
Other biological processes	**0.30%**		**3%**

Table 5.4 Functional categorization " Biological Process" of 0 hr-air and 8hr-O_3 protein lists.

Pie chart, 5.1

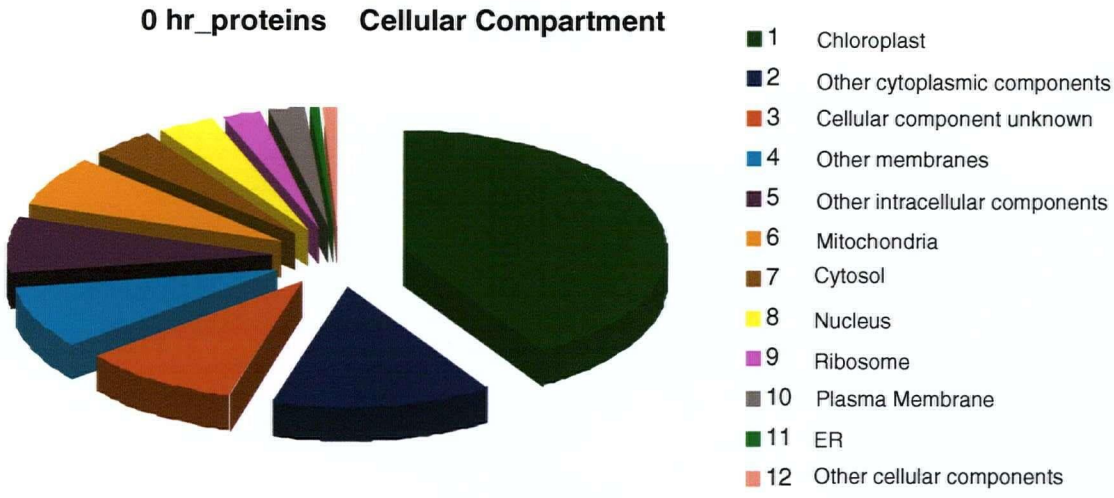
0 hr_proteins Cellular Compartment
1 Chloroplast
2 Other cytoplasmic components
3 Cellular component unknown
4 Other membranes
5 Other intracellular components
6 Mitochondria
7 Cytosol
8 Nucleus
9 Ribosome
10 Plasma Membrane
11 ER
12 Other cellular components

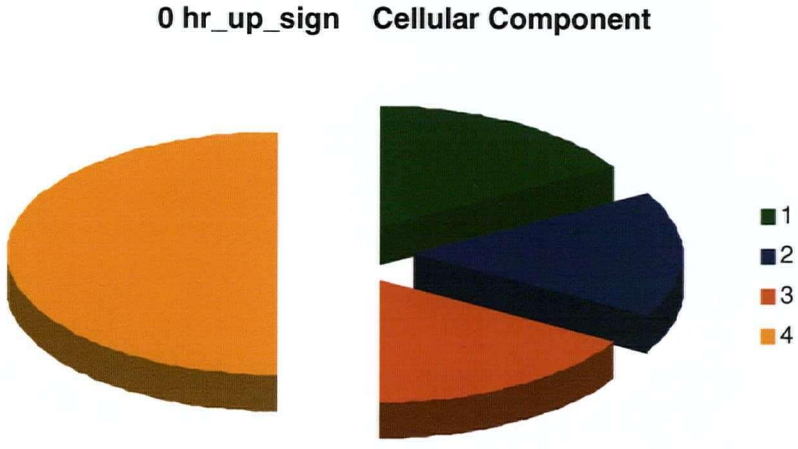
0 hr_up_sign Cellular Component
1
2
3
4

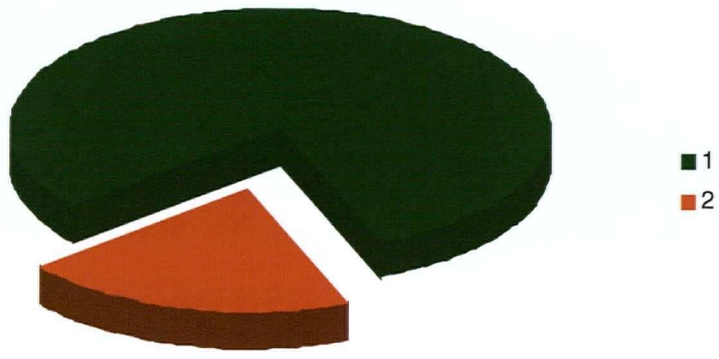
0 hr_down_sign Cellular Component
1
2

Pie chart, 5.2

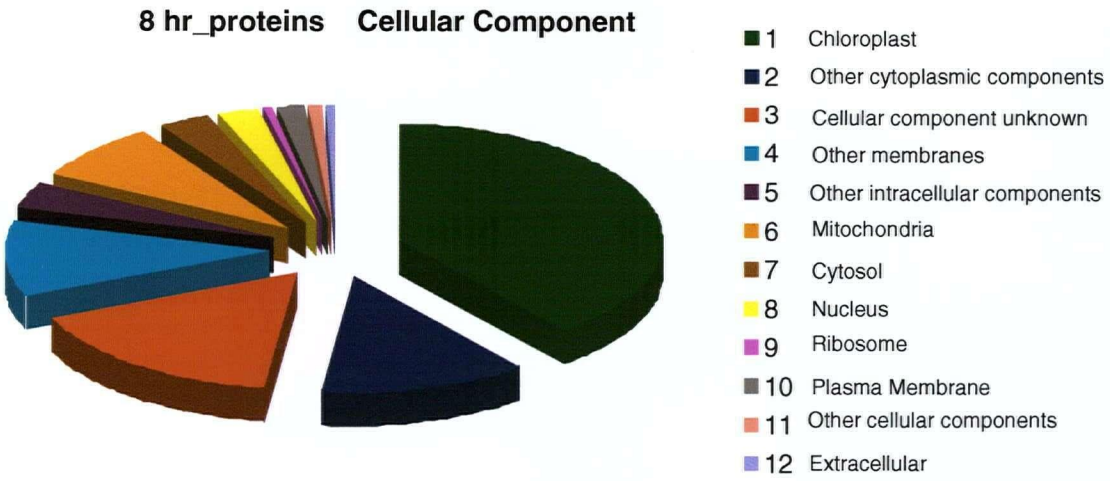
8 hr_proteins Cellular Component
1 Chloroplast
2 Other cytoplasmic components
3 Cellular component unknown
4 Other membranes
5 Other intracellular components
6 Mitochondria
7 Cytosol
8 Nucleus
9 Ribosome
10 Plasma Membrane
11 Other cellular components
12 Extracellular

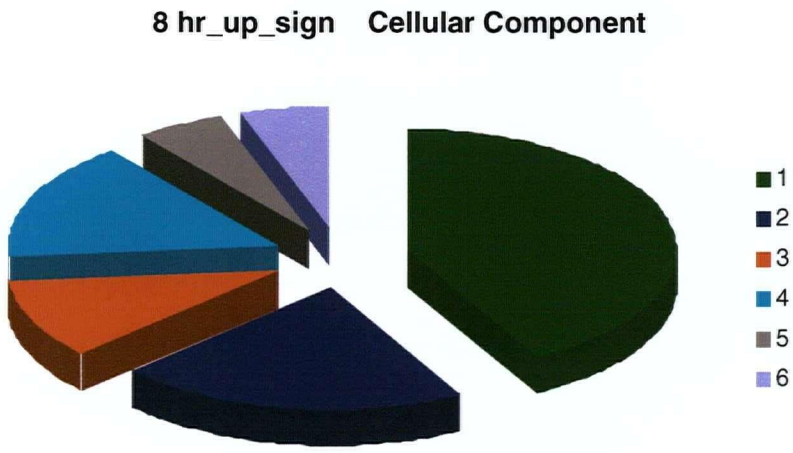
8 hr_up_sign Cellular Component
1
2
3
4
5
6

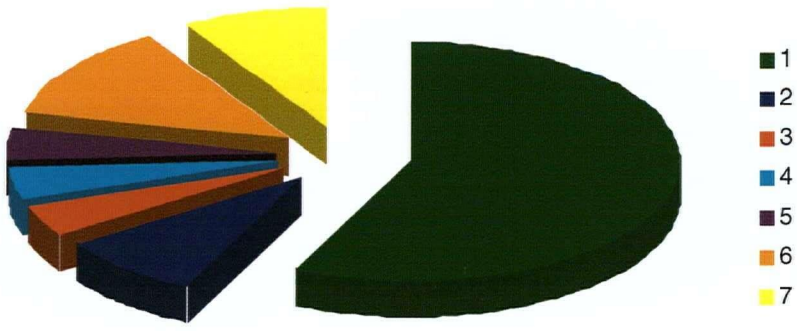
8 hr_down_sign Cellular Component
1
2
3
4
5
6
7

Pie chart, 5.3

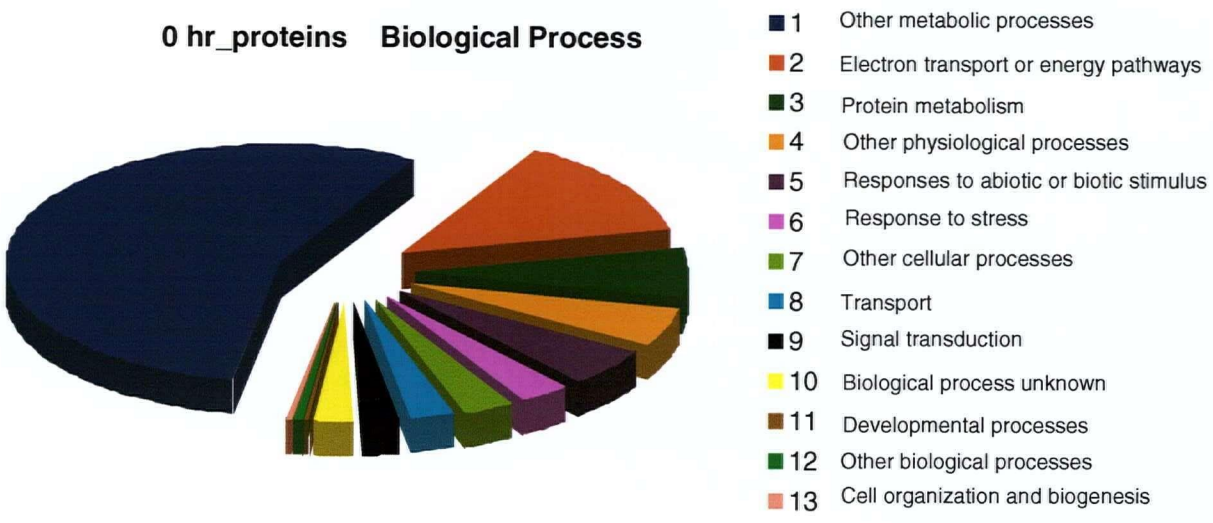
0 hr_proteins Biological Process
1 Other metabolic processes
2 Electron transport or energy pathways
3 Protein metabolism
4 Other physiological processes
5 Responses to abiotic or biotic stimulus
6 Response to stress
7 Other cellular processes
8 Transport
9 Signal transduction
10 Biological process unknown
11 Developmental processes
12 Other biological processes
13 Cell organization and biogenesis

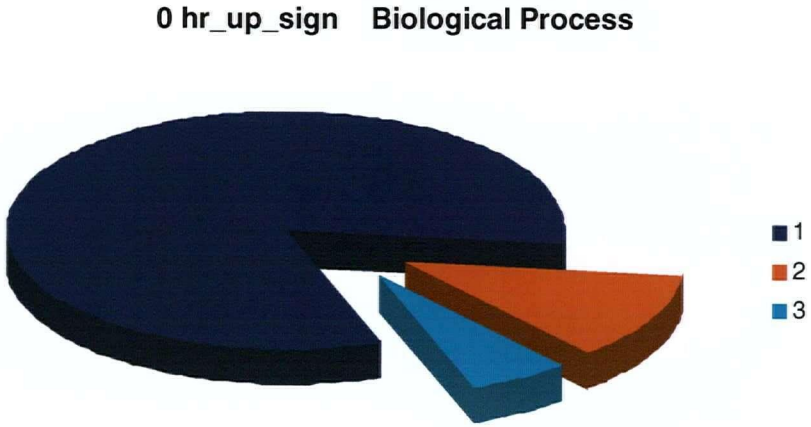
0 hr_up_sign Biological Process
1
2
3

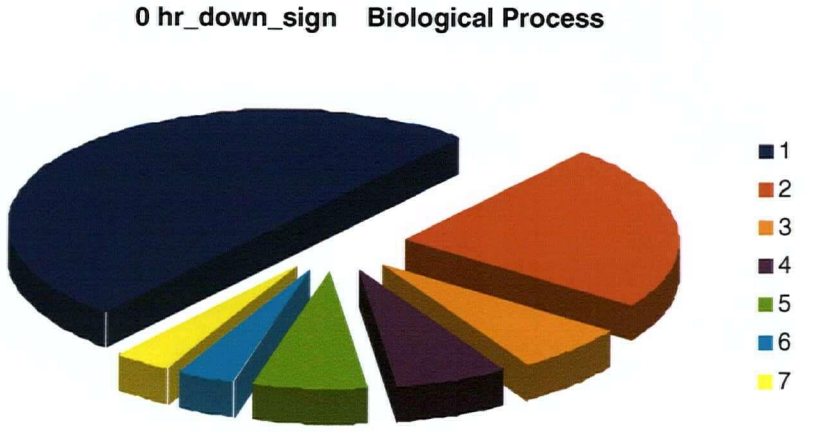
0 hr_down_sign Biological Process
1
2
3
4
5
6
7

Pie chart, 5.4

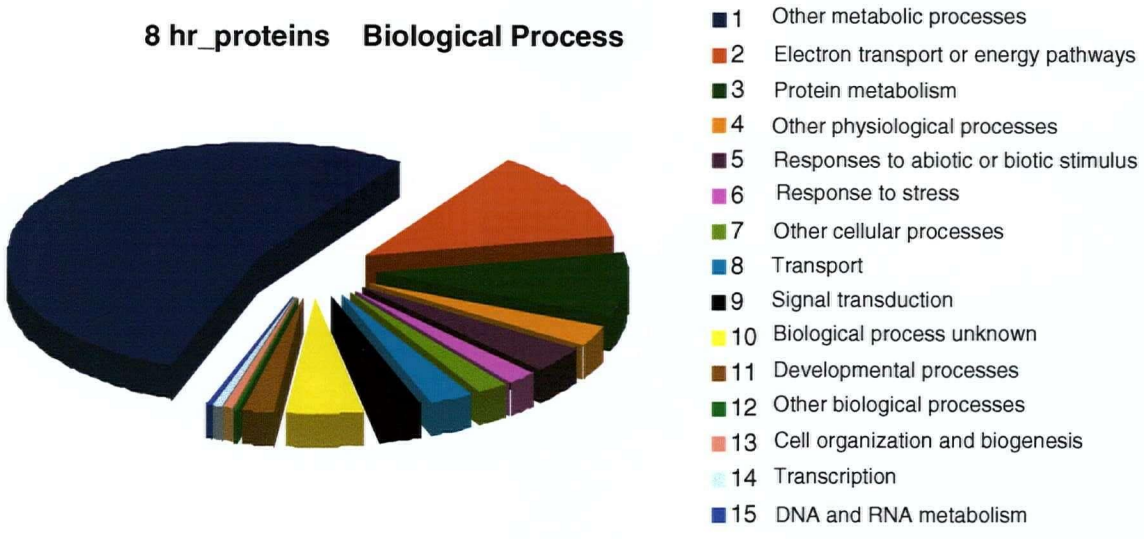
8 hr_proteins Biological Process
1 Other metabolic processes
2 Electron transport or energy pathways
3 Protein metabolism
4 Other physiological processes
5 Responses to abiotic or biotic stimulus
6 Response to stress
7 Other cellular processes
8 Transport
9 Signal transduction
10 Biological process unknown
11 Developmental processes
12 Other biological processes
13 Cell organization and biogenesis
14 Transcription
15 DNA and RNA metabolism

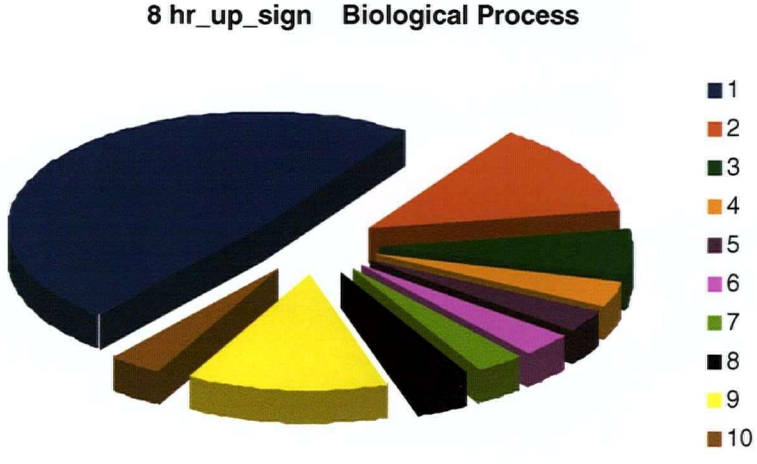
8 hr_up_sign Biological Process
1
2
3
4
5
6
7
8
9
10

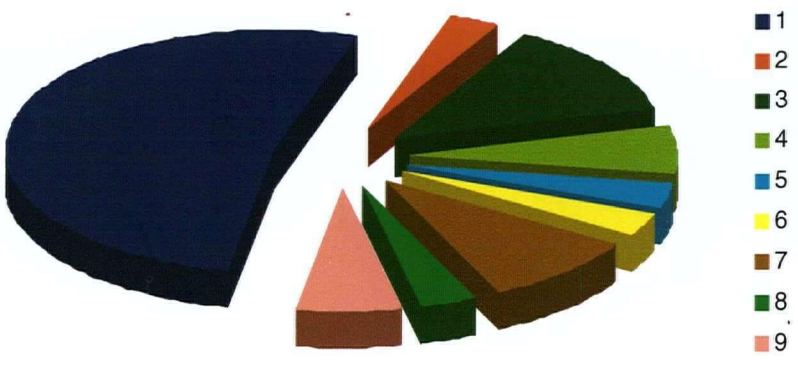
8 hr_down_sign Biological Process
1
2
3
4
5
6
7
8
9

5.4 Discussion

An inevitable consequence of aerobic life is the continual accumulation of reactive oxygen species (ROS) such as superoxide radical ($^{\bullet}O_2^-$), singlet oxygen ($^1O_2$), hydrogen peroxide (H_2O_2), hydroperoxide ($HO_2^{\bullet}$), and hydroxyl radical ($^{\bullet}OH$). These ROS are produced in unstressed cells as a result of normal plant growth and metabolic events; for example, as byproducts of mitochondrial and chloroplastic electron transfer, lipid β-oxidation, cell wall cross-linking and lignin formation (Asada 1992; Foyer et al., 1994; Noctor and Foyer, 1998). Plants have evolved to protect themselves by constitutively producing a basal level of antioxidant molecules, such as glutathione, ascorbate, phenylpropanoids, flavonoids, and polyamines (reviewed by Salin, 1987; Foyer et al., 1994; Kangasjärvi et al., 1994) and enzymes, including superoxide dismutases (SODs), ascorbate peroxidases (APXs), peroxiredoxins (PRXs), monodehydroascorbate reductase (MDH), and glutathione reductase (GR) (Alscher et al., 1991; Bowler et al., 1992; and Santos et al., 1998), which help to protect them from the potential damaging effects of these endogenous ROS (Conklin and Last, 1995; Roa et al., 1995; Kangasjärvi et al., 1996; Boldt and Scandalio, 1997; Sanderman, 1997).

The ability of plants to deal with basal levels of ROS thus involves a highly complex ROS scavenging system. However, when plants are subjected to intense or protracted assaults from environmental stressors such as ground-level ozone (O_3) (Pellinen et al., 1999), ultra-violet radiation (UVR) (Green and Fluhr, 1995), and pathogens (Legendre et al., 1993), abnormal amounts of ROS are produced, resulting in oxidative stress. As a result of this increased ROS presence, plants respond by

further activating their antioxidant defenses in order to protect themselves against the potential injurious effects of oxidative reactions with membranes and macromolecules in their cells.

Since ozone strongly and rapidly induces the activation of MPK6 in WT *Arabidopsis* plants (**Fig. 5.4**), I wanted to determine the role(s) that this signalling species might play in the overall response to ozone-induced stress. Through the use of RNA interference-based (RNAi) suppression, I have shown that MPK6 participates in managing the overall response to oxidant-induced stress in *Arabidopsis thaliana*. I have also shown, with the use of the MPK3 loss-of-function genotype that the closely-related MPK3 also plays an important role in the ability of *Arabidopsis* plants to respond to ozone-induced stress. I also have preliminary results that indicate that the upstream MAPKK, MKK5, is important in the overall response to ozone-induced stress in *Arabidopsis* and that ozone-induced signals therefore likely flow through MKK5 to MPK3 and MPK6.

In my loss-of-function studies, varying degrees of MKK5 suppression were obtained, but my inability to recover fully suppressed transgenic plants may point to the potential importance of MKK5 function in other processes such as seed development and/or germination. This was not the case with the MPK6-RNAi lines, where the recovery of almost completely silenced lines was common. This indicates that, if MKK5 is participating in other signaling pathways, it does so without requiring the presence of MPK6, its proposed downstream target. It could be that there is some threshold-level of MKK5 needed for proper signaling in development.

None of these transgenic lines (MPK3, MPK6 and MKK5) showed signs of spontaneous lesion formation under normal growth conditions. However, the MPK3-DG genotype had a germination rate of <50% which is far less than that of the MKK5- and AtMPK6-RNAi genotypes. While the initial (T_1) MPK6-RNAi seedlings had a high mortality rate when transferred from selection medium to soil, this was not the case for later generations and it seems likely that the original observation was unrelated to the transgene. It is interesting to note that the double (MPK3/6)-DG loss-of-function genotype cannot be recovered from MPK3-DG X MPK6-DG crosses (Dr. Xin Li, personal communication).

The most salient difference between the MKK5/MPK3/6 transgenics and WT plants is that the kinase-suppressed transgenic plants are all more sensitive to ozone. This is indicative of a direct role for these kinases in controlling the oxidative-stress response to ozone. The ozone-induced tissue damage for all transgenic lines resembled that elicited during the hypersensitive response (HR), which is consistent with the fact that both HR- and ozone-induced cell death have been shown to involve the accumulation of elevated levels of ROS (including hydrogen peroxide).

Partial suppression of MKK5 was also sufficient to attenuate the ozone-induced activation of two MAPKs, one of which is MPK6. This result is consistent with published data showing that constitutively active MKK5 is capable of activating both MPK3 and MPK6 (Ren et al., 2002) and that RNAi-silencing of SIPK (the orthologue of MPK6) in tobacco plants leads to increased ozone-induced cell death, with a concomitant increase in leaf-localized hydrogen peroxide (Samuel & Ellis, 2002). It is worth noting that the time-course of MAPK activation induced by ozone in the MKK5-

suppressed lines mirrors that seen in WT plants. Only the strength of activation of the two MAPKs is reduced in the MKK5-suppressed background. Overall, the preliminary results I obtained from my attempts to manipulate MKK5 function for MKK5 are interesting, but the topic clearly needs further work to substantiate them.

By contrast, the activation profile of MPK3 in the MPK6-RNAi lines is radically altered during ozone treatment, in a manner analogous to the activation of WIPK in a SIPK-suppressed background (Samuel & Ellis, 2002). MPK6 appears to play an important role in the regulation of MPK3, and the reciprocal seems to be true for MPK3. The regulatory mechanism(s) underpinning this interplay could be direct or indirect. There are a number of examples of mammalian MAPKs regulating the activities of other MAPKs. Zhang et al. (2001) demonstrated that the direct association between p38α and ERK1&2 led to inhibition of ERK1&2 phosphotransferase activities which was independent of MEK1 phosphorylation. They hypothesized that activated p38 may sequester ERK1&2 and sterically block phosphorylation of these MAP kinases by MEK1/2. Both dual-specificity phosphoprotein phosphatases (MKP) and serine/threonine-specific phosphatases have also been connected with the inactivation of MAPK signalling systems in mammals and plants (Brondello et al., 1997; Meskiene et al., 1998; Ulm et al., 2001; Westermarck et al., 2001).

It may be that MPK6 and MPK3 each target a specific, cognate phosphatase, which in turn removes one or both of the activation-loop phosphates from the other kinase, leaving that kinase inactive. A different possibility is that, just as with some mammalian signalling systems, one kinase physically sequesters its partner/target kinase thus preventing its activation. This 'pas de deux' between MPK3 and MPK6

highlights a previously unknown level of regulation in plant MAPK signalling. It will be interesting to find out if this type of reciprocal-regulation exists between any other plant MAPKs, MAPKKs and/or MAPKKKs and if so, what the biological implications might be.

It is important to realize that the ozone-sensitivity observed in MPK6-RNAi and the MPK3-DG loss-of-function genotypes could be a result of the promiscuous activities of the mis-regulated MAPK: MPK3 (in the MPK6-RNAi plants) or the MPK6 (in the MPK3-DG plants). At this point it is difficult to assess the relative importance of the physical loss of either MAPK vs. the enhancement of the activity of the other. It is known that both the intensity and duration of MAPK activation are important in the overall outcome of a signalling event. For example, mammalian PC12 cells undergo proliferation after transient MAPK activation in response to epidermal growth factor (EGF), but these same cells undergo growth arrest after sustained MAPK activation in response to nerve growth factor (NGF) (Davis, 1993; Cobb and Goldsmith, 1995; and Marshall, 1995). Consistent with this observation, Menke et al. (2004) reported that the MPK3 activation profile observed in their AtMPK6-silenced plants after treatment with various pathogens was similar to that seen in WT plants. These different outcomes with respect to MPK3 misregulation might be related to the nature of the different stressors and/or to the duration of their exposure.

The goal of proteomics is to identify all the proteins in an organism, to understand their patterns of expression in different cell types, and ultimately to characterize their post-translational modifications, interactions, and structure. In the spirit of this endeavor, I used isotope-coded affinity tagging (ICAT) technology to

examine ozone-induced changes in protein expression in *Arabidopsis thaliana*, where the proteomes of both WT and MPK6-RNAi genotypes were compared before and after an ozone challenge.

The observation that specific proteins differ in their abundance between WT and MPK6-RNAi plants even in the absence of ozone challenge may indicate that the constitutive loss of this MAPK has had metabolic consequences that affect amino acid metabolism and catabolism, electron transport or energy pathways, and molecular functions, including electron carrier-, catalytic-, oxidoreductase-, transporter-, and transaminase-activity. One of the more interesting 0 hr-air proteins found to be down-regulated in the R(6-7) genotype is a 5-formyltetrahydrofolate cyclo-ligase (5-FCL) family member (At1g76730). The 5-FCL catalyzes the irreversible, ATP-dependent conversion of 5-formyltetrahydrofolate to 5, 10-methenyltetrahydrofolate, and is located predominantly, if not exclusively, in the plant mitochondria. The substrate for 5-FCL, 5-formyltetrahydrofolate, is capable of inhibiting serine hydroxymethyltransferase (SHMT), which is crucial to photorespiration (Roje et al., 2002). If the level of 5-FCL expression is reduced in R(6-7) plants, this could possibly result in an accumulation of 5-formyltetrahydrofolate, which could reduce photorespiration capacity in this genotype.

Another of the 0hr-air proteins whose expression level is also lower in the RNAi genotype compared to WT is a chloroplast [Fe•S] protein, ferrodoxin (At1g60950). Ferrodoxin is located on the stromal surface of the thylakoid membrane, and functions in the photosynthetic electron transport chain. The observation that the level of

ferrodoxin is much lower in the R(6-7) genotype might indicate an overall decrease in the photosynthetic capacity of this genotype.

A number of the 8 hr-O_3 proteins whose expression levels are elevated in the R(6-7) genotype compared with the WT, are known to be involved in the antioxidant response to oxidative stress: chloroplast peroxiredoxin-Q (prxQ) (At3g26060.1); cytosolic monodehydroascorbate reductase (At3g52880.1); and cytosolic glutathione reductase (At3g24170.1).

Glutathione (GSH) (γ-Glu-Cys-Gly) is a major water-soluble antioxidant in plant cells. It is capable of directly reducing most active oxygen species; however, it reacts rather slowly with hydrogen peroxide. An important role for GSH is in the reduction of dehydroascorbate to ascorbate, the major substrate for reductive detoxification of hydrogen peroxide in plants, in the ascorbate-glutathione cycle (**Fig. 14**) (Foyer and Halliwell, 1976; Groden and Beck, 1979; and Nakano; Asada, 1980; reviewed in Foyer et al., 1998). Ascorbate can be regenerated from MDHA directly via the action of monodehydroascorbate reductase, or by the spontaneous disproportionation of MDHA into ascorbate and dehydroascorbate (DHA). Ascorbic acid is regenerated from DHA by dehydroascorbate reductase, in a reaction in which reduced glutathione (GSH) is simultaneously oxidized to form GSSG. GSH is then regenerated from GSSG in the presence of NADPH by glutathione reductase (Sharma and Davis, 1997). The components of this cycle exist in both chloroplast and cytosol (Foyer, 1993; and Foyer et al., 1998), and mitochondria, glyoxysomes, and peroxisomes (Jiménez et al., 1997).

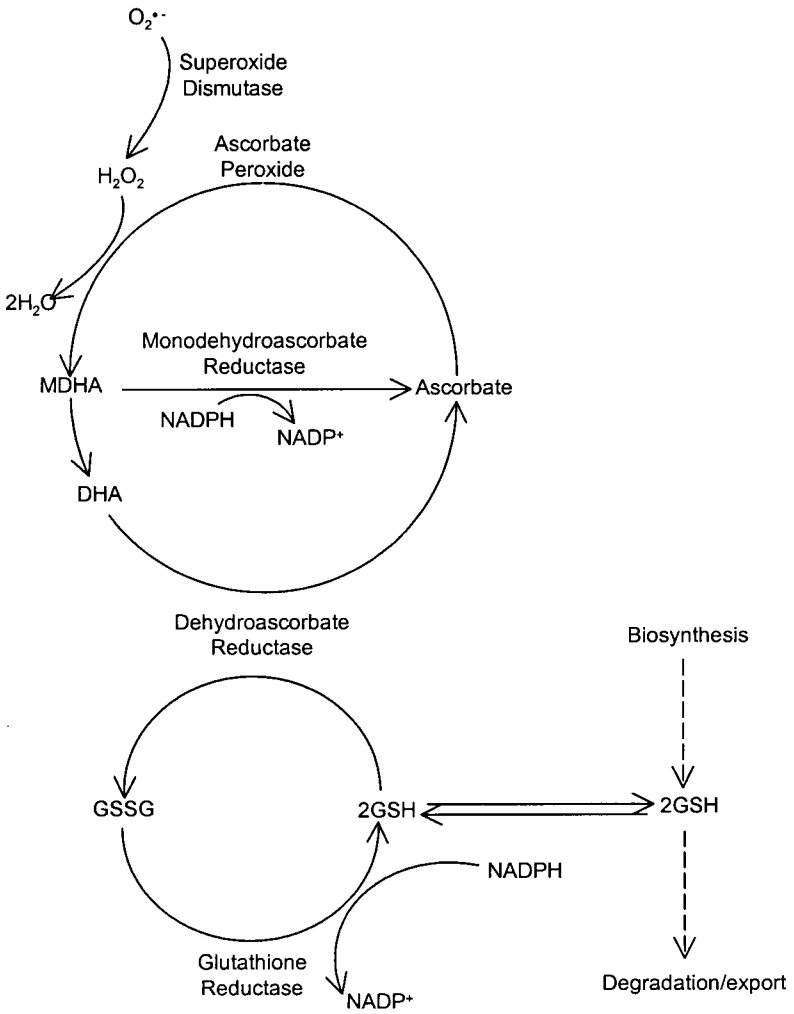

Fig. 14 Schematic representation of the relationships between glutathione biosynthesis and export together with interactions between the reduced and oxidized forms of glutathione and scorbate in removal of hydrogen peroxide. Hydrogen peroxide reacts with ascorbic acid in the company of ascorbate peroxidase forming monodehydroascorbate (MDHA). The regeneration of ascorbate can proceed from MDHA directly by the action of monodehydroascorbate reductase, or via the spontaneous disproportionation of MDHA into ascorbate and dehydroascorbate (DHA). Then, ascorbic acid is regenerated from DHA in a reaction catalyzed by dehydroascorbate reductase, in which reduced glutathione (GSH) Is oxidised into GSSG. GSH is regenerated in the company of NADPH by glutathione reductase. Borrowed and modified from (Foyer et al., 1998).

There were other antioxidant-related proteins detected in the 8 hr-O_3 sample, (catalase 3 (At1g20620.1), a peroxidase (At3g49120.1), catalase 2 (At4g35090.1), and glutathione peroxidase (At2g25080.1) which is predominantly involved in the detoxification of lipid peroxides (Eshdat et al., 1997), but expression differentials of these antioxidant-associated proteins were not significantly different between the two genotypes. This does not mean their protein expression levels may not be elevated compared to control levels, just that their levels were similar in WT and RNAi genotypes after 8 hr of ozone fumigation, indicating the loss of MPK6 function did not interfered with any response of their protein accumulation levels to ozone.

It is difficult to determine the importance of increased ratios of these specific antioxidant enzymes, given the fact that the *Arabidopsis* genome codes for so many antioxidant proteins. The fact that the MPK6-RNAi genotype shows leaf damage only after 24 hrs of ozone fumigation (500 ppb), indicates that there is only a relatively subtle change in the ability of this genotype to respond to acute oxidant stress. Consistent with this, the level of hydrogen peroxide accumulation in the leaves of ozone-treated MPK6-RNAi plants appear to be similar to those in WT plants. There is a slight but detectable difference however, in the two genotypes (WT and MPK6-RNAi) at 8 hr.

A more novel member of the antioxidant-related proteins with an elevated abundance in the MPK6-RNAi genotype compared with the WT genotype is prxQ, a plant homologue of the bacterioferritin co-migratory protein (Bcp). prxQ reduces hydroperoxides, which can form as direct byproducts of ozone-induced lipid oxidation, using electrons derived from NADPH through the thioredoxin (Trx)/Trx reductase

pathway or from some unknown reducing agent(s) (Jacobson et al., 1989; Chae et al., 1994; Kwon et al., 1994; Dietz et al., 2002).

And finally, the gene product of MAM1 (At5g23010), methylthioalkymalate synthase had the largest protein expression differential among the up-regulated 8hrO_3 proteins. Methylthioalkymalate synthase is an important enzyme in biosynthesis of alkyl glucosinolates, hallmark natural products in the crucifers, where they are thought to play an important role in plant defense (Chen et al., 2003).

In summary, I have used RNA interference-based (RNAi) suppression technology to demonstrate that both MPK6 and MKK5 are important in the overall response to ozone-induced oxidative stress, that MPK6 is needed for proper MPK3 function, and that the ozone-induced activation of MPK3 and MPK6 passes through MKK5. The MKK5 results are preliminary, but deserve further analysis. In addition, with the use of the (MPK3)-DG loss-of-function genotype, I have shown that MPK3 is also important in the response to ozone in *Arabidopsis* and that MPK3 in needed for proper MPK6 function. Finally, I employed isotope-coded affinity tagging (ICAT) analysis to both identify and quantify differences in protein profiles between WT and AtMPK6-RNAi genotypes.

Functional classification of the proteins from ozone treated tissue that were differentially expressed in the MPK6-suppressed and WT backgrounds was conducted based on the GO ontology system (**Table 5.4, p152**). The majority of the 0 hr-air and 8 hr-O_3 proteins are annotated as being located in the chloroplast, while the rest are associated with the mitochondria, nucleus, and cytosol. The categories of 'other metabolic processes', electron transport, energy pathways or antioxidant-related make

up the bulk of the 0 hr-air and 8 hr-O_3 protein entries with an assortment of other categories covering the rest of the protein entries.

Chapter 6

Concluding remarks and future directions

The overall goal of the research described in this thesis was to provide insight into the role of MAP kinases in plant responses to ozone- and ultra-violet (UV) radiation-induced oxidative stress. Ozone and UV, both environmentally relevant inducers of oxidative stress, represent two of the most pervasive environmental stresses to which plants, as well as metazoans, can be exposed. The specific objectives in this study were to determine the identity of the oxidant-induced MAPKs and to establish whether manipulation of the expression of these kinases would leed to alterations in a plant's overall ability to respond to oxidative stress. These investigations led to the identification of the oxidant-induced MAPKs, to a receptor-based model for ozone-induced MAPK signalling, and to the identification of an oxidant-induced MAPKK. The work also introduced me to the use of ICAT, a relatively new, high-throughput quantitative proteomic platform, which I was able to employ in my analysis of plant MAPK signalling.

The negative effects of ground level ozone and ultra-violet radiation on plants are well established, but the underlying mechanisms leading to these harmful effects are not well understood. The use of different mutants, and of transgenic plants impaired in signalling have helped me to illuminate the complex responses to oxidative stress in plants. It is now clear that MAPKs such as MPK6 and SIPK play important

roles in the overall ability of plants to deal with oxidative stress. The future direction of this research needs to have a large-scale focus, one that includes the use of high-throughput proteomic platforms such as ICAT and 2D gel electrophoresis combined with mass spectrometry and full-genome microarray technology. An endless supply of *Arabidopsis* signalling mutants wouldn't hurt!

Here is a list of possible future experiments that could be conducted by incoming students:

MKK5 work

- Q-PCR analysis of the most highly suppressed MKK5-RNAi lines in order to obtain a more accurate assessment of their levels of MKK5 suppression.

- Use Q-PCR to analyze multiple MKK5 lines to ascertain if MKK4 expression, is elevated in the R(5-2) line. If MKK4 expression is truly elevated, it might point to a scenario in which MKK4 can compensate for the loss of MKK5.

- To gain additional insight into the role(s) of MKK5 in transducing ozone-derived signals, perform a transcriptional "full-genome microarray" and proteomic profile "ICAT" comparison of ozone-treated WT and MKK5-RNAi plants, before and after (2 hr and 8 hr) treatment with ozone.

- I have also developed an MKK4-RNAi genotype. I have not had time to analyze this genotype beyond collecting a number of putative positive (T_1) lines which grew on selection medium. The same experiments need to be undertaken with this genotype as have been carried out with the MKK5-RNAi lines. It would also be very informative to produce a (MKK4 X MKK5) double mutant, if this combination is not lethal.

MPK6/MPK3

- Complete a more thorough ICAT protein profiling analysis of the ozone-treated MPK6-RNAi genotype looking at more lines grown under different conditions (i.e. greenhouse or growth chamber), each with at least two biological replicates. This level of analysis would give us a better idea of the reliability of our initial results. The big question: Can we obtain the same list of differentially expressed proteins (MPK6-RNAi/WT) each time the experiment is conducted?

- Since the double (MPK3/6)-DG loss-of-function genotype cannot be recovered from MPK3-DG X MPK6-DG crosses, an inducible double mutant should be constructed. For instance, transform the MPK6-DG genotype with an inducible vector carrying the MPK3-RNAi construct. These inducible, double mutants would give us a better understanding of the roles played by these two kinases. This approach can also be extended to the MKK loss-of-function mutants, MKK4 and MKK5.

- The data obtained from the individual loss-of-function genotypes, along with the double genotypes, would help us to make informed decisions on identifying potential targets of MPK3, MPK6, MKK4, and MKK5. Once we have a better idea of the identities of these targets, their analysis could begin. This process will help us to obtain a more complete picture of the roles that these kinases play in regulating the overall response to ozone/oxidant-induced stress.

In closing, I would like to talk a little about the history of *Arabidopsis thaliana*, the main model organism for my research. It is always desireable to know the history of the "horse" you are betting on. I have therefore put together a chronology of the most salient time points in the history of *Arabidopsis thaliana*, starting when it was first found in the Harz Mountains of Germany, in the 1570's, to the sequencing of it's genome in 2002 (reviewed in Plant physiology, the Lehle seeds website: http://www.*Arabidopsis*.com/; Somerville and Koornneef, 2002; and Meyerowitz, 2001).

The history of *Arabidopsis thaliana*

1570's *Arabidopsis thaliana* was discovered by Johannes Thal (hence, *thaliana*) in the Harz Mountains, though he called it *Pilosella siliquosa*.

1753 Linneaeus assigns names of *Pilosella siliquosa minor* as well as Arabis *thaliana* to *Arabidopsis*.

1873 Alexander Braun publishes first non-taxonomic paper on a mutant (presumably agamous) *Arabidopsis* plant found near Berlin.

1841 Taxonomist Gustav Heynhold renames Arabis *thaliana* as *Arabidopsis thaliana* (L.) Heynh. in honor of Johnannes Thal.

1907 E. Strasburger's graduate student, Friedrich Laibach, correctly observes that *Arabidopsis* has only 5 chromosomes (2n=10); the lowest odd number known up at that time for a plant; upon graduation, Laibach promptly discontinues working with *Arabidopsis* for the next 30 years.

1935 Russian genetist N.N. Titova, on a Russian expedition to find plants as potential model systems for genetics, rejects *Arabidopsis* because its chromosomes, miscounted as n=3, were too small.

1937 F. Laibach begins collecting *Arabidopsis* ecotypes.

1943 F. Laibach first recognizes the potential of *Arabidopsis* as model system for genetics.

1947 Laibach's graduate student E. Reinholz publishes first collection of induced mutations; discovers that late flowering can be induced in an early flowering type by X-rays.

1950's J. Langridge and K. Napp-Zinn's research demonstrates utility of *Arabidopsis* for laboratory studies.

1965 First International *Arabidopsis* Conference held in Göttingen, Germany; F. Laibach retires and G. Röbbelen at the University of Göttingen, Germany assumes curator role for Laibach's ecotype collection.

1967 Lee-Chen with Burger and Steinitz-Sears create first *Arabidopsis* trisomics; W.J. Feenstra reports using clear plastic sleeves to facilitate seed harvest; G.P. Redéi reports using a dilute agar solution to facilitate seed planting.

1970 G. Rédei publishes first major review article published in Bibliographica Genetica vol 20, No. 2, 1970, pp. 1- 151.

1975 G. Rédei publishes second major review article published in Ann. Rev. Genet. (1975) vol. 9,111-127.

1983 M. Koornneef publishes first detailed genetic map published.

1984 Genome size and complexity characterized.

1985 First promoted as model for molecular genetics.

1986 Transformation with Agrobacterium reported.

1986 First *Arabidopsis* gene sequence published.

1989 First T-DNA tagged mutant gene cloned.

1993 High-efficiency transformation established

1996 *Arabidopsis* Genome Initiative organized.

1997 Physical maps of all 5 chromosomes completed.

1998 *Arabidopsis* featured in Science genome issue.

1999 Chromosomes II and IV sequenced.

2000 Chromosomes I, III and V sequenced completing genome sequence.

2001 Increased emphasis on functional and comparative genomics.

2002 *Arabidopsis* first species whose entire genome placed on a Microarray.

Bibliography

Abe, M.K., Kartha, S., Karpova, A.Y., Li, J., Liu, P.T., Kuo, W.L. and Hershenson, M. B. (1998) Hydrogen peroxide activates signal-regulated kinase via protein kinase C, Raf-1, and MEK1. Am. J. Respir. Cell Mol Biol. **18**: 562-569.

Adam, A.L., Pike, S., Hoyos, M.E., Stone, J.M., Walker, J.C. and Novacky, A. (1997) Rapid and transient activation of a myelin basic protein kinase in tobacco leaves treated with harpin from *Erwinia amylovora*. Plant Physiol. **115**: 853-861.

Aebersold, R. and Mann, M. (2003) Mass spectrometry-based proteomics. Nature **13**: 198-207

Aharon, G. et al. (1998) Regulation of a plant plasma membrane Ca^{2+}-channel by TG-α-1, a heterotrimeric G protein I subunit homologue. FEBS Lett. **424**:17-21.

Alessi, D.R., Cuenda, A., Cohen, P., Dudley, D.T. and Saltiel, A. R. (1995) PD 098059 is a specific inhibitor of the activation of mitogen-activated protein kinase kinase in vitro and in vivo. J. Biol. Chem. **270**: 27489-27494.

Allen, L.J., MacGregor, K.B., Koop, R.S., Bruce, D.H., Karner, J., Brown, A.W. (1999) The Relationship Between Photosynthesis and a Mastoparan-Induced Hypersensitive Response in Isolated Mesophyll Cells. Plant Physiol. **119**: 1233-1241.

Allen, R.G. and Tresini, M. (2000) Oxidative stress and gene regulation. Free Radic. Biol. Med. **28**: 463-99.

Alscher, R.G., Erturk, N., Heath, L.S. (2002) Role of superoxide dismutases (SODs) in controlling oxidative stress in plants. J. Exp. Bot. **53**: 1331–1341.

Asada, K. (1992) Ascorbate peroxidase - a hydrogen peroxide-scavenging enzyme in plants. Physiol. Plant. **85**: 235-241.

Asai, T., Tena, G., Plotnikova, J., Willmann, M. R., Chiu, W. L., Gomez-Gomez, L., Boller, T., Ausubel, F.M. and Sheen, J. (2002) MAP kinase signalling cascade in *Arabidopsis* innate immunity. Nature **415**: 977-983.

Assmann, S. M. (2002) Heterotrimeric and unconventional GTP binding proteins in plant cell signalling. Plant Cell, Supplemental, **S**: 355-S373.

Atkinson, M.M., Midland, S.L., Sims, J.J. and Keen NT (1996) Syringolide 1 triggers Ca^{2+} influx, K^+ efflux, and extracellular alkalization in soybean cells carrying the disease-resistance gene *Rpg4*. Plant Physiol. **112**: 297–302.

Atkinson, M.M., Keppler, L.D., Orlandi, E.W., Baker, C.J. and Mischke, C.F. (1990) Involvement of plasma membrane calcium influx in bacterial induction of the K^+/H^+ and hypersensitive responses in tobacco. Plant Physiol. **92**: 215–221.

Baker, C.J. and Orlandi, E.W. (1995) Active oxygen in plant / pathogen interactions. Ann. Rev. Phytopathol. **33**: 304-321.

Baker, C.J., Orlandi, E.W. and Mock, N.M. (1993) Harpin, an elicitor of the hypersensitive response in tobacco caused by *Erwinia amylovora*, elicits active oxygen production in suspension cells. Plant Physiol. **102**:1341-1344.

Baldwin, I.T., Schmelz, E.A. and Ohnmeiss, T.E. (1994) Wound-induced changes in root and shoot jasmonic acid pools correlate with induced nicotine synthesis in *Nicatina sylvestris* SPEGAZZINI and COMES. J. Chem. Ecol. **20**: 2139-2157.

Banno, H., Hirano, K., Nakamura, T., Irie, K., Nomoto, S., Matsumoto, K. and Machida, Y. (1993) NPK1, a Tobacco gene that encodes a protein with a domain homologous to yeast BCK1, STE11, and Byr2 protein kinases. Mol. Cell. Biol. **13**: 4745-4752.

Bellincampi, D., Dipierro, N., Salvi, G., Cervone, F. and De Lorenzo, G. (2000) Extracellular H_2O_2 induced by oligogalacturonides is not involved in the inhibition of the auxin-regulated *rolB* gene expression in tobacco leaf. Plant Physiol. **122:** 1379-1385.

Bell, E. and Mullet, J., E. (1993) Charachterization of an *Arabidopsis* lipoxygenase gene responsive to methyl jasmonate and wounding. Plant Physiol. **103**: 1133-1137.

Betsholtz, C., Johnson, A., Heldin, C.-H. and Westermark, B. (1986) Efficient reversion of simian sarcoma virus transformation and inhibition of growth factor-induced mitogenesis by suramin. Proc. Natl. Acad. Sci. U.S.A. **83**: 6440-6444.

Blagoev, B., Kratchmarova, I., Ong, S.E., Nielsen, M., Foster, L.J., Mann, M. (2003) A proteomic stragety to elucidate functional protein-protein interactions applied to EGF signaling. Nat. Biotech. **3**: 315-318.

Blechert, S., Brodschelm, W., Holder, S., Kammerer, L., Kutchan, T.M., Mueller, M.J., Xia, Z-Q. and Zenk, M.H. (1995) The octadecanoic pathway: Signal molecules for the regulation of secondary pathways. Proc. Natl. Acad. Sci. U.S.A. **92**: 4099-4105.

Blumwald, E., Aharon, G.S. and Lam, B. C-H. (1998) Early signal transduction pathways in plant-pathogen interactions. TIBS **3**: 342-345.

Boldt, R., and Scandalios, J. G. (1997) Influence of UV-light on the expression of the *Cat2* and *Cat3* catalase genes in maize. Free Radic. Biol. Med. **23**: 505–514.

Boller, T. (1991) Ethylene in pathogenesis and disease resistance. *In* A. K. Mattoo and J. C. Suttle (eds.), The Plant Hormone Ethylene. CRC Press, Boca Raton, Florida, pp. 293-314.

Bolwell, G.P. (1996) The origin of the oxidative burst in plants. Biochem. Soc. Trans. **24**: 438-442.

Bolwell, G.P. (1999) Role of active oxygen species and NO in plant defense responses. Curr Opin Plant Biol. **2**:287-94.

Boulton, T.G., Nye, S.H., Robbins, D.G., Ip, N.Y., Radziejewska, E., Morgenbesser, S.D., Depinho, R.A., Panayotatos, N., Cobb, M.H. and Yancopoulos, G.D. (1991) ERKs: a family of serine/threonine kinases that are activated and tyrosine phosphorylated in response to insulin and NGF. Cell **65**: 663-675.

Boveris, A. and Chance, B. (1973) The mitochondrial generation of hydrogen peroxide. General properties and effect of hyperbaric oxygen. Biochem. J. **134**: 707-716.

Boveris, A., Cadenas, E. and Stoppani, A.O.M. (1976) Biochem. J. **156**: 435-444.

Bowler, C., Van Montagu, M. and Inze, D. (1992) Superoxide dismutase and stress tolerance. Ann. Rev. Plant Physiol. Plant Mol. Biol. **43**:83-116.

Braidot, E., Petrussa, E., Vianello, A. Marci, F. (1999) Hydrogen peroxide generation by higher plant mitochondria oxidizing complex I or complex II substrates. FEBS. **451**: 347-350.

Brederode, F.T., Linthorst, H.J., Bol, J.F. (1991) Differential induction of acquired resistance and PR gene expression in tobacco by virus infection, ethephon treatment, UV light and wounding. Plant Molecular Biology **17**: 1117–1125.

Brendley, B.W. and Pell, E.J. (1998) Ozone-induced changes in biosynthesis of Rubisco and associated compensation to stress in foliage of hybrid poplar. Tree Physiol **18**:81-90.

Brisson, L.F., Tenhaken, R. and Lamb, C. (1994) Function of oxidative cross-linking of cell wall structureal proteins in plant disease resistance. Plant Cell **6**: 1703-1712.

Brondello, J.M., Brunet, A., Pouyssegur, J., and McKenzie, F.R. (1997) The dual specificity mitogen-activated protein kinase phosphatase-1 and -2 are induced by the p42/p44 MAPK cascade. J. Biol. Chem. **272**: 1368–1376.

Brunet, A. and Pouyssegur, J. (1997) Mammalian MAP kinase modules: how to transduce specific signals. Essays Biochem. **32**:1-16.

Bush, D.S., Biswas A.K., Jones, R.L. (1989) Gibberellic-acid-stimulated Ca^{2+} accumulation in endoplasmic reticulum of barley aleurone: Ca^{2+} transport and steady-state levels. Planta **178**: 411-420.

Cadenas, E. (1995) Mechanisms of oxygen activation and reactive oxigen species detoxification. *In Oxidative Stress and Antioxidant Defenses in Biology* (Ahmad, S., ed.). New York: Chapman and Hall, **pp**1-61.

Camp, W.V., Montagu. M.V. and Inze, D. (1998) H_2O_2 and NO: redox signals in disease resistance. TIPS. **3**: 330-334.

Caselli, A., Marzocchini, R., Camici, G., Manao, G., Moneti, G., Pieraccini, G. and Ramponi, G. (1998) The inactivation mechanism of low molecular weight phosphotyrosine-protein phosphatase by H_2O_2. J. Biol. Chem. **273**: 32554-32560.

Cerutti, P.A. (1985) Pro-oxidant states and tumor promotion. Science **227**: 375-381.

Chae H.Z., Robinson K., Poole L.B., Church G., Storz G. and Rhee S. G. (1994) Cloning and sequencing of thiol-specific antioxidant from mammalian brain: alkyl hydroperoxide reductase and thiol-specific antioxidant define a large family of antioxidant enzymes. Proc. Natl. Acad. Sci. U.S.A. **91**: 7017-7021.

Chahdi, A., Daeffler, L., Giel, J.P., Landry, Y. (1998) Drugs interacting with G protein α subunits: selectivity and perspectives. Fundam. Clin. Pjarmacol. **12**: 121-132.

Chameides, W.L., Kasibhatla, P.S., Yienger, J. and Levy II, H. (1994) Growth of continental-scale metro-agro-plexes, regional ozone pollution, and world food production. Science **264:** 74-77.

Chamnongpol, S., Willekens, H., Moeder, W., Langebartels, C., Sandermann, H. Jr., Van Montagu, M., Inze, D. and Van Camp, W. (1998). Defense activation and enhanced pathogen tolerance induced by H_2O_2 in transgenic tobacco. Proc. Natl. Acad. Sci. U.S.A. **95:** 5818-5823.

Chandra, S. and Low, P.S. (1997) Measurement of Ca^{2+} fluxes during elicitation of the oxidative burst in aequorin-transformed tobacco cells. J. Biol. Chem. **272:** 28274-28280.

Chen F., Tholl D., D'Auria J.C., Farooq A., Pichersky E. and Gershenzon J. (2003) Biosynthesis and emission of terpenoid volatiles from *Arabidopsis* flowers. Plant Cell **15**: 481-494.

Chen, Z., Malamy, J., Henning, J., Conrath, U., Sanches-Casas, P. ,Silva, H. Ricigliano, J. and klessig, D. F. (1995) Induction, modification, and transduction of the salicylic acid signal in plant defense responses. Proc. Natl. Acad. Sci. U.S.A. **92**: 4134-4137.

Chong, H., Vikis, H.G. and Guan, K.-L. (2003) Mechanisms of regulating the Raf kinase family. Cell. Signal. **15**: 463-469.

Clark-Lewis, I., Sanghera, J.S. and Pelech, S. L. (1991) Definition of a consensus sequence for peptide substrate recognition by p44mpk, the meiosis-activated myelin basic protein kinase. J. Biol. Chem. **266**:15180-15184.

Clayton, H., Knight, M.R., Knight, H., McAinsh, M.R. and Hetherington, A.M. (1999) Dissection of the ozone – induced calcium signature. The Plant J. **17**: 575-579.

Clough, S. J., Bent, A.F. (1998) Floral dip: a simplified method for Agrobacterium-mediated transformation of *Arabidopsis thaliana*. Plant J. **16**:735-43.

Cobb, M.H. and Goldsmith, E.J. (1995) How MAP kinases are regulated. J. Biol. Chem. 270:14843-14846.

Coleman, M.D., Dickerson, R.E., Isebrands, J.G., and Karnosky, D.F. (1995) Carbon utilization allocation and partitioning in aspen clones varying in sensitivity to tropospheric ozone. Tree Physiol. **15**: 593-604.

Conklin, P.L. and Last, R.L. (1995) Differential accumulation of antioxidant mRNAs in *Arabidopsis thaliana* exposed to ozone. Plant Physiol. **109:** 203-212.

Constabel, C. P., Bergey, D. R. and Ryan, C. A. (1995) Systemin activates synthesis of wound-inducible tomato leaf polyphenol oxidase via the octadecanoid defense signaling pathway. Proc. Natl. Acad. Sci. U.S.A. **92**: 407–411.

Corpas, F.J., Barroso, J.B. and del Rio, L.A. (2001) Peroxisomes as a source of reactive oxygen species and nitric oxide signal molecules in plant cells. TIPS. **6**: 145-150.

Costa, V. and Moradas-Ferreira, P. (2001) Oxidative stress and signal transduction in *Saccharomyces cerevisiae*: insights into ageing, apoptosis and diseases. Mol. Aspects of Med. **22**: 217-246.

Dai, Q., Yan, B., Haung, S., Liu, X., Peng, S., Miranda, M.L.L., Chavez, A.Q., Vergara, B.S., Olszyk, D.M. (1997) Response of oxidative stress defense systems in rice (*Oryza sativa*) leaves with supplemental UV-B radiation. Physiol. Plant. **101**: 301-308.

Darrall, N.M. (1989) The effect of air pollutants on physiological processes in plants. Plant Cell Environ. **12**: 1-30.

Davis, R.D. (1993) The mitogen-activated protein kinase signal transduction pathway. J. Biol. Chem. **268**: 14553-14556.

Delladone, M., Xia, Y., Dixon, R.A. and Lamb, C. (1998) Nitric oxide functions as a signal in plant disease resistance. Nature **394**: 585-588

Demple, B. (1996) Redox signaling and gene control in the *Escherichia coli* soxRS oxidative stress regulon - a review. Gene **179**: 53-57.

Desikan, R., Clarke, A., Atherfold, P., Hancock, J.T. and Neill, S. J. (1999) Harpin induces mitogen-activated protein kinase activity during defense responses in *Arabidopsis thaliana* suspension cultures. Planta **210**: 97-103.

Desikan, R., Hancock, J.T., Coffey, M.J. and Neill, S. J. (1996) Generation of active oxygen in elicited cells of *Arabidopsis thaliana* is mediated by a NADPH oxidase-like enzyme. FEBS letters **382**: 213-217.

Dietz, K.J., Horling, F., König, J. And Baier, M. (2002) The function of the chloroplast 2-cysteine peroxiredoxin in peroxide detoxification and its regulation. J. Exp. Bot. **53**: 1321-1329.

Draper, J. (1997) Salicylate, superoxide synthesis and cell suicide in plant defense. TIPS. **2**:162-165.

Eckey-Kaltenbach, H., Ernst, D., Heller, W. and Sandermann Jr, H. (1994) Biochemical plant responses to ozone. Plant Physiol. **104**: 67 - 74.

Ecker, J.R. (1995) The ethylene signal transduction pathway in plants. Science **268**: 667–675.

Etheridge, N., Trusov, Y., Verbelen, J.P., Botella, J.R. (1999) Characterization if ATDRG1, a member of a new class of GTP-binding proteins in plants. Plant Mol. Biol. **39**: 1113-1126.

Farmer, E.E. and Ryan, C.A. (1990) Interplant communication: Airborne methyl jasmonate induces synthesis of proteinase inhibitors in plant leaves. Proc. Natl. Acad. Sci. U.S.A. **87**: 7713–7716.

Feher, J., Csomos, G. and Vereckei, A. (1987) Free radical reactions in medicine (Feher, J., Csomos, G. and Vereckei, A., eds.). Berlin: Springer-Verlag, **pp**. 19-37.

Felle, H. (1988) Auxin causes oscillations of cytoplasmic free calcium and pH in *Zea mays* L coleotiles. Planta **174**: 495-499.

Foyer, C.H., Descourvieres, P. and Kunert, K. J. (1994) Protection against oxygen radicals: an important defence mechanism studied in transgenic plants. Plant Cell Environ. **17**: 507-523.

Foyer, C.H. and Halliwell, B. (1976) The presence of glutathione and glutathione reductase in chloroplasts: a proposed role in ascorbic acid metabolism. Planta **133**: 21-25.

Franklin-Tong, V.E., Drobak, B.K., Allan, A.C., Watkins, P.A.C., Trewavas, A. J. (1996) Growth and pollen tubes of *Papaver rhoeas* is regulated by a slow-moving calcium wave propagated by inositol 1,4,5-triphosphate. Plant Cell **8**: 1305-1321.

Fujisawa, Y., Kato, H., Iwasaki, Y. (2001) Structure and function of heterotrimeric G proteins in plants. Plant Cell Physiol. **42**: 789-794.

Fujisawa, Y., Sawaki, S., Kato, H., Asahi, T. and Iwasaki, Y. (2001) Biochemical reponses of rice cells to mastoparan 7, an activator of heterotrimeric G proteins. Plant Biotech. **18**: 241-249.

Goormachtig, S., Capoen, W., James, E.K. and Holster, M. (2004) Switch from intracellular to intercellular invasion during water stress-tolerant legume nodulation. Proc. Natl. Acad. Sci. U.S.A. **101**: 6303-6308.

Gotor, C., Lam, E., Cejudo, F.J. and Romero, L.C. (1996) Isolation and analysis of the soybean *SGA2* gene (cDNA) encoding a new member of the plant G-protein family of signal transducers. Plant Mol. Biol. **32**: 1227-1234

Graier, W.F., Hoebel, B.G., Paltauf-Doburzynska, J. and Kostner, G.M. (1998) Effects of superoxide anions on endothelial Ca^{2+} signaling pathways. Arterioscler. Thromb. Vasc. Biol. **18**: 1470-1479.

Green, R. and Fluhr, R. (1995) UV-B-induced PR-1 accumulation is mediated by active oxygen species. Plant Cell **7**: 203-212.

Greenbaum, D., Colangelo, C., Williams, K. and Gerstein, M. (2003) Comparing protein abundance and mRNA expression levels on a genomic scale. Genome Biol. **4**: article 117.

Grimes, H.D., Perkins, K.K. and Boss, W.F. (1983) Ozone degrades into hydroxyls under physiological conditions. Plant Physiol. **72**: 1016 -1020.

Groß, S., Knebel, A., Tenev, T., Neininger, A., Gaestel, M., Herrlich, P. and Böhmer, F.D. (1999) Inactivation of protein-tyrosine phosphatases as mechanism of UV-induced signal transduction. J. Biol. Chem. **37**: 26378-23386.

Groden, D. and Beck, E. (1979) H_2O_2 destruction by ascorbate-dependent systems from chloroplasts. Biochim Biophy. Acta **546**: 426-433.

Guidi, L., Nali, C., Lorenzini, G. ,Filippi, F. and Soldatini, G.F. (2001) Effect of chronic ozone fumigation on the photosynthetic process of poplar clones showing different sensitivity. Environ. Pollut. **113**: 245-254.

Gundlach, H., Muller, M.J., Kutchan, T.M. and Zenk, M.H. (1992) Jasmonic acid is signal transducer in elicitor-induced plant cell cultures. Proc. Natl. Acad. Sci. U.S.A. **89**: 2389-2393.

Gutkind, J.S. (1998) The pathways connecting G protein-coupled receptors to the nucleus through divergent mitogen-activated protein kinase cascades. J. Biol. Chem. **273**: 1839-1847.

Guyton, K.Z., Liu, Y., Gorospe, M., Xu, Q. and Holbrook, N.J. (1996) Activation of mitogen-activated protein kinase by H_2O_2. J. Biol. Chem. **271**: 4138 - 4142.

Gygi, S.P., Rochon, Y., Franza, B.R. and Aebersold, R. (1999) Correlation between protein and mRNA abundance in yeast. Mol. Cell. Biol. **19:** 1720-1730.

Hahlbrock, K., Scheel, D., Logemann, E., Nurnberger, T., Parniske, M., Reinold, S., Sacks, W.R. and Schmelzer, E. (1995) Oligopeptide elicitor-mediated defense gene activation in cultured parsley cells. Proc. Natl. Acad. Sci. U.S.A. **92**: 4150-4157.

Hammod-Kosack, K.E. and Jones J.D.G. (1996) Resistance gene-dependent plant defense responses. Plant Cell **8**: 1773-1791.

Han, D.K., Eng, J., Zhou, H. and Aebersold, R. (2001) Quantitative profiling of differentiation-induced microsomal proteins using isotope-coded affinity tags and mass spectrometry. Nature Biotech. **19**: 946-951.

Hanks, S.K. and Hunter, T. (1995) The eukaryotic protein kinase superfamily: kinase (catalytic) domain structure and classification. FASEB. J. **9**: 576-596.

Hardie, D.G. (1999) Plant protein serine/threonine kinases: classification and function. Annu. Rev. Plant Physiol. Plant Mol. Biol. **50**: 97-131.

Heagle, A.S. (1989) Ozone and crop yield. Ann Rev Phytopathology **27**: 397-423.

Heath, R.I. (1988) Biochemical mechanisms of pollutant stress. *In Assessment of crop loss from air pollutants* (Heck, W.N., Taylor, O, C. and Tingey, D.T., eds.). London: Elsevier, **pp**. 259-286.

Heck, W.W., Cure, W.W., Rawlings, J. O., Zaragoza, L.J., Heagle, A. S., Heggestad, H.E., Khout, R.J., Kress, L.W. and Temple, P.J. (1984) "Assessing impacts of ozone on agricultural crops: I. Overview," Journal of the Air Pollution Control Association, **34**: 729-735.

Heck, W.W., Cure, W.W., Rawlings, J. O., Zaragoza, L.J., Heagle, A. S., Heggestad, H.E., Khout, R.J., Kress, L.W. and Temple, P.J. (1984) "Assessing impacts of ozone on agricultural crops: II. Crop yield functions and alternative exposure statistics," Journal of the Air Pollution Control Association, **34**: 810-817.

Hewitt, N.C., Kok, G.L. and Fall, R. (1990) Hydroperoxides in plants exposed to ozone mediate air pollution damage to alkene emitters. Nature **344**: 56-58.

Hirt, H. (1997) Multiple roles of MAP kinases in plant signal transduction. TIPS **2**: 11-15.

Höller, C., Freissmuth, M. and Nanoff, C. (1999) G proteins as drug targets. CMLS, Cell. Mol. Life Sci. **55**: 257-270.

Holsters, M., de Waele, D., Depicker, A., Messens, E., van Montagu, M. And Schell, J. (1978) Transfection and transformation of Agrobacterium tumefaciens. Mol. Gen. Genet. **163**: 181-187.

Hosang, M. (1985) Suramin binds to platelet growth factor and inhibits its biological activity. J. Cell Biochem. **29**: 265-273.

Hrabak, E.M., Dickmann, L.J., Satterlee, J.S., and Sussman, M.R. (1996) Characterization of eight new members of the cal-modulin-like domain protein kinase gene family from *Arabidopisis thaliana.* Plant Mol. Biol. **31**:405-412.

Ichimura, K., Tena, G., Henry,Y., Zhang, S., Hirt, H., Ellis, B.E., Morris, P.C., Wilson, C., Champion, A., Innes, R.W., Sheen, J., Ecker, J.R., Scheel, D., Klessig, D.F., Machida, Y., Mundy, J., Ohashi, Y., Kreis, M., Heberle-Bors, E., Walker, J.C. and Shinozaki, K. (2002) Mitogen-activated protein kinase cascades in plants. Nomenclature of *Arabidopsis* MAP kinases (MPKs)and MAP kinase kinases (MKKs). Trends in Plant Science **7**: 301-308.

Ishikawa, A., Tsubouchi, H., Iwasaki, H. and Asahi, T. (1995) Molecular cloning and characterization of a cDNA for the α subunit of a G protein from rice. Plant Cell **36**: 353-359.

Izumi, C., Schroeder, M., Schroeder, J.I. (2004) Reactive oxygen species activation of plant Ca^{2+} channels. A signaling mechanism in polar growth hormone transduction, stress signaling, and hypothetically mechanotransduction. Plant Phys. **135**: 702-708.

Jabs, T. (1999) Reactive oxygen intermediates as mediators of programmed cell death in plants and animals. Biochem. Pharmacol. **57**: 231-245.

Jabs, T., Dietrich, R.A. and Dangl, J. (1996) Initiation of runaway cell death in an *Arabidopsis* mutant by extracellular superoxide. Science **273**: 1853-1856.

Jacobson, F.S., Morgan, R. W., Christman, M. F. and Ames, B. N. (1989) An alkyl hydroperoxide reductase from Salmonella typhimurium involved in the defense of DNA against oxidative damage. J. Biol. Chem. **264**: 1488-1496.

Jane, L. and Marc, R. K. (2002) Protection against heat stress-induced oxidative damage in *Arabidopsis* involves calcium, abscisic acid, ethylene, and salicylic acid. Plant Physiol. **128**: 682–695.

Jansen, M.A.K., Gaba, V. and Greenburg, B.M. (1998) Higher plants and UV-B radiation: balancing damage, repair and acclimation. TIPS **3**: 131-135.

Jaspers, I., Chen, L.C. and Flescher, E. (1998) Induction of interleukin-8 by ozone is mediated by tyrosine kinase and protein kinase A, but not by protein kinase C. J. Cell. Physiol. **177**: 313-323.

Jespersen, H.M., Kjaersgård, I. V. H., Østergaard, L., Welinder, K. G. (1997) From sequence analysis of three novel ascorbate peroxidases from *Arabidopsis thaliana* to structure, function and evolution of seven types of ascorbate peroxidase. Biochem. J. **326**: 305–310.

Jiménez, A., Hernandez, J.A., del Rio, L.A. and Sevilla, F. (1997) Evidence for the presence of the ascorbate-glutathione cycle in mitochondria and peroxisomes of pea leaves. Plant Physiol. **114**: 275-284.

Johnson, G.L. and Lapadat, R. (2002) Mitogen-activated protein kinase pathways mediated by ERK, JNK, and p38 protein Kinases. Science **298**: 1911-1912.

Jonak, C., Ökrész, L., Bögre, L. and Hirt, H. (2002) Complexity, cross talk and integration of plant MAP kinase signalling. Curr. Opin. Plant Biol. **5**: 415-424.

Jonak, C., Kiegerl, S., Ligterink, W., Barker, P.J.E., Huskisson, N.S. and Hirt, H. (1996) Stress signaling in plants: a mitogen-activated protein kinase pathway is activated by cold and drought. Proc. Natl. Acad. Sci. U.S.A. **93**:11274-11279.

Jones, A.M. (2002) G-protein-coupled signaling in *Arabidopsis*. Curr. Opin. Plant Biol. **5**: 402-407.

Jones, H.D., Smith, S.J., Desikan, R., Plankidou-Dymock, S., Lovegrove, A. and Hooley, R. (1998) Heterotrimeric G proteins are implicated in gibberellin induction of α-amylase gene expression in wild oat aleurone. Plant Cell **10**: 245-254.

Kamata, H. Hirata, H. (1999) Redox regulation of cellular signalling. Cell Signal. **1**:1-14.

Kangasjarvi, J., Talvinen, J., Utriainen, M. and Karjalainen, R. (1994) Plant defense systems induced by ozone. Plant, Cell and Environ. **17**: 783-794.

Kanofsky, J.R. and Sima, P.D. (1995) Singlet oxygen generation from the reaction of ozone with plants. J. Biol. Chem. **270**:7850-7852.

Karnik, S.S., Gogonea, C., Patil, S., Saad, Y. and Takezako, T. (2003) Activation of G-protein-coupled receptors: a common molecular mechanism. Trends in Endocrin. Med. **14**: 431-437.

Kauss, H. and Jeblick, W. (1996) Influence of salicylic acid on the induction of competence for H_2O_2 elicitation. Plant Physiol. **111**: 755-763.

Kawano, T., Sahashi, N., Takahashi, K., Uozumi, N. and Muto, S. (1998) Salicylic Acid induces superoxide generation followed by an increase in cytosolic calcium ion in tobacco suspension culture: The earliest events in signal transduction. Plant Cell Physiol. **39**: 721-730.

Kay, K. and James, A. I. (1996) Superoxide accelerates DNA damage by elevating free-iron levels (hydrogen peroxide / Fenton reaction / oxidative stress / hydroxyl radical / oxygen toxicity). Proc. Natl. Acad. Sci. U.S.A. **93**:13635-13640.

Keller, A., Nesvizhskii, A.I., Kolker, E., Aebersold, R. (2002) Empirical statistical model to estimate the accuracy of peptide identifications made by MS/MS and database search. Anal. Chem. **74**: 5383-5392.

Kiichi, H., Minoru, M., Satoshi, I., Akira, N., Kenjiro, M. and Junji, Y. (1997) AP-1 transcriptional activity is regulated by a direct association between thioredoxin and Ref-1. Proc. Natl. Acad. Sci. U.S.A. **15**: 3633–3638.

Klinker, J.F., Hageluken, A., Grunbaum, L., Heilmann, I., Nurnburg, B., Harhammer, R., Offermanns, S., Schwaner, I., Ervens, J., Wenzel-Seifert, K. et al., (1994) Mastoparan may activate GTP hydrolysis by Gi-proteins in HL-60 membranes indirectly through interaction with nucleoside diphosphate kinase. Biochem. J. **304**: 377-383.

Knetsch, M.L.W., Wang, M., Snaar-Jagalska, B.E. and Heimovaara-Dijkstra, S. (1996) Abscisic acid induced mitogen-activated protein kinase activation in barley aleurone protoplasts. Plant Cell **8**: 1061-1067.

Koch, J.R., Creelman, R.A., Eshita, S.M., Seskar, M., Mullet, J.E. and Davis, K.R. (2000) Ozone sensitivity in hybrid poplar correlates with insensitivity to both salicylic acid and jasmonic acid. The role of programmed cell death in lesion formation. Plant Physiol.**123**: 487-96.

Koch, J.R., Scherzer, A.J., Eshita, S.M. and Davis, K.R. (1998) Ozone sensitivity in hybrid poplar is correlated with the lack of defense-gene activation. Plant Physiol. **118**: 1243-1252.

Kong, W., Shiota, S., Shi, Y., Nakayama, H. and Nakauama, K. (2000) A novel peroxiredoxin of the plant Sedum lineare is a homologue of Escherichia coli bacterioferritin co-migratory protein (Bcp). Biochem. J. **351**: 107–114.

Kovtun, Y., Chiu, W.-L., Tena, G. and Sheen, J. (2000) Functional analysis of oxidative stress-activated mitogen-activated protein kinase cascade in plants. **P7**: 2940-2945.

Kowaltowski, A.J. and Vercesi, A.E. (1999) Mitochondrial damage induced by conditions of oxidative stress. Free radical biol. Med. **26**: 463-471.

Kuge, S., Arita, M., Murayama, A., Maeta, K., Izawa, S., Inoue, Y. and Nomoto, A. (2001) Regulation of the yeast Yap1p nuclear export signal is mediated by redox signal-induced reversible disulfide bond formation. Mol. Cell. Biol. **21**: 6139-6150.

Kuge, S., Jones, N. and Nomoto, A. (1997) Regulation of yAP-1 nuclear localization in response to oxidative stress. EMBO **16**: 1710-1720.

Kumar, D. and Klessig, D.F. (2000) Differential induction of tobacco MAP kinases by the defense signals nitric oxide, salicylic acid, ethylene, and jasmonic acid. Mol. Plant Microbe Inter.**13**: 347-351.

Krupa, S.V. and Manning, W.J. (1988) Atmospheric ozone: Formation and effects on vegetation. Environ. Pollut. **50**:101-137.

Kyriakis, J. M., Banerjee, P., Nikolakaki, E., Dai, T., Rubie, E. A., Ahmad, M. F., Avruch, J. and Woodgett, J. R. (1994) Nature **369**: 156-160.

Lamb, C. and Dixon, R.A. (1997) The oxidative burst in plant disease resistance. Annu. Rev. Plant Mol. Biol. **48**: 251-275.

Lander, H.M., Ogiste, J.S., Teng, K.K. and Novogrodsky, A. (1995) p21ras as a common signaling target of reactive free radicals and cellular redox stress. J. Biol. Chem. **270**: 21195-21198.

Langebartels, C., Heller, W., Fuhrer, G., Lippert, M., Simons, S. and Sandermann, H. Jr (1998) Memory effects in the action of ozone on conifers. Ecotoxicol. Environ. Saf. **41**: 62-72.

Lawton, M. A., Yamamoto, R. T., Hanks, S. K. and Lamb, C. J. (1989) Molecular cloning of plant transcripts encoding protein kinase homologs. Proc. Natl. Acad. Sci. U.S.A. **86**: 3140-3144.

Lebrun-Garcia, A., Ouaked, F., Chiltz, A. and Pugin, A. (1998) Activation of MAPK homologues by elicitors in tobacco cells. Plant J. **15**: 773-781.

Lee, J., Klessig, D.F., and Nurnberger, T. (2001) A harpin binding site in tobacco plasma membranes mediates activation of the pathogenesis-related gene HIN1 independent of extracellular calcium but dependent on mitogen-activated protein kinase activity. Plant Cell **13**: 1079-1093.

Lee, S., Choi, H., Suh, S., Doo, I. S., Oh, K.Y., Choi, E.J., Schroeder-Taylor, A.T., Low, P.S. and Lee, Y. (1999) Oligogalacturonic acid and chitosan reduce stomatal aperture by inducing the evolution of reactive oxygen species from guard cells of tomato and Commelina communis. Plant Physiol. **121**: 147-152.

Lee, Y.-R.J. Assmann, S.M. (1999) *Arabidopsis thaliana* 'extra-large GTP-binding protein' (AtXLG1): a new class of G-protein. Plant Mol. Biol. **40**: 55-64.

Legendre, L., Heinstein, P.F. and Low, P.S. (1992) Evidence for participation of GTP-binding proteins in elicitation of the rapid oxidative burst in cultured soybean cells. J. Biol. Chem. **267**: 20140-20147.

Legendre, L., Yuch, Y.G., Crain, R., Haddock, N. and Heinstein, P.F. (1993) Phospholipase C activation during elicitation of the oxidative burst in cultured plant cells. J. Biol. Chem. **268**: 24559-24563.

Levine, A., Pennell, R.I., Alverez, M.E., Palmer, R. and Lamb, C. (1996) Calcium-mediated apoptosis in plant hypersensitive disease resistance response. Curr. Biol. **6**: 427-437.

Levine, A., Tenhaken, R., Dixon, R. and Lamb, C. (1994) H_2O_2 from the oxidative burst orchestrates the plant hypersensitive disease resistance response. Cell **79**: 583-593.

Li, X., Lassner, M. and Zhang, Y. (2002) Deleteagene: a fast neutron deletion mutagenesis-based gene knockout system for plants. Comp. Func. Genom. **3**: 158-160.

Li, X., Zhang, H., Ranish, J., and Aebersold, R. (2003) Automated Statistical Analysis of Protein Abundance Ratios from Data Generated by Stable-Isotope Dilution and Tandem Mass Spectrometry. Anal. Chem. **75**: 6648-6657.

Ligterink, W., Kroj, T., Nieden, U., Hirt, H. and Scheel, D. (1997) Receptor-mediated activation of a MAP kinase in pathogen defense of plants. Science **276**: 2054-2057.

Lois, R. (1994) Accumulation of UV-absorbing flavonoids induced by UV-B radiation in *Arabidopsis thaliana* L. Planta **194**: 498-503.

Lois, R. and Hahlbrock, K. (1992) Differential wound activation of members of the phenylalanine ammonia-lyase and 4-coumarate: CoA ligase gene families in various organs of parsley plants. Z Naturforsch **47**: 90-94.

Ma, H., Yanofsky, M. and Meyerowitz, E. M. (1990) Molecular cloning and characterization of GPA1, a G protein alpha subunit gene from *Arabidopsis thaliana*. Proc. Natl. Acad. Sci. U.S.A. **87**: 3821-3825.

Maccarrone, M., Veldink, G.A. and Vligenthart, J.F.G. (1992) Thermal injury and ozone stress affect soybean lipoxygenases expression. FEBS Letters **309**: 225-230.

A.-H.-Mackerness, S., Fred, J.C., Jordan, B. and Thomas, B. (2001) Early signaling components in ultraviolet-B responses: distinct roles for different reactive oxygen species and nitric oxide. FEBS Letters. **489**: 237-242.

A.-H.-Mackerness, S., Surplus, S.L., Blake, P., John, C.F., Buchanan-Wollaston, V., Jordan, B.R. and Thomas, B. (1999) Ultraviolet-B-induced stress and changes in gene expression in *Arabidopsis thaliana*: role of signalling pathways controlled by jasmonic acid, ethylene and reactive oxygen species. Plant, Cell and Environ. **22**: 1413-1423.

Madronich, S., McKenzie, R.L., Björn, L.O. and Caldwell, M.M. (1998) Changes in ultraviolet radiation reaching the Earth's surface. J. Photochem. Photobiol. **46**: 5-19.

Mahady, G. B., Liu, C. and Beecher, C.W.W. (1998) Involvement of Protein Kinase and G Proteins in the Signal Transduction of Benzophenanthridine Alkaloid Biosynthesis. Phytochemistry **48**: 93-102.

Manning, W.J. and Krupa, S.V. (1992) Experimental methodology for studying the effects of ozone on crops and trees. In: Surface level ozone exposures and their effects on vegetation. (Lefohn, A.S., ed.). Chelsea, MI: Lewis Publishers, **pp**. 93-153.

Marinissen, M.J. and Gutkind, J.S. (2001) G-protein-coupled receptors and signaling networks: emerging paradigms. Trends in Pharm. Sci. **22**: 368-376.

Marshall, C, J. (1995) Specificity of receptor tyrosine kinase signaling: transient versus sustained extracellular signal-regulated kinase activation. Cell **80**: 179-185.

Mason, M.G. and Botella, J.R. (2000) Completing the heterotrimer: isolation and characterization of an *Arabidopsis thaliana* G protein γ-subunit cDNA. Proc. Natl. Acad. Sci. USA. **97**: 14784-14788.

McCurdy, T.R. (1994) Concentration of ozone in the lower troposphere (ambient air). In Tropospheric ozone:human health and agricultural impacts (McKee, D. J., ed.). Boca Raton, FL: Lewis Publishers, **pp**. 19-37.

Mehdy, M.C. (1994) Active oxygen species in plant defense against pathogens. Plant Physiol. **105**: 467-472.

Melan, M.A., Dong, X. Endara, M.E., Davis, K.R., Ausubel, F.M. and Peterman, T.K. (1993) An *Arabidopsis thaliana* lipoxygenase gene is induced by pathogens, abscisic acid, and methyl jasmoate. Plant. Physiol. **101**: 441-450.

Menke, F.L.H., van Pelt, J.A., Pieterse, C.M.J. and Klessig, D.F. (2004) Silencing of the mitogen-activated protein kinase MPK6 compromises disease resistance in *Arabidopsis*. The Plant Cell **16**:897-907.

Meskiene, I., Bogre, L., Glase, W., Balog, J., Brandstotter, M., Zwerger, K., Ammerer, G., and Hirt, H. (1998) MP2C, a plant protein phosphatase 2C, functions as a negative regulator of mitogen-activated protein kinase pathways in yeast and plants. Proc. Natl. Acad. Sci. U.S.A. **95**: 1938–1943.

Miles, G.P., Samuel, M.A. and Ellis, B.E. (2002) Suramin inhibits oxidant –induced MAPK signalling in plants. Plant Cell Environ. **25**: 521-527.

Miles, G.P., Samuel, M.A., Jones, A.M. and Ellis, B.E (2004) Mastoparan rapidly activates plant MAP Kinase signaling independent of heterotrimeric G proteins. Plant Physiol. **134**: 1332-1336.

Milligan, S.A., Owens, M.W. and Grisham, M.B. (1998) Differential regulation of Extracellular signal-regulated kinase and Nuclear factor-κB signal transduction pathways by hydrogen peroxide and tumor necrosis factor. Arch. Biochem. Biophys. **352**: 255-262.

Millward, T.A., Zolnierowicz, S. and Hemmings, B. A. (1999) Regulation of protein kinase cascades by protein phosphatase 2A. TIBS **24**: 186-191.

Mittler, R., Herr, E.H., Orvar, B.L., van Camp, W., Willekens, H., Inze, D. and Ellis, B.E. (1999) Transgenic tobacco plants with reduced capability to detoxify reactive oxygen intermediates are hyperresponsive to pathogen infection. Proc. Natl. Acad. Sci. U.S.A. **96**: 14165-70.

Mizoguchi, T., Hayashida, N., Yamaguchi-Shinozaki, K., Kamata, H. and Shinozaki, K. (1993) ATMPKs: a gene family of plant MAP kinases in *Arabidopsis thaliana*. FEBS **336**: 440-444.

Mizoguchi, T., Ichimura, K. and Shinozaki, K. (1997) Environmental stress response in plants: the role of mitogen-activated protein kinases. TIBTECH **15**:15-19.

Morgan P.W. and Drew M.C. (1997). Ethylene and plant responses to stress. Physiol. Plant. **100**: 620-630.

Morris, P.C. (2001) MAP kinase signal transduction pathways in plants. New Phytol. **151**: 67-89.

Mudd, J.B., Dawson, P.J., Tseng, S. and Liu, F.P. (1997) Reaction of ozone with protein tryptophans: Band III, serum albumin, and cytochrome C. Arch. Biochem. Biophys. **338**: 143-149.

Mur, L.A., Bi, Y.M., Darby, R.M., Firek, S. and Draper, J. (1997) Compromising early salicylic acid accumulation delays the hypersensitive response and increases viral dispersal during lesion establishment in TMV-infected tobacco. Plant J. **12**: 1113-1126.

Nakano, Y. and Asada, K. (1980) Spinach chloroplasts scavenge hydrogen peroxide on illumination. Plant, Cell and Physiology **21**: 1295-1307.

Nashida, M., Maruyama, Y., Tanaka, R., Kontani, K., Nagao, T. and Kurose, H. (2000) $G\alpha_i$ and $G\alpha_o$ are target protein of reactive oxygen species. Nature **408**: 492-495.

Nathan, C. (1995) Natural resistance and nitric oxide. Cell **82**: 873-876.

Nishihama, R., Banno, H., Shibata, W., Hirano, K., Nakashima, M., Usami, S. and Machida, Y. (1995) Plant homologues of MAPK (Mitogen-Activated Protein Kinase) Signal Pathways in Yeast and Animal Cells. Plant Cell Physiol. **36**: 749-757.

Noctor, G., Arisi, A.-C.M., Jouanin, L., Kunert, K.J., Rennenberg, H. and Foyer, C. (1998) Glutathione: biosynthesis, metabolism and relationship to stress tolerance explored in transformed plants. J. Exp. Bot. **49**: 623-647.

Noctor, G. and Foyer, C.H. (1998) A re-evaluation of the ATP:NADPH buget during C_3 photosynthesis: a contribution from nitrate assimilation and its associated respiratory activity? J. of Exp. Bot. **49,** 1895-1908.

Noctor, G and Foyer, C.H. (2000) Homeostasis of adenylate status during photosynthesis in a fluctuating environment. J. of Exp. Botany **51**: 347-356.

Norgauer, J., Eberle, M., Lemke, H.D. and Aktories, K. (1992) Activation of human neutrophils by mastoparan. Reorganisation of the cytoskeleton, formation of

phosphatidylinositol 3, 4, 5-triphosphate, secretion up-regulation of complement receptor type 3 and superoxide anion production are stimulated by mastoparan. Biochem. J. **282**: 393–397.

O'Donnell, P.J., Calvert, C., Atzorn, R., Wasternack, C., Leyser, H.M.O. and Bowles, D.J. (1996) Ethylene as a signal mediating the wound response of tomato plants. Science **274**: 1914–1917.

Ohlsson, A.B., Berglund, T., Komlos, P. and Rydstrom, J. (1995) Plant defense metabolism is increased by the free radical-generating compound AAPH. Free Radic. Biol. Med. **19**: 319-327.

O'Kane, D., Gill, V., Boyd, P. and Burdon, R. (1996) Chilling, oxidative stress and antioxidant responses in *Arabidopsis thaliana* callus. Planta **198**: 371-377.

Okano, Y., Takagi, H., Tohmatsu, T., Saito, K. and Nozawa, Y. (1985) A wasp venom mastoparan-induced polyphosphoinositide breakdown in rat peritoneal mast cells. FEBS Lett. **188**: 363-366.

Oliver, S., Formento, P., Fichel, J. L., Etienne, M. C., & Milano, G. (1990) Epidermal growth factor receptor expression and suramin cytotoxicity *in vitro*. Eur. J. Cancer **26**: 867-871.

Olson, P.D. and Varner, J.E. (1993) Hydrogen peroxide and lignification. Plant J. **4**: 887-892.

Orozco-Cardenas, M. and Ryan, C.A. (1999) Hydrogen peroxide is generated systemically in plant leaves by wounding and systemin via the octadecanoid pathway. Proc. Natl. Acad. Sci. U.S.A. **96**: 6553-6557.

Orvar, B.L. and Ellis, B.E. (1997) Transgenic tobacco plants expressing antisense RNA for cytosolic ascorbate peroxidase shows increases susceptibility to ozone injury. Plant J. **11**: 1297-1305.

Patton, R.L. and Garraway, M.O. (1986) Ozone-induced necrosis and increased peroxidase activity in hybrid poplar leaves. Environ. Exp. Bot. **26**: 137-141.

Pauls, K.P. and Thompson, J.E. (1980) In vitro simulation of senescence-related membrane damage by ozone-induced lipid peroxidation. Nature **283**: 504-506.

Pellinen, R., Palva, T. and Kangasjärvi, J. (1999) Subcellular localization of ozone-induced hydrogen peroxide production in birch (*Betula pendula*) leaf cells. Plant J. **20**: 349-356.

Penninckx, I.A., Eggermont, K., Terras, F.R., Thomma, B.P., De Samblanx, G.W., Buchala, A., Metraux, J.P., Manners, J.M. and Broekaert, W.F. (1996) Pathogen-induced systemic activation of a plant defensin gene in *Arabidopsis* follows a salicylic acid-independent pathway. Plant Cell. **8**: 2309-2323.

Peus, D., Meves, A., Vasa, R.A., Beyerle, A., O'Brien, T. and Pittelkow (1999) H_2O_2 is required for UVB-induced EGF receptor and downstream signaling pathway activation – ten years after. Free Radic. Biol. and Med. **27**: 1197-1202.

Piedras, P., Hammond-Kosack, K.E., Harrison, K. and Jones, J.D.G. (1998) Rapid, Cf-9- and Avr9-dependent production of active oxygen species in tobacco suspension cultures. Mol. Plant Microbe interact. **11**: 1155-1166.

Pollack, M. and Richard, M. (1990) Suramin blockade of insulin-like growth factor I-stimulated proliferation of human osteosarcoma cells. J. Natl. Cancer. Inst. **82**:1349-1352.

Potter, S., Uknes, S., Lawton, K., Winter, A.M., Chandler, D., DiMaio, J., Novitzky, R., Ward, E. and Ryals, J. (1995) Regulation of a hevein-like gene in *Arabidopsis*. Mol. Plant Microbe Interact. **6**: 680-685.

Poyton, R.O. and McEwen, J.E. (1996) Crosstalk between nuclear and mitochondrial genomes. Annu. Rev. Biochem. **65**: 563-607.

Prasad, T., Anderson, M.D., Martin, B.A. and Stewart, C.R. (1994) Evidence for chilling-induced stress in maize seedlings and a regulatory role for hydrogen peroxide. Plant Cell **6**: 65-74.

Predieri, S., Norman, H. A., Krizek, D. T., Pillai, P., Mirecki, R. M. and Zimmerman, R. H. (1995) Influence of UV-B radiation on membrane lipid composition and ethylene evolution in Doyenne d'Hiver pear shoots grown in vitro under different photosynthetic photon fluxes. Environ. Exp. Bot. **2**: 151-160.

Price, A., Knight, M., Knight, H., Cuin, T., Tomos, D. and Ashenden, T. (1996) Cytosolic calcium and oxidative plant stress. Biochem. Soc. Trans. **24**: 479-483.

Pryor, W.A., Squadrito, G.L. & Friedman, M. (1995) The cascade mechanism to explain **ozone** toxicity: The role of lipid ozonation products. Free Radical Biol. Med. **19**: 935–941.

Ranish, J.A., Yi, E.C., Leslie, D.M., Purvine, S.O., Goodlett, D.R., Eng, J., Aebersold, R. (2003) The study of macromolecular complexes by quantitative proteomics. Nat. Gen. **33**: 349-355.

Rao, M.V., Koch, J.R., and Davis, K.R. (2000) Ozone: a tool for probing programmed cell death in plants. Plant Mol. Biol. **44**: 345-358.

Rao, M.V., Lee, H., Creelman, R.A., Mullet, J.E. and Davis, K.R. (2000)

Jasmonic Acid Signaling Modulates Ozone-Induced Hypersensitive Cell Death. Plant Cell **12:** 1633-1646.

Rao, M.V., Paliyath, G. and Ormrod, D.P. (1996) Ultraviolet-B- and ozone-induced biochemical changes in antioxidant enzymes of *Arabidopsis thaliana*. Plant Physiol. **110**: 125-136.

Reich, P.B. and Amundson, R.G. (1985) Ambient levels of O_3 reduce net photosynthesis in tree and crop species. Science **230**: 566-570.

Reinbothe, S., Mollenhauer, B. and Reinbothe, C. (1994) JIPs and RIPs: The regulation of plant gene expression by jasmonates in response to environmental cues and pathogens. Plant Cell **6**: 1197-1209.

Ren, D., Yang, Y. and Zhang, S. (2002) Cell death is associated with hydrogen peroxide production in *Arabidopsis*. JBC **277**: 559-565.

Rentel, M.C., Lecourleux, D., Ouaked, F., Usher, S.L., Peterson, L., Okamoto, H., Knight, H., Peck, S.C., Grierson, C.S., Hirt, H. and Knight, M.R. (2004) OXI1 kinase is necessary for oxidative burst-mediated signalling in *Arabidopsis*. Nature **427**: 858-861.

Retzlaff, W.A., Williams, L.E. and Dejong, T.M. (1991) The effect of different atmospheric ozone partial pressures on photosynthesis and grown of nine fruit and nut tree species. Tree Physiol. **8**: 93-105.

Rich, P.R. and Bonner Jr. W.D. (1978) Arch. Biochem. Biophys. **188**: 206-213.

Ries G, et al. (2000) Elevated UV-B radiation reduces genome stability in plants. Nature **406**: 98-101.

Roje, S., Janave, M.T., Ziemak, M.J. and Hanson, A.D. (2002) Cloning and characterization of mitochondrial 5-formyltetrahydrofolate cycloligase from higher plants. JBC **277**: 42748-42754.

Rojo, E., Zouhar, J., Carter, C., Kovaleva, V. (2003) A unique mechanism for protein processing and degradation in *Arabidopsis thaliana*. Proc. Natl. Acad. Sci. U.S.A. **100**: 7389-7394.

Romeis, T., Piedras, P., Zhang, S. and Klessig, D.F. Hirt, H. and Jones, J. (1999) Rapid Avr9- and Cf-9 dependent activation of MAP kinases in tobacco cell cultures and leaves, Convergence of resistance gene, elicitor, wound and salicylate response. Plant Cell, **11**: 273-287.

Roos, W., Dordschbal, B., Steighardt, J., Hieke, M. ,Weiss, D. and Saalbach, G. (1999) A redox-dependent, G protein-coupled phospholipase A of the plasma membrane is involved in the elicitation of alkaloid biosynthesis in *Eschscholtzia californica*. Biochem. Biophys. Acta **1448**: 390-402.

Rozema, J., Staaij J.V.D., Björn L.O. & Caldwell M. (1997) UV-B as an environmental factor in plant life: stress and regulation. Tree **12**: 22-28.

Runeckles, V.C. and Chevone, B.I. (1992) Crop responses to ozone. *In* Surface Level Ozone Exposures and their Effects on Vegetation (Lofohn, A. S., ed.) Chelsea, MI: Lewis Publishers, **pp**. 189-270.

Runeckles, V.C. and Krupa, S.V. (1994) The impact of UV-B radiation and ozone on terrestrial vegetation. Environ. Pollut. **83**:191-213.

Runeckles, V.C. and Vaatnou, M. (1997) EPR evidence for superoxide anion formation in leaves during exposure to low levels of ozone. Plant Cell Environ. 20: 306-314.

Saalbach, G., Natura, G., Lein, W., Buschmann, P., Dahse, I., Rohrbeck, M. and Nagy, F. (1999) The α-subunit of a heterotrimeric G-protein from tobacco, NtGPα1, functions in K^+ channel regulation in mesophyll cells. J. Exp. Bot. **50**: 53-61.

Sachsenmaier, C., Radler-Poul, A., Zinck, R., Nordheim, A., Herrlich, P. and Rahmsdorf, H.J. (1994) Involvement of growth factor receptors in the mammalian UVC response. Cell **78**: 963-972.

Saintanis, C.J., Riga-Karandinos, A.N. and Karandinos, M.G. (2001) Effects of ozone on chlorophyll and quantum yield of tobacco (*Nicotiana tabacum* L.) varieties. Chemosphere **42,** 945-953.

Sagi, M. and Fluhr, R. (2001) Superoxide production by the gp91phox NADPH oxidase plant homologue: modulation of activity by calcium and TMV. Plant Physiol. **126**: 1281-1290.

Salter, L. and Hewitt C. N. (1992) Ozone-hydrocarbon interactions in plants. Phytochemistry **31**: 4045–4050.

Samanta, S., Perkinton, M.S., Morgan, M. and Williams, R.J. (1998) Hydrogen peroxide enhances signal-responsive arachidonic acid release from neurons: role of mitogen-activated protein kinase. J. Neurochem. **70**: 2082-2090.

Samuel, M.A. and Ellis, B.E. (2002) Double jeopardy: both overexpression and suppression of a redox-active plant mitogen-activated protein kinase Render Tobacco plants ozone sensitive. Plant Cell **14**: 2059-2069.

Samuel, M.A., Miles, G.P. and Ellis, B.E. (2000) Ozone treatment rapidly activates MAP kinase signaling in plants. Plant J. **22**: 367-376.

Sandermann, H., Ernst, D., Heller, W. and Langerbartels, C. (1998) Ozone: an abiotic elicitor of plant defence reactions. TIPS **3**: 47-50.

Sano, H., Seo, S., Orudgev, E., Youssefian, S., Ishizuka, K. and Ohashi, Y. (1994) Expression of the gene for a small GTP binding protein in transgenic tobacco elevates endogenous cytokinin levels, abnormally induces salicylic acid in response to wounding, and increases resistance to tobacco mosaic virus infection. Proc. Natl. Acad. Sci. USA **91**: 10556-10560.

Santos, M., Gousseau, H., Lister, C., Foyer, C., Creissen, G., Mullineaux, P. (1996) Cytosolic ascorbate peroxidase from *Arabidopsis thaliana* L. is encoded by a small multigene family. Planta **198**: 64–69.

Satterlee, J.S. and Sussman, M.R. (1998) Unusual membrane-associated protein kinases in higher plants. J. Membrane Biol.**164**: 205-213.

Scandalios J. G. (1997) Molecular genetics of superoxide dismutases in plants. In: Scandalios JG, ed. *Oxidative Stress and the Molecular Biology of Antioxidant Defenses.* Cold Spring Harbor, NY, USA: Cold Spring Harbor Laboratory Press, 27-68.

Schenk, P.W. and Snaar-Jagalska, B.E. (1999) Signal perception and transduction: the role of protein kinases. Biochim. Biophys. Acta **1449**: 1-24.

Scherer, G.F.E. (1992) Stimulation of growth and phospholipase A_2 by the peptides mastoparan and melittin and by the auxin 2, 4-dichlorophenoxyacetic acid. Plant Growth Regul. **11**: 153-157.

Schraudner, M., Ernst, D., Langerbartels, C. and Sandermann, H. (1992) Biochemical responses to ozone. Activation of the defense-related proteins β-1,3-glucanase and chitinase in tobacco leaves. Plant Physiol. **99**: 1321-1328.

Schraudner, M., Moeder, W., Wiese, C. and Camp, W.V. (1998) Ozone-induced oxidative burst in the ozone biomonitor plant, tobacco Bel W3. Plant J. **16**: 235-245.

Schwacke, R. and Hager, A. (1992) Fungal elicitors induce a transient release of active oxygen species from cultured spruce cells that is dependent on $Ca2^{+}$ and protein-kinase activity. Planta **187**: 136-141.

Seo, S., Okamoto, M., Seto, H., Ishizuka, K., Sano, H. and Ohashi, Y. (1995) Tobacco MAP Kinase: a possible mediator in wound signal transduction pathways. Science **270**: 1988-1992.

Sharma, Y.K. and Davis, K.R. (1994) Ozone-induced expression of stress-related genes in *Arabidopsis thaliana*. Plant Physiol. **105**: 1089-1096.

Sharma, Y.K. and Davis, K.R. (1997) The effects of ozone on antioxidant responses in plants. Free Radical Biol. Med. **23**: 480-488.

Sharma, Y.K., Leon, J., Raskin, I. and Davis, K.R. (1996) Ozone-induced responses in *Arabidopsis thaliana*: The role of salicylic acid in the accumulation of defense-related transcripts and induced resistance. Proc. Natl. Acad. Sci. U.S.A. **93**: 5099-5104.

Shapiro, M. A. (1980) Turbulent mixing within tropopause folds as a mechanism for the exchange of chemical constituents between the stratosphere and troposphere, J. Atmos. Sci. **37**: 994-1004.

Shiu, S.-H. and Bleecker, A. B. (2001) Receptor-like kinases from *Arabidopsis* form a monophyletic gene family related to animal receptor kinases. Proc. Natl. Acad. Sci. U.S.A. **98**: 10763-10768.

Sies, H. (1991) Oxidative stress: Introduction. *In* Oxidative Stress: Oxidants and Antioxidants (Sies, H., ed.). London: Academic Press, **pp**. xv-xxii.

Sills, R.C., Hong, H.L., Greenwell, A., Herbert, R.A., Boorman, G.A. and Devereux,T.R. (1995) Increased frequency of K-*ras* mutations in lung neoplasms from female B6C3F1 mice exposed to ozone for 24 or 30 months. Carcinogenesis **16**: 1623–1628.

Spiegel, A.M. and Weinstein, L.S. (2004) Inherited diseases involving G proteins and G protein-coupled receptors. Ann. Rev. Med **55**: 27-39.

Sticher, L., Mauch-Mani, B. and Métraux, J.P. (1997) Systemic acquired resistance. Annu. Rev. Phytopath. **35**: 235 – 270.

Stockwell, W.R., Kirchner, F., Kuhn, M. and Seefeld, S. (1997) New Mechanism for Regional Atmospheric Chemistry Modeling. J. Geophys. Res. **102**: 25847-25879.

Stratmann, J.W., Scheer, J. and Ryan, C.A. (2000) Suramin inhibits initiation of defense signaling by systemin, chitosan, and a β-glucan elicitor in suspension-cultured *Lycopersicon peruvianum* cells. Proc. Natl. Acad. Sci. U.S.A. **97**: 8862-8867.

Stratmann, J.W., Stelmach, B.A., Weiler, E.W. and Ryan, C.A. (2000) UVB/UVA radiation activates a 48 kDa myelin basic protein kinase and potentiates wound signaling in tomato leaves. J. Photochem. Photobiol. **71**: 116-123.

Storz, G. and Imlay J.A. (1999) Oxidative stress. Curr. Opin. Microbiol. **2**:188-94.

Storz, G., Tartaglia, L. A. and Ames, B.N. (1990) Transcriptional regulator of oxidative stress-inducible genes: direct activation by oxidation. Science **248**: 189-194.

Suzuki, K. and Shinshi, H. (1995) Transient activation and tyrosine phosphorylation of a protein kinase in tobacco cells treated with a fungal elicitor. Plant Cell **7**: 639-647.

Suzuki, K., Yano, A. and Shinshi, H. (1999) Slow and prolonged activation of the p47 protein kinase during hypersensitive cell death in a culture of tobacco cells. Plant Physiol. **119**: 1465-1472.

Taher, M.M., Garcia, J.G. and Natarajan, V. (1993) Hydroperoxide-induced diacylglycerol formation and protein kinase C activation in vascular endothelial cells. Arch. Biochem. Biophys. **303**: 260- 266.

Takahashi, K., Isobe, M. and Muto, S. (1998) Mastoparan induces an increase in cytosolic calcium ion concentration and subsequent activation of protein kinases in tobacco suspension culture cells. Biochem. Biophys. Acta **1401**: 339-346.

Tanoue, T. and Nishida, E. (2003) Molecular recognitions in the MAP kinase cascades. Cell. Signal. **15**: 455-462.

Teige, M., Scheikl, E., Eulgem, T., Dóczi, R., Ichimura, K., Shinozaki, K., Dangl, J.L. and Hirt, H. (2004) The MKK2 pathway mediates cold and salt stress signaling in *Arabidopsis*. Mol. Cell. **15**: 141-152.

Tena, G., Asai, T., Chiu, W.L. and Sheen, J. (2001). Plant mitogen-activated protein kinase signaling cascades. Curr Opin Plant Biol. **4**: 392-400.

Tenhaken, R., Levine, A., Brisson, L.F., Dixon, R.A. and Lamb, C. (1995) Function of the oxidative burst in hypersensitive disease resistance. Proc. Natl. Acad. Sci. U.S.A. **92**: 4158-4163.

Toone, W.M. and Jones, N. (1998) Stress-activated signalling pathways in yeast. Genes Cells **3**: 485-498.

Torres, M.A., Dangl, J.L. and Jones, J.D.G. (2002) *Arabidopsis* $gp91^{phox}$ homologues *AtrbohD* and *AtrbohF* are required for accumulation of reactive oxygen intermediates in the plant defense response Proc. Natl. Acad. Sci. U.S.A. **99**: 517-522.

Tucker, E. B. and Boss, W. F. (1996) Mastoparan-induced intracellular Ca^{2+} fluxes may regulate cell-to-cell communication in plants. Plant Physiol. **111**: 459–467.

Tuomainen, J., Betz, C., Kangasjärvi, J., Ernst, D., Yin, Z. H., Langebartels, C. and Sandermann, Jr. H. (1997) Ozone induction of ethylene emission in tomato plants: Regulation by differential transcript accumulation for the biosynthetic enzymes. The Plant J. **12**: 1151–1162.

Turrens, J.F. and Boveris, A. (1980) Generation of the superoxide anion by NADPH dehydrogenase of bovine heart mitochondria. Biochem. J. **191**: 421-427.

Ulm, R., Revenkova, E., di Sansebastiano, G.P., Bechtold, N., and Paszkowski, J. (2001) Mitogen-activated protein kinase phosphatase is required for genotoxic stress relief in *Arabidopsis*. Genes Dev. **15**: 699–709.

Ullah, H., Chen, J.G., Temple, B., Boyes, D.C., Alonso, J.M., Davis, K.R., Ecker, J.R. and Jones, A.M. (2003) The β-subunit of the *Arabidopsis* G protein negatively regulates auxin-induced cell division and affects multiple developmental processes. Plant Cell **15**: 393-409.

Ullah, H., Chen, J.G., Young, J.C., Im, K.H., Sussman, M.R. and Jones, A.M. (2001) Modulation of cell proliferation by heterotrimeric G protein in *Arabidopsis.* Science **292**: 2066-2069.

Usami, S., Banno, H., Ito, Y., Nishihama, R. and Machida, Y. (1995) Cutting activates a 46-kilodalton protein kinase in plants. Proc. Natl. Acad. Sci. U.S.A. **92**: 8660-8664.

Vernooij, B., Fredrich, L., Morse, A., Reist, R., Kolditz-Jawhar, Ward, E., Uknes, S., Kessmann, H. and Ryals, J. (1994) Salicylic acid is not the translocated signal responsible for inducing systemic aquired resistance but is required in signal ransduction. Plant Cell **6**:959-965.

Von Haller, P.D., Yi, E., Donohoe, S., Vaughn, K., Keller, A., Nesvizhskii, A.I., Li, E.J., Goodlett, D.R., Aebersold, R. Watts, J.D. (2003) The application of new software tools to quantitative protein profiling via isotope-coded affinity tag (ICAT) and tandem mass spectrometry: II. Evaluation of tandem mass spectrometry methodologies for large-scale protein analysis, and the application of statistical tools for data analysis and interpretation. Mol. Cell Proteomics **7**: 428-442.

Wang, X.Q., Ullah, H., Jones, A.M. and Assmann, S.M. (2001) G protein regulation of ion channels and abscisic acid signaling in Arabidopdid guard cells. Science **292**: 2070-2072.

White, P.J. and Broadley, M. R. (2003) Calcium in plants. Anns. of Botany **92**: 487-511.

Wilson, C., Eller, N., Gartner, A., Vicente, O. and Heberle-Bors, E. (1993) Isolation and characterization of a tobacco cDNA clone encoding a putative MAP kinase Plant Mol Biol. **23**: 543-551.

Weiss, C.A., Garnaat, C.W., Mukai, Y., Hu, Y. and Ma, H. (1994) Isolation of cDNAs encoding guanine nucleotide-binding protein β-subunit homologues from maize (ZGB1) and *Arabidopsis* (AGB1). Proc. Natl. Acad. Sci. U.S.A. **91**: 9554-9558.

Westermarck, J., Li, S.P., Kallunki, T., Han, J., and Kahari, V.M. (2001) p38 mitogen-activated protein kinase-dependent activation of protein phosphatases 1 and 2A inhibits MEK1 and MEK2 activity and collagenase 1 (MMP-1) gene expression. Mol. Cell. Biol. **21**: 2373–2383.

Wise, A., White, I.R. and Millner, P.A. (1993) Stimulation of guanosine 5'-O-(3-thio) triphosphate binding to higher plant plasma membranes by the mastoparan-analogue, Mas 7. Biochem. Soc. Trans. **21:** 228S.

Xing, T., Higgins, V.J. and Blumwald, E. (1997) Race-specific elicitors of *Cladosporium fulvum* promote translocation of cytosolic components of NADPH oxidase to the plasma membrane of tomato cells. Plant Cell **9**: 249–259.

Yalpani, N., Enyedi, A.J., Leon, J. and Raskin, I. (1994) Ultraviolet light and ozone stimulate accumulation of salicylic acid, pathogenesis-related proteins and virus resistance in tobacco. Planta **193**:372-376.

Yang, T. and Poovaiah, B.W. (2002) Hydrogen peroxide homeostasis: Activation of plant catalase by calcium / calmodulin. PNAS **99**: 4097-4102.

Yang, S.-H., Sharrocks, A.D. and Whitmarsh, A.J. (2003) Transcriptional regulation by the MAP kinase signaling cascades. Gene **320**: 3-21.

Yano, A., Suzuki, K., Uchimiya, H. and Shinshi, H. (1998) Induction of hypersensitive cell death by a fungal protein in cultures of tobacco cells. MPMI **11**: 115-123.

Yi, E.C., Lee, H., Aebersold, R., Goodlett, D.R. (2003) A microcapillary trap cartridge-microcapillary high-performance liquid chromatography electrospray ionization emitter device capable of peptide tandem mass spectrometry at the attomole level on an ion trap mass spectrometer with automated routine operation. Rapid Comm. in Mass Spec. **17**: 2093-2098.

Zhang, H., Shi, X., Hampong, M., Blanis, L. and Pelech, S. (2001) Stress-induced Inhibition of ERK1 and ERK2 by direct interaction with p38 MAP Kinase J. Biol. Chem. **276**: 6905-6908.

Zhang, S. and Klessig, D.F. (1997) Salicylic acid activates a 48-kD MAP Kinase in Tobacco. The Plant Cell **9**: 809-824.

Zhang, S. and Klessig, D.F. (1998) Resistance gene *N*-mediated *de novo* synthesis and activation of a tobacco mitogen-activated protein kinase by tobacco mosaic virus infection. Proc. Natl. Acad. Sci. U.S.A. **95**: 7433-7438.

Zheng, M., Åslund, F. Storz G. (1998) Activation of the OxyR transcription factor by reversible disulfide bond formation. Science **279**: 1718-1721.